

Resource Constrained Adaptive Evolution of Mollusc Shell Form

A Dissertation

Presented in Partial Fulfillment of the Requirements for the
Degree of Doctor of Philosophy

with a

Major in Bioinformatics and Computational Biology

in the

College of Graduate Studies

University of Idaho

By

T. Mason Linscott

Major Professor: Christine Parent, Ph.D.

Committee Members: Luke Harmon, Ph.D.; Paul Hohenlohe, Ph.D.;

Craig McGowan, Ph.D.

Department Administrator: Paul Hohenlohe, Ph.D.

August 2021

Authorization to Submit Dissertation

This dissertation of T. Mason Linscott, submitted for the degree of Doctor of Philosophy with a Major in Bioinformatics and Computational Biology and titled “**Resource Constrained Adaptive Evolution of Mollusc Shell Form**,” has been reviewed in final form. Permission, as indicated by the signatures below, is now granted to submit final copies to the College of Graduate Studies for approval.

Major Professor: _____ Date: _____
Christine Parent, Ph.D.

Committee Members: _____ Date: _____
Luke Harmon, Ph.D.

_____ Date: _____
Paul Hohenlohe, Ph.D.

_____ Date: _____
Craig McGowan, Ph.D.

Department Administrator: _____ Date: _____
Paul Hohenlohe, Ph.D.

Abstract

All life has evolved within a set of extrinsic constraints imposed by the environment. Environmental constraints can limit the scope of evolution and distribution of species in predictable ways when taken in the context of intrinsic, genetically coded metabolic mechanisms. For example, species that require a limiting macronutrient for trait synthesis may only express enlarged or elaborate traits in areas or time periods of abundant macronutrient availability. As many functionally important traits for a variety of organisms have been proposed to be modulated by these eco-physiological constraints (EPC), EPCs have been invoked as one of the major driver of historical and contemporary spatial patterns of biodiversity.

The study of EPC dynamics entails aspects of physiology, systematics, biogeography, adaptation, and speciation. One approach to characterize how EPCs dynamics may affect diversification is to examine evolutionary and spatial patterns of trait expression in a single system where EPC dynamics are partially understood, and then test for similar spatial/evolutionary patterns across physiologically similar systems. The aim of the present work is to use Mountainsnails (*Oreohelix*), marine molluscs, and calcium carbonate (CaCO_3) availability as a framework to gain a better understanding of how EPC dynamics may affect diversification and species distributions. First, I conducted phylogenetic analyses of *Oreohelix* to examine how species limits are associated with the evolution of a resource-intensive trait (calcareous shell ornaments). I found that ornamented *Oreohelix* have evolved recently and that ornamentation is not associated with delimited species units. Second, I utilized species distribution models and shell biometrics to examine whether ornamented *Oreohelix* are associated with calcareous bedrock and if ornamentation confers greater shell strength. I show that ornamented *Oreohelix* are generally restricted to calcareous rock environments and stronger than smooth *Oreohelix* save those smooth forms sampled from calcareous environment Third, I extend the CaCO_3 EPC framework to all marine molluscs and ask whether ornamented marine molluscs are restricted to regions of greater CaCO_3 availability and if they will be more greatly affected by future ocean acidification compared to smooth or sea slug molluscs. Ornamented molluscs were found at higher frequency in CaCO_3 environments but were shown to be less affected by future anthropogenic ocean acidification compared to smooth forms which are commonly expressed at higher latitudes.

Acknowledgements

I am grateful to my advisor Christine Parent for her insightful feedback on my ideas and supporting me throughout the projects covered in this dissertation. I would like to thank Joel Sauder, Kate Holcomb, Jeff Sorenson, Samantha Ferguson, and Christina Sato for facilitating permits and providing logistic support while conducting fieldwork in Idaho, Utah, Arizona, New Mexico, and Washington, respectively. This work would not have been possible without the diligent collections or information provided by a number of academic and public field personnel: Lusha Tronstad, Paul Hendricks, Tom Burke, Hillary Boyd, Bill Gaines, Ann Sprague, Judy Hoder, Janet Millar, Eric Wagner, and Kevin Wheeler. Special thanks are given to Mark A. Ports for several stimulating discussions and providing a number of samples from the state of Nevada. I would also like to acknowledge the support of Heather Robeson and the University of Colorado Museum of Natural History for providing samples for the first Chapter. Additional collection samples were provided by John Slapcinsky and the University of Florida Museum of Natural History. I am grateful to John Phillips, Kelly Martin, Andrew Rankin, and Nicole Recla for comments on different chapters. I would also like to thank Benji Oswald for helping to facilitate GPU resources at the University of Idaho Computation Resource Core. Several fruitful conversations on sequencing approaches with Bernandette Johnson, Amanda Stahlke, Megan Ruffley, Dan New, and Matt Fagan have also helped me determine the path forward in regards to sequencing approaches and I am grateful for their shared expertise. This work was funded by an NSF Graduate Research Fellowship program award to T. Mason Linscott (NSF 1842399) and through the NSF Idaho EPSCoR GEM3 Program under award number OIA-1757324.

Dedication

This work is dedicated to all those who have aided me during my studies at the University of Idaho. Principal among these is my partner, Valerie Linscott, whose companionship I have cherished for many years. With good fortune and dedication, I pray to remain worthy of her counsel, compassion, and strength for as long as fate allows.

My friends and the greater community at both the University of Idaho and the University of Tulsa have also played a great role in shaping my career and person that I am today. First, I must thank Christine Parent and Ron Bonett for being benevolent mentors who have guided my research down productive and enjoyable paths. I would also like to thank Daniel Caetano, Yannik Roell, Katie Peterson, Amanda Stahlke, and Johnathan Kaiser for welcoming me back to academia after my commitment faltered during my first year as a graduate student. John Phillips has been a close friend and resourceful mentor whose love of science and drive I have tried to emulate. Many of John's suggested improvements can be found herein. Another close friend, Andrew Rankin, has improved my research by his continual skepticism of adaptive evolution and retelling of humorous anecdotes during our many field outings.

Lastly, I would like to dedicate this work to my fellow BCB students. They have been a welcoming and friendly group of scientists whose passions and sharp minds have helped me understand the type of colleague I aspire to become.

Table of Contents

Authorization to Submit.....	ii
Abstract.....	iii
Acknowledgements.....	iv
Dedication.....	v
Table of Contents.....	vi
List of Tables.....	viii
List of Figures.....	ix
CHAPTER 1: Assessing species number and genetic diversity of the Mountainsnails	
(Oreohelicidae)	1
Abstract.....	1
Introduction.....	1
Materials and Methods.....	7
Results.....	12
Discussion.....	16
CHAPTER 2: CaCO₃ availability constrains biomineralization expression and	
distribution of Mountainsnails (<i>Oreohelix</i>).....	23
Abstract.....	23
Introduction.....	23
Materials and Methods.....	27
Results.....	31
Discussion.....	37
CHAPTER 3: Recognizing and predicting global patterns of mollusc ornamentation	
expression through machine-learning	43
Abstract.....	43
Introduction.....	43
Materials and Methods.....	46
Results.....	49
Discussion.....	57

References.....	60
Appendix A: Copyright from Conservation Genetics for Chapter 1	76
Appendix B: Supplementary Tables and Figures for Chapter 1	78
Appendix C: Supplementary Tables and Figures for Chapter 2	82
Appendix D: Supplementary Tables and Figures for Chapter 3	104

List of Tables:

Chapter 1: Table 1	3
Chapter 1: Table 1	35
Chapter 2: Table 2	36
Chapter 3: Table 1	52
Chapter 3: Table 2	53
Chapter 1: Supplementary Table 1	80
Chapter 1: Supplementary Table 2	81
Chapter 2: Supplementary Table 1	94
Chapter 2: Supplementary Table 2	96
Chapter 2: Supplementary Table 3	97
Chapter 2: Supplementary Table 4	98
Chapter 2: Supplementary Table 5	100
Chapter 2: Supplementary Table 6	101
Chapter 2: Supplementary Table 7	102
Chapter 2: Supplementary Table 8	103

List of Figures:

Chapter 1: Figure 1	8
Chapter 1: Figure 2	14
Chapter 1: Figure 3	15
Chapter 2: Figure 1	32
Chapter 2: Figure 2	33
Chapter 2: Figure 3	38
Chapter 2: Figure 4	39
Chapter 3: Figure 1	51
Chapter 3: Figure 2	55
Chapter 3: Figure 3	56
Chapter 1: Supplementary Figure 1	78
Chapter 1: Supplementary Figure 2	79
Chapter 2: Supplementary Figure 1	86
Chapter 2: Supplementary Figure 2	87
Chapter 2: Supplementary Figure 3	88
Chapter 2: Supplementary Figure 4	89
Chapter 2: Supplementary Figure 5	90
Chapter 2: Supplementary Figure 6	91
Chapter 2: Supplementary Figure 7	92
Chapter 2: Supplementary Figure 8	93
Chapter 3: Supplementary Figure 1	104
Chapter 3: Supplementary Figure 1	105

CHAPTER 1: Assessing species number and genetic diversity of the Mountainsnails (Oreohelicidae)

“Assessing Species Number and Genetic Diversity of the Mountainsnails (Oreohelicidae)”
Conservation Genetics 21, pages 971–985 (2020)”

Abstract:

One of the current challenges facing conservation biologists is a lack of resolution of species boundaries in threatened groups residing in at-risk areas. This is particularly key for habitats like calcareous outcrops that are known to harbor a high degree of endemic species that may also possess extensive morphological variation. Here, we construct the first time-calibrated phylogeny and evaluate species number of the limestone endemic Mountainsnails (Oreohelicidae), a highly-threatened and phenotypically variable family of land snails from Western North America, using sequence fragments of the mitochondrial gene Cytochrome Oxidase subunit I (COI) from 50 recognized taxonomic species and subspecies. We found four highly supported clades that span wide geographic areas from southern Canada to northern Mexico. Using three species delimitation approaches, we identified a largely concordant set of 15 putative species, which represents less than a third the expected number of species given the current taxonomy and our dataset composition. Our results reveal that this is largely a result of two of the delimitation approaches lumping much of the taxonomic diversity of Oreohelicidae into a single species that possesses remarkable shell form variation and convergence. Moreover, we discuss the suitability of these approaches to delimiting clades with recent divergence, which is not uncommon for limestone endemic fauna and flora. To improve management decisions in montane limestone endemics, our research highlights the need for increased molecular and ecological studies of these isolated and phenotypically variable species.

Introduction:

Regions of high resource availability tend to be associated with high biodiversity (Storch et al. 2005, Cardinale et al. 2009, Cline et al. 2018) and are often sources for conflicts between extractive industries and environmental agencies over access to and protection of resources (Sontter et al. 2018). This conflict is particularly salient for the management of sensitive species

restricted in distribution to areas rich in minerals targeted by industry for extraction (e.g., mining or quarrying). Such extractive activities can alter the distribution of mineralogical resources, which may in turn have detrimental effects on the composition of communities and persistence of resident species at multiple spatiotemporal scales (Miranda et al. 2004, Erskine et al. 2014, Che-Castaldo and Neel 2016, Murguia et al. 2016, Sonter et al. 2018).

Calcareous substrates derived from calcium carbonate (CaCO_3) bedrock (e.g., limestone, dolomite, and marble) are known to harbor endemic diversity and locally adapted populations (Kruckeberg 1969, Baskin and Baskin 1988, Schilthuizen 1994, Clements et al. 2006), and these same areas are some of the most at-risk sites from industrial mineral development for aggregate, cement, and agricultural applications (Tropek et al. 2010, Che-Castaldo and Neel 2016). Conservation plans for these areas seek to balance societal needs for carbonate rock and the habitat requirements of endemic species occupying calcareous outcrops, but developing management plans for these communities is non-trivial (Clements 2008). One major hindrance in the development of management plans for these areas is that many limestone endemic fauna (snails: Alonso et al. 1985, Gittenberger 1991, Frest and Johannes 1997, Teshima et al. 2003, Haskell and Pan 2013; arthropods: Bauer 1989) and flora (Baskin and Baskin 1988, Rajakaruna 2004, Rajakaruna 2017, Wang et al. 2017) possess a high degree of phenotypic variation within and between limestone outcrops, which can make species classification difficult. As many regulatory agencies protect taxa at the species level (Mace 2004, Frankham et al. 2012), there is a need to describe species and interspecific relationships in these communities so that conservation plans can be developed. However, because morphology-based delimitations can be misleading in limestone endemics due to a high degree of homoplastic characters (Conti et al. 1999, Giokas 2000, Elejalde et al. 2008), molecular data are oftentimes needed to evaluate morphology-based systematics of poorly studied taxa.

The Mountainsnails (family: Oreohelicidae) are a calciphilous family of montane-endemic land snails that includes two genera: *Radiocentrum* and *Oreohelix*—purportedly the most diverse genus of land snails in North America (82 currently recognized taxonomic species and subspecies; Pilsbry 1939, Nekola 2014). Many members of Oreohelicidae are restricted to single mountains, canyons, or only a few limestone outcrops within a given mountain range (Pilsbry 1939, Frest and Johannes 1997, Weaver et al. 2008). The narrow range of many *Oreohelix* species and potential threat of industrial and road development have contributed to

Table 1:

Scientific Name	Global Status	Federal Status	State	State Status	Sampled in Current Study
<i>Oreohelix alpina</i>	G2	NL	US: MT	S1	-
<i>Oreohelix amariradix</i>	G1G2	NL	US: MT	S1S2	1
<i>Oreohelix anchana</i>	GH	NL	US: AZ US: AZ,	SNR	-
<i>Oreohelix barbata</i>	G1	FS:S	NM	S1,S1	1
<i>Oreohelix californica</i>	G1	NL	US: CA	SNR	-
<i>Oreohelix carinifera</i>	G1	NL	US: MT	S1	-
<i>Oreohelix concentrata</i>	G2	NL	MX: CH	SNR; SNR	1
<i>Oreohelix confragosa</i>	G1	NL	US: AZ US: SD,	S1	-
<i>Oreohelix cooperi</i>	G1Q	FS:S	WY	S2, S1	1
<i>Oreohelix elrodi</i>	G2G3Q	NL	US: MT	S1	1
<i>Oreohelix eurekensis</i>	G2	NL	US: UT	S1	-
<i>Oreohelix eurekensis uinta</i>	G1	NL	US: UT	SNR	-
<i>Oreohelix grahamensis</i>	G2	FS:S	US: AZ	S2	1
<i>Oreohelix hammeri</i>	GX	NL	US: ID US: CA,	S1	1
<i>Oreohelix handi</i>	G1	NL	NV	SNR, S1	1
<i>Oreohelix haydeni alta</i>	G1	NL	US: CO	SNR	-
<i>Oreohelix haydeni betheli</i>	-	NL	US: CO	SNR	1
<i>Oreohelix haydeni bruneri</i>	-	NL	US: CO	SNR	1
<i>Oreohelix haydeni corrugata</i>	G2	NL	US: UT	S1	1
<i>Oreohelix haydeni haydeni</i>	-	NL	US: UT	S2	-
<i>Oreohelix haydeni hesperia</i>	G2T1	NL	US: ID	S1	1
<i>Oreohelix haydeni hybrida</i>	-	NL	US: UT	SNR	1
<i>Oreohelix haydeni mixta</i>	-	NL	US: CO	SNR	-
<i>Oreohelix haydeni oquirrhensis</i>	-	NL	US: UT	SNR	1
<i>Oreohelix haydeni perplexa</i>	G2T1T3	NL	US: ID	SNR	1
<i>Oreohelix hemphilli</i>	G2T1T3	NL	US: NV	S2	1
<i>Oreohelix hendersoni</i>	G1G3	NL	US: CO	SNR	1
<i>Oreohelix houghi</i>	G1	NL	US: AZ	SNR	1
<i>Oreohelix howardi</i>	G1	NL	US: UT	SNR	1
<i>Oreohelix idahoensis idahoensis</i>	G1	BLM:S	US: ID	S1	1
<i>Oreohelix idahoensis baileyi</i>	G1	NL	US: ID	S1	1
<i>Oreohelix intersum</i>	G1T1	NL	US: ID	S1	1
<i>Oreohelix jaegeri</i>	G1	NL	US: NV	S1	-
<i>Oreohelix jugalis</i>	G1	BLM:S	US: ID	S1	1
<i>Oreohelix junii</i>	G1G2	NL	US: WA	S2S3	1
<i>Oreohelix litoralis</i>	G2	NL	US: NM	S1	-

<i>Oreohelix loisae</i>	G1	NL	US: NV	S2	1
<i>Oreohelix magdalenae</i>	G1G3	NL	US: AZ	S1	1
<i>Oreohelix metcalfei acutidiscus</i>	G2	FS:S	US: NM	SNR	-
<i>Oreohelix metcalfei concentrica</i>	G2T1	FS:S	US: NM	SNR	1
<i>Oreohelix metcalfei cuchillensis</i>	G2T1	NL	US: NM	S1	-
<i>Oreohelix metcalfei hermosensis</i>	G2T1	FS:S	US: NM	SNR	-
<i>Oreohelix metcalfei metcalfei</i>	G2T1T2	FS:S	US: NM	SNR	1
<i>Oreohelix metcalfei radiata</i>	G2T1	FS:S	US: NM US: NV,	SNR	1
<i>Oreohelix neomexicana</i>	G2T2	NL	TX	S3, SNR	1
<i>Oreohelix nevadensis</i>	G3	NL	US: NV	S1	1
<i>Oreohelix parawanensis</i>	G1	NL	US: UT	S1	1
<i>Oreohelix peripherica newcombi</i>	G1	NL	US: UT	SNR	-
<i>Oreohelix peripherica peripherica</i>	G2	NL	US: UT	SNR	1
<i>Oreohelix peripherica wasatchensis</i>	G2T1T2	NL	US: UT	S1	1
<i>Oreohelix peripherica weberiana</i>	-	NL	US: UT	SNR	1
<i>Oreohelix pilsbryi</i>	G2T1	FS:S	US: NM US: MT,	S1	-
<i>Oreohelix pygmaea pygmaea</i>	G1	FS: S	WY	S1, S1	1
<i>Oreohelix pygmaea maculata</i>	-	NL	US: WY US: MT,	SNR	-
<i>Oreohelix strigosa berryi</i>	G5T2	NL	WY	S1S2, SH	-
<i>Oreohelix strigosa buttoni</i>	-	NL	US: UT	SNR	-
<i>Oreohelix strigosa capax</i>	G5T2Q	NL	US: ID	SNR	-
<i>Oreohelix strigosa delicata</i>	G5T1 G5T5	NL NL	US: OR, WA	S1, S1	1
<i>Oreohelix strigosa depressa</i>			US: MT, NM, NV, WY	SNR, S2S3, S2?, SNR	1
<i>Oreohelix strigosa fragilis</i>	-	NL	US: ID, UT	SNR	1
<i>Oreohelix strigosa goniogyra</i>	G5T1	BLM:S	US: ID	S1	1
<i>Oreohelix strigosa nogalensis</i>	G5T2	FS:S	US: NM	S1	1
<i>Oreohelix strigosa strigosa</i>	-	NL	US: WA	S5	1
<i>Oreohelix subrudis</i>	G5	NL	CAN: AB, BC, SK; US: AZ, CO, ID, MT,	SU, S3, SNR; SNR, SNR, S5, S3, S3, SNR, SNR	1

			NM, NV, WA, WY		
<i>Oreohelix swopei</i>	G1	FS:S	US: NM	S1	-
			US: ID,		
<i>Oreohelix tenuistriata</i>	GH	NL	UT	SH, SNR	1
<i>Oreohelix variabilis</i>	G2Q	NL	US: OR	S2	1
<i>Oreohelix vortex</i>	G2?	BLM:S	US: ID	S1	1
<i>Oreohelix waltoni</i>	G1	BLM:S	US: ID	S1	1
<i>Oreohelix yavapai clutei</i>	-	NL	US: AZ	SNR	-
<i>Oreohelix yavapai cummingsi</i>	G5T3Q	NL	US: UT	S1	-
<i>Oreohelix yavapai extremitatis</i>	G5TNR	NL	US: AZ, MT, WY	SNR, SNR, SNR	-
<i>Oreohelix yavapai fortis</i>	-	NL	US: AZ	SNR	-
<i>Oreohelix yavapai magnicornu</i>	-	NL	US: WY	SNR	-
<i>Oreohelix yavapai mariae</i>	G5T1	NL	US: MT	S1	-
<i>Oreohelix yavapai profundorum</i>	-	NL	US: AZ	SNR	-
<i>Oreohelix yavapai yavapai</i>	G5	NL	US: AZ	S1	1
<i>Radiocentrum avalonense</i>	G1	NL	US: CA	S1	1
<i>Radiocentrum chiricahuana</i>	G2	NL	US: AZ	SNR	1
<i>Radiocentrum clappi</i>	G2	NL	US: AZ	SNR	-
			US: NM,		
<i>Radiocentrum ferrissi</i>	G1	NL	TX	S1, S1	-
<i>Radiocentrum hachetanum</i>	G2	NL	US: NM	S1	-

Table 1: Oreohelicidae species sampling and conservation status at federal and state levels. NatureServe ranks correspond to global (G) or state (S) on a scale of 1-5 with 5 being the least threatened. NR, U, Q, T correspond to not ranked, unrankable due to possible lack of information, questionable taxonomic status, and intraspecific status, respectively. Federal sensitive species status abbreviations BLM stands for Bureau of Land Management and FS for Federal Forest Service.

the listing of over half of the family as critically imperiled (G1 or S1 rank) or imperiled (G2 or S2 rank) by NatureServe and local state governments (Table 1; NatureServe 2019). However, conserving oreohelcid diversity is complicated by a lack of systematic knowledge of the group. Many of the current taxonomic units of Oreohelcidae were described based on shell characters that may be prone to homoplasy, phenotypic plasticity, or a high degree of intraspecific variation (Henderson 1918, Anderson et al. 2007, Chak 2007). Given this, as well as a few molecular studies suggesting a lack of support for recognized taxonomic units (Chak 2007) and molecular-based evidence for cryptic species (Weaver et al. 2008), management officials are hesitant to develop conservation plans or federally list threatened Oreohelcid species without both morphological and molecular support for current taxonomic statuses (Federal Register 2005, 2006, 2011).

The primary morphological characters used for delimiting Oreohelcid species are genitalia and shell morphology (Pilsbry 1938, Ports 2004). Genitalia morphology is relatively conserved in *Oreohelix* (Pilsbry 1938) with only three genitalia types being recorded and named after the nominal species of each group (*O. strigosa*, *O. subrudis*, and *O. yavapai* types). These have served to define the major groups from which the genus has been organized. Given the relatively conserved genital morphology of the group compared to other land snails (Pilsbry 1938), shell morphology has been primarily invoked for species or subspecies delineation in combination with geographical isolation. However, species delimitation based on shell morphology has resulted in the description of several species complexes within the major genitalia groups. Within these complexes, it is common to find gradients of intergrading shell forms with the extremes usually being ascribed as species or subspecies. One of the major shell characters used for species delimitation in *Oreohelix* is shell ornamentation (e.g., increased shell biomineralization such as spiral ribs, vertical ribs, prominent keel; Figure 1) but it is also a character with a high degree of variation between populations (Fairbanks 1975, Weaver et al. 2008), which has made morphological species classification challenging for experts and conservation officials. Morphological identification is further complicated by ornamentation convergence within and between the major genitalia groups (e.g., the spiral ribs of *O. haydeni* and *O. pilsbryi*, Figure 1; Pilsbry 1938). These parallelisms of shell form across the genus have led previous authors to suggest much of shell form variation in the group may be

environmentally driven (Henderson 1918), but the exact environmental associations of these characters remains elusive (Anderson et al. 2007, Weaver et al. 2008).

In this study, we present the first family-wide molecular phylogeny of Oreohelicidae to assess species status and determine the diversification branching pattern and timing among species. We combined previously published sequences with newly generated sequence data from hitherto unsampled species to produce both maximum-likelihood and Bayesian phylogenetic reconstructions, as well as employ coalescent-based delimitation and barcode gap detection methods. The results of our study improve on our understanding of oreohelcid systematics and provide an important resource for the management and conservation of this threatened group.

Materials and Methods:

Sampling

Field personnel collected specimens from a total of 274 localities across the western United States between 1998—2019 (Figure 2). Collected adult snails were preserved in 95% ethanol. Additional tissue samples were taken from collections at the Junius Henderson Museum, University of Colorado, Boulder and the Florida Museum of Natural History, University of Florida, Gainesville (Appendix Table 1). Samples were identified as either recognized or proposed (Frest and Johannes 1997) taxonomic units using a combination of geographic location, shell, and genitalia characters when available (Pilsbry 1939, Burke 2014).

DNA sequencing, genotyping, and dataset composition

Genomic DNA was extracted from muscle tissue removed from the foot of each animal using a DNeasy Blood and Tissue Kit (Qiagen, Valencia, CA) per the manufacturer's protocols. Partial sequences of the mitochondrial COI gene were amplified by PCR with primers LCO1490/HCO2198 (5'-TAAACTTCAGGGTGACCAAAAATCA-3' and 5'-GGTCAACAAATCATAAAGATATTGG-3'; Folmer et al. 1994). All PCRs were performed in 25 μ l reactions containing 2 μ l DNA, 18 μ l water, 2.5 μ l buffer, 0.75 μ l of 50 mM MgCl₂, 0.5 μ l of 10 mM dNTPs, 1 μ l of 10 μ M forward and reverse primer, and 0.25 μ l of 5U/ μ l of New England Biolabs Taq polymerase. The PCR conditions were as follows: an initial denaturation step at 95°C for 2 minutes, followed by 30 cycles of 95°C for 35 seconds, 52°C for 60 seconds, 72°C for 45 seconds, and finalized with a final extension step at 72°C for 5 minutes. To verify amplifications, amplicons were electrophoresed in a 1% agarose gel. PCR

Figure 1:

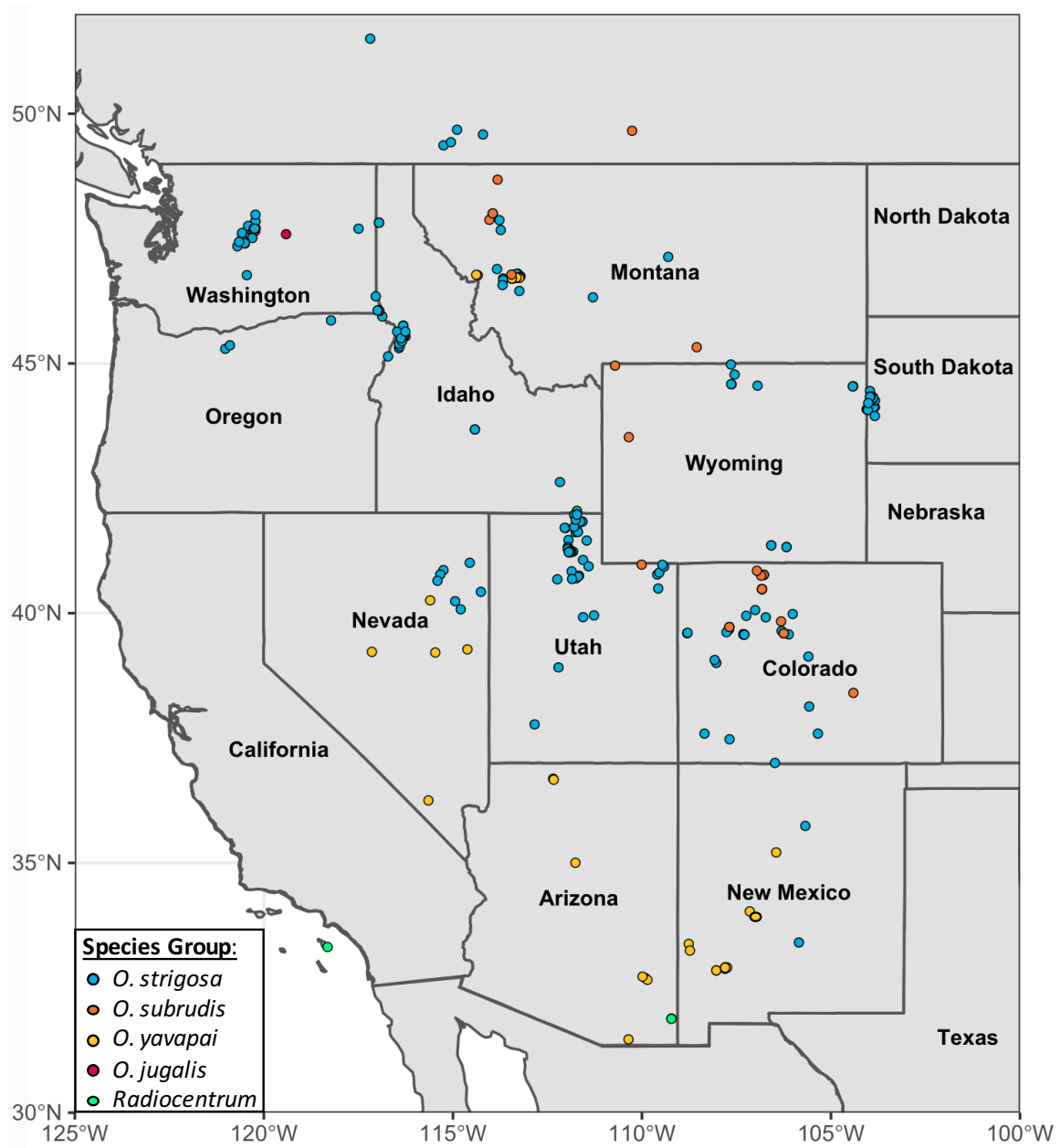


Figure 1: Sampling localities color coded by species group. Blue corresponds to the *O. strigosa* group, orange to the *O. subrudis* group, yellow to the *O. yavapai* group, red to the *O. jugalis* group, and green to the *Radiocentrum* group.

products were then purified using the Qiaquick PCR cleanup kit (Qiagen). Bi-directional DNA Sanger sequencing was outsourced to Eurofins MWG Operon, Louisville, KY, USA (<http://www.eurofins.fr>). Chromatograms in both directions were compared and consensus sequences were assembled using Chromas v.2.6.2 (Technelysium, <http://www.technelysium.com.au/chromas.html>).

We added to these data a set of 261 homologous *Oreohelix* sequences from GenBank from previous molecular studies of the group (Weaver 2006, Chak 2007, Weaver et al. 2008, van Paridon 2017, Dempsey et al. 2020). In addition, we added a single individual of *Megomphix* to serve as an outgroup as previous morphological studies have indicated Oreohelicidae and Megomphicidae may be sister families (Emberton 1991). The combined 861 sequence dataset contained representatives of 60.9% (52 species) of all currently recognized species and subspecies in Oreohelicidae. Multiple sequence alignments were constructed using the MAFFT online webserver (<https://mafft.cbrc.jp/alignment/server/>) (Kato et al. 2019) specifying a gap opening penalty of 5 and using the remaining default values. The initial 572bp alignment contained COI fragments ranging in length from 296 to 572bp with a mean sequence length of 565bp. No indels or premature stop codons were observed. Identical sequences (357 sequences) matched another from the same or nearby locality and were removed prior to phylogenetic analysis for a final alignment of 504 sequences.

Phylogenetic analyses

We first selected a model of nucleotide sequence evolution using the corrected Akaike information criterion (AICc) and decision theory (Minin et al. 2003), implemented by the automodel command in PAUP* v4.0152 (preview release; Swofford 2003). The JC+ Γ model was chosen for our dataset. Phylogenetic relationships were then inferred using maximum-likelihood performed in RAxML (Stamatakis 2006), specifying the JC+ Γ model and conducting ten replicate runs. Nodal support was assessed using 100 bootstrap replicates with two tree searches per bootstrap. We used the resulting ML phylogeny to test the assumption that the data set has evolved in a clock-like fashion by testing for a global molecular clock in PAUP* using the likelihood-ratio test (LRT) of Felsenstein (1988). As the strict clock model was rejected, the relaxed clock model was used for subsequent analyses. Additionally, we tested the level of genetic saturation at the COI gene using DAMBE7 (Xia 2018) using the 'Xia method' (Xia et al. 2003) and visually assessed saturation using the R package 'ape'

(Paradis and Schliep 2018). Visual inspection was accomplished by plotting uncorrected genetic distances vs corrected genetic distances using the Gamma shape parameter value from the PAUP* automodel command (JC+ Γ ; Gamma shape parameter= 0.666; Supplemental Figure 3). The saturation test in DAMBE using the default parameters indicated little saturation (P-values < 0.001; proportion of invariant sites: 0.407). The slope of uncorrected to corrected genetic distances indicates weak to moderate saturation at 25-30% sequence divergence (Supplemental Figure 3). These analyses indicate weak-to-moderate saturation, which may cause relationships and divergence time estimates at the deeper nodes to be more uncertain (Xia et al. 2003).

We estimated the timing of *Oreohelix* divergence events by inferring an absolute evolutionary timescale using a fossil calibration point implemented in BEAST v1.8.4 (Heled & Drummond 2009). Past systematic revisions have placed nearly all previously ascribed *Oreohelix* fossils into the genus *Radiocentrum* (Roth 1986, Pierce and Constenius 2001). Of the few *Oreohelix* fossils remaining, most are from the Quaternary with only a single Oreohelicid in the early Miocene (20.8 MYA) from the Deep River Formation (Roth and Emburton 1994), though the validity of the assignment of this fossil to the genus *Oreohelix* is not certain (Roth 2019, Personal Communication). As it appears *Radiocentrum* has been present since at least the late Cretaceous and *Oreohelix* possibly since the early Miocene, we chose to fossil calibrate using the earliest date for the Deep River formation to allow for the possibility that *Oreohelix* is a relatively recent emergence from recent *Radiocentrum* as conjectured by Pierce and Constenius (2001). To have another suitable calibration for comparison, we used fossil records of *Oreohelix* from the mid-Blancan age Shooting Iron Formation as a calibration point (Love 1989). For the Deep River fossil calibration, we used a log-normal prior distribution with an offset of 20.8 MYA, mean of 3.0 MYA, and standard deviation of 1.5 MYA for estimating the split between *Oreohelix* and *Radiocentrum*. We used a log-normal distribution with an offset of 3.8 MYA, mean of 3.0 MYA, and standard deviation of 1.5 MYA for the Shooting Iron Calibration. We ran and subsequently combined four independent MCMC chains each of 100 million generations, sampling every 5000 generations, and discarding the first 20% as burn-in using LogCombiner (Rambaut and Drummond, 2007) for both calibration points. Convergence was assessed visually using TRACER v. 1.7.1

(Rambaut and Drummond, 2007) and by verifying greater than 200 effective sample size for all parameters estimated.

Species delimitation

To delimit species, we first used the Automatic Barcode Gap Discovery (ABGD) method (Puillandre et al. 2012) through the online server (<https://bioinfo.mnhn.fr/abi/public/abgd/abgdweb.html>) with the default settings. The ABGD method compares pairwise genetic distances from gene fragments to differentiate smaller intraspecific divergence from greater interspecific divergence. ABGD then delimits sequences into groups over a user specified range of maximal intraspecific divergence values and reports the number of groups for each recursively determined maximal intraspecific divergence value (Puillandre et al. 2012).

We then implemented the multi-threshold Generalized Mixed Yule Coalescent (GMYC) method (Pons et al. 2006, Fujisawa and Barraclough 2013) with our ultrametric BEAST chronogram in R (R Core Team 2019). The single threshold GMYC model seeks a global threshold that delimits between species-level to population-level processes by separately modelling the fit of within- vs. between-species branching models resulting in a given ultrametric tree. The method operates by finding the maximum likelihood (ML) solution of a model incorporating diversification between species using a Yule speciation process and branching within species using a neutral coalescent (Pons et al. 2006). The multi-model approach relaxes the assumption that all speciation events are older than all coalescent events in the tree (Fujisawa and Barraclough 2013) and allows for the fitting of multiple thresholds across individual clades of the tree.

Finally, we used the multi-rate Poisson Tree Process (mPTP) model (Kapli et al. 2017) with our RAxML tree operated through the online server (<https://mcmc-mptp.h-its.org/mcmc/>) to delimit species. The PTP model group seeks to delimit species by modelling branching processes based on the number of accumulated expected substitutions between subsequent speciation events. The underlying assumption is that each substitution has a chance to generate a branching event with branching events being more probable within than between species. The original PTP is a two-parameter model that assumes models within and between species branching using a single coalescent and speciation parameter, respectively (Kapli et al. 2017). In contrast to the original PTP (Zhang et al. 2013), mPTP is more robust to sampling- and

population-specific biases in empirical datasets by assigning each delimited species a distinct intra-specific coalescent distribution instead of assuming a single global distribution for all delimited species. We used default parameters for the mPTP analyses.

Results:

Phylogenetic analyses

All Bayesian and maximum-likelihood approaches were concordant in topology for major clades (Figure 1, Supplementary Figure 1), so we chose to focus our discussion of the results to the time-calibrated BEAST tree. The 95% highest posterior density (HPD) of our mean substitution rate for the early Miocene Deep River fossil *Oreohelix* was 0.00442-0.0131 substitutions/site/MYA (mean 0.00889), which is outside the range of substitution reported for other terrestrial gastropods at the COI gene (0.028 - 0.130 substitutions/site/MYA; Van Riel et al., 2005). Using the Shooting Iron mid-Blancan age fossil as a calibration point, we recovered a 95% HPD of 0.0261 – 0.068 substitutions/site/MYA (mean 0.0449) for our mean substitution rate which fits well within the range of mean substitution rates recovered from other terrestrial gastropods. Given the previously discussed concerns regarding the generic assignment of the Deep River formation fossil specimen used for calibration, and that it resulted in an abnormally low mean substitution rate, we focus the remaining sections of the paper on the Shooting Iron formation calibration results.

Radiocentrum and *Oreohelix* were recovered as reciprocally monophyletic with a high degree of posterior probability (PP) for all Bayesian analyses (Figure 1; 1.00 PP). The 95% highest posterior density (HPD) of the split between *Oreohelix* and *Radiocentrum* encompassed the estimated earliest split between them using fossils (mean divergence date: 6.37 MYA; 95% HPD: 4.08-10.46 MYA). The *Oreohelix* genitalia groups proposed by Pilsbry (1938) were recovered as monophyletic and correspond to major deep splits in the tree, with the exception of the *O. jugalis/junii* species group which was placed within the *O. subrudis* group by Solem (1975)(Figure 1): Clade A is a weakly supported group (0.55 PP; mean divergence date: 4.99 MYA; 95% HPD: 3.00-8.28 MYA) that includes all members of the *O. yavapai* species group from Arizona, Montana, Nevada, and New Mexico; Clade B unites samples from Idaho and Washington (1.00 PP; mean divergence date: 1.19 MYA; 95% HPD: 0.37-2.34 MYA) as part of the *O. jugalis/junii* species group; Clade C contains all samples of the *O. subrudis* genitalia group (1.0 PP; mean divergence date: 1.90 MYA; 95% HPD: 0.84-

3.29 MYA), which includes samples from Colorado, Montana, New Mexico, Nevada, Utah, and Wyoming. Clade D comprises approximately two-thirds of the samples, including all of the samples of the *O. strigosa* genitalia group from Colorado, Idaho, Nevada, New Mexico, Oregon, Utah, Canada, and Washington (1.0 PP; mean divergence date: 2.25 MYA; 95% HPD: 1.06-3.78 MYA).

Species delimitation

ABGD resulted in a narrow range of delimited species (15–16) across the specified default prior range of maximal distance (0.001 – 0.1) but with relatively stable estimates of 16 *Oreohelix* species between prior maximal distances of 0.0129 to 0.03594. These results were largely concordant with the 15 species delimited by mPTP (Figure 1). The only differences between the approaches were whether *O. barbata* was delimited into one or two species and whether *Radiocentrum* were delimited into one or three species. Both approaches delimited one new species from the Kaibab National Forest. Many of the delimited species for these approaches were located in the southwest U.S., with both approaches splitting many previously taxonomically recognized southwestern species into multiple species. *O. grahamensis* and *O. barbata* were delimited into three and two species, respectively. Clade D with the largest number of recognized taxonomic species (29 species) was lumped into a single delimited species unit in all analyses excluding GMYC. The *O. metcalfei* complex (Clade A) from New Mexico (four species) and *O. haydeni/yavapai* Montana complex (three species) were also delimited as a single species. Using the criteria that a delimited species is threatened if all the previous taxonomic units that constitute the new delimited species are listed as NatureServe rank G2 or higher, we found 11 threatened species using these two approaches (Supplemental Table 1). The multi-model GMYC delimited a mean of 264 species ($p < 0.00001$ CI: 260–269 species), which is well beyond any previous estimate of species number in Oreohelcidae.

Figure 2:

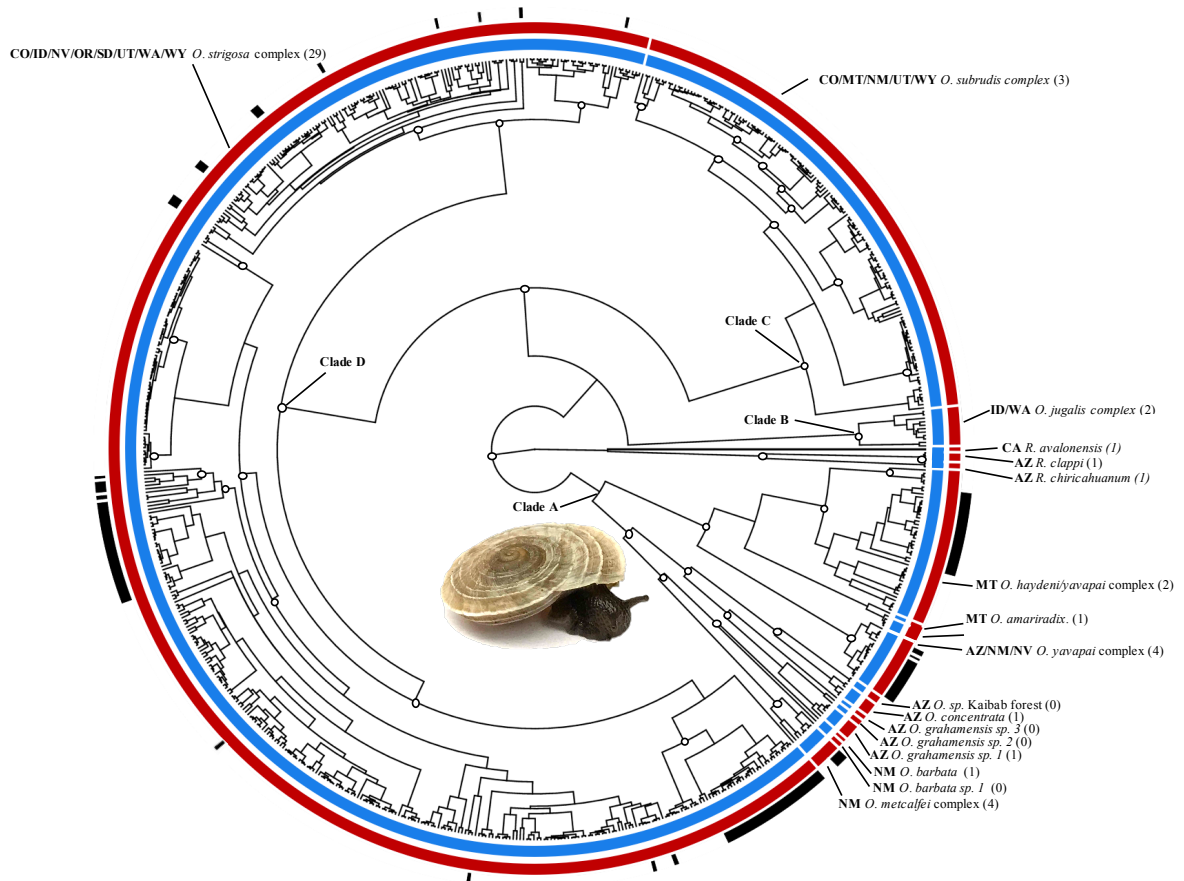


Figure 2: Beast chronogram with delimited species according to species delimitation method. The blue circle depicts the 15 species delimited by mPTP and red circle the 16 by ABGD. The outer ring indicates ornamentation presence (black) and absence (white). Delimited species are annotated with taxonomic names and state location. Numbers in parentheses are the number of previously recognized taxonomic units included under the newly delimited species. Nodes with hollow circles represent clades with greater than 0.80 posterior probability.

Figure 3:

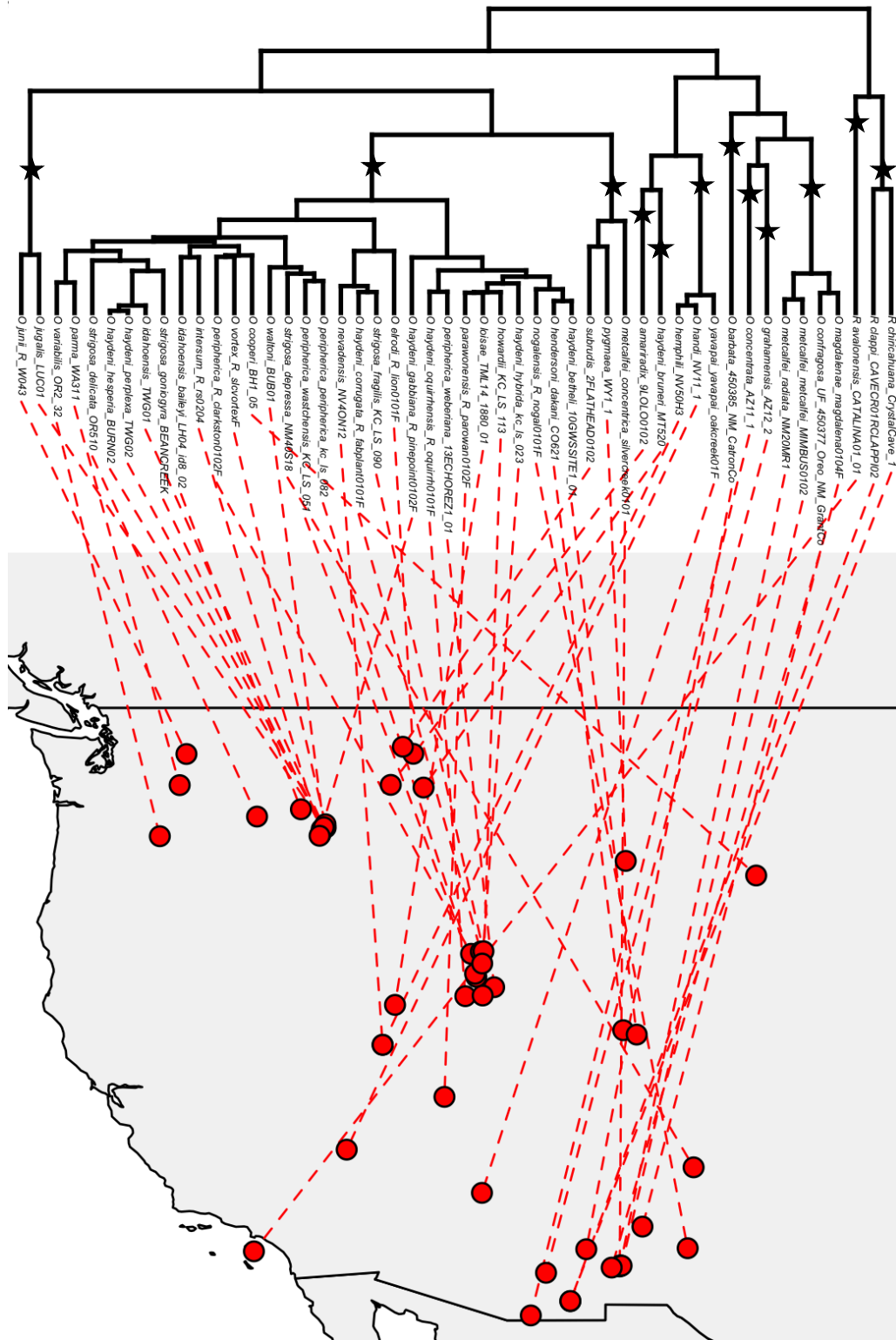


Figure 3: Geophylogeny of recognized taxonomic units. Stars on the phylogeny indicate delimited species. Undescribed or cryptic species are not presented.

Discussion:

Patterns of molecular divergence and morphological convergence

Accurate divergence time estimates between clades can provide key insights into historical demographic processes or ecological factors associated with diversification between species, either of these may in turn provide crucial information for the management of threatened species (Crandall 2009). Here, we employ a single mitochondrial gene (COI) to reconstruct the evolutionary history of Oreohelicidae, which limits 1) our perspective of the evolutionary history of the group, by only having one gene history for comparison, and 2) our power to estimate accurate divergence times and determining species relationships, due to the size of the gene fragment (Heled and Drummon 2009). Many different gene histories are possible, which may not accurately represent the true ‘species tree’, and this realization should temper the reader’s interpretation and application of the single gene history results outlined herein (Rannala and Yang 2017). However, there is often substantial phylogenetic information contained in a single gene, which can be utilized for understanding the processes that have shaped the diversity of extant endangered taxa and can also provide a foundation for future conservation genetic work. Previous authors have considered *Oreohelix* an ancient genus in a ‘stage of prolific speciation’ (Henderson 1918; Pilsbry 1938). Our finding that *Oreohelix* and *Radiocentrum* split in the early Pliocene to late Miocene (Supplemental Figure 1), with a mean date in the late Miocene (6.37 MYA), confirms that *Oreohelix* is a relatively recent split from *Radiocentrum* as opposed to an ancient Cretaceous split proposed by Pilsbry (1938). We also find that many currently recognized taxonomic species are polyphyletic, yet morphologically distinct. Together, these results indicate that extant Oreohelicidae are relatively younger than previously thought and that several forms have arisen convergently in geographically separated localities.

Many recognized species of conservation concern were found to be polyphyletic, indicating that the characters used for species delimitation may not be suitable for diagnosing species (Figure 1). Most of the polyphyletic species fall within the *O. strigosa* species complex (Clade D) but also include members of the Montana *O. haydeni/yavapai* complex (Clade A). Four of the polyphyletic species of conservation concern appear to be the result of distinct shell ornamentation morphologies used for species classification evolving multiple times separately (e.g., *O. haydeni*, *O. peripherica*, *O. idahoensis*, *O. hemphilli*). For example, the homoplastic

shell character of spiral ribs used for assigning specimens to *O. haydeni* must have evolved separately no fewer than 11 times across widely geographically separated areas (Figure 1). In contrast, there are examples of recently diverged, sympatric, and possibly cryptic lineages of *Oreohelix* displaying the same shell morphology and co-occurring at the same site (Weaver et al. 2008). Indeed, the rapid evolution of ornamented shell characters across distinct, phylogenetically separated clades (e.g., *O. haydeni*; this study) and convergence of ornamentation in the same locality in separate lineages (e.g., *O. peripherica*; Weaver et al. 2008) indicates ornamentation can evolve quickly, and possibly in response to environmental conditions.

What are the possible factors that may be driving parallelisms of shell form and resulting polyphyletic taxonomic units in Oreohelcidae? Previous studies have hypothesized that ornamentation results in increased mechanical strength, increased surface water adhesion, decreased evaporation, and decreased insolation (Giokas 2008). Any of these proposed benefits could promote ornamentation evolution for the *Oreohelix* species that occupy arid environments or localities with a high density of predators. However, the occurrence of ornamentation across geographically separate areas that differ substantially in climatic and biotic conditions may indicate that no single axis of selection may be driving ornamentation evolution across Oreohelcidae. Ornamentation may have multiple functions in different environmental contexts, which may make disentangling any functional benefit of ornamentation difficult without a more comprehensive assessment of the climatic and biotic conditions across the geographical distribution of a given lineage.

While the function of terrestrial mollusk shell ornamentation may be elusive, it has been proposed that many forms of molluscan ornamentation are associated with regions rich in calcium carbonate (Alonso et al. 1985, Teshina et al. 2003, Watson et al. 2012). The greater availability of calcium carbonate in these regions may allow for increased shell biomineralization and ornamentation expression. In *Oreohelix*, all ornamented species save one (*O. waltoni*) are restricted to limestone, marble, or dolomite outcrops (Linscott et al. in prep). Conversely, many thin shelled ‘hairy’ forms of *Oreohelix* are solely found on volcanic rock (Frest and Johannes 1997). Further, *Oreohelix* ornamentation expression decreasing along transects crossing geologic boundaries where the rock type shifts from predominantly calcium carbonate to another composition (e.g., *O. idahoensis* and *O. waltoni*; Pilsbry 1938, Linscott

and Parent in prep.) may indicate that ornamentation expression is plastic or locally selected for in calcareous environments. Local selection according to edaphic or geological factors can promote adaptive divergence and possible speciation (Clements et al. 2006, reviewed in Rajakaruna 2017). However, many smooth or unadorned *Oreohelix* species occupy similar calcareous bedrock habitat as ornamented forms, which may indicate a degree of standing genetic variation is necessary for ornamentation to evolve. Ornamentation expression is predominantly expressed in the large *O. strigosa* species complex (Clade D) as well as in the *O. yavapai* complex (Clade A). Within these clades, ornamented types (e.g., keel, horizontal ribs, vertical ribs) are very recently diverged from a smooth or another ornamented phenotype (Figure 1). If local adaptation to edaphic or geologic factors is occurring in *Oreohelix*, our estimates of species number may be underestimated given that divergence may be recent and lineage sorting has not fully occurred (Rajakaruna 2007).

Species number and conservation implications

Delimiting the boundaries between species is a challenging and necessary task for informed management of threatened groups. Generally, it is expected that regions of long temporal stability and isolation will possess a high degree of phylogenetic diversity and well-demarcated species boundaries (Moritz 2002). In such regions, it is expected that single gene phylogenetic reconstructions and species estimation approaches will reasonably capture the evolutionary history of a group (Reid and Carstens 2012). However, secondary contact or recent divergence can make the delimitation of species and conservation units challenging, particularly when there is limited molecular data (Leaché et al. 2014, Jackson et al. 2017). Resolving species relationships in these situations require multiple-genes or genomic sampling to understand the extent of admixture and/or genome-wide adaptive divergence. Scenarios of secondary contact or recent divergence are rarely detected before a first-pass molecular delimitation has taken place; single gene reconstructions are suitable for determining the clades that need greater molecular sampling and for delimiting moderate to highly diverged lineages.

There was substantial conflict in the number of species between GMYC and the non-ultrametric tree based approaches. GMYC delimited a mean of 264 species, which is more than five-fold increase in species number given our taxonomic sampling. The unrealistic number of species generated by GMYC is possibly due to a combination of possible model violations including our choice of priors for our divergence time analysis (Birth-Death tree prior over a

coalescent tree prior; Monaghan et al. 2009), the proportion of singletons in the data, and/or the predominant composition of the rapidly splitting *O. strigosa* clade in our dataset (Reid and Carstens 2012, Talavera et al. 2013). However, even when we used a coalescent tree prior, pruned singletons from our tree, and removed the *O. strigosa* clade we still recovered extremely high estimates of species number (Supplemental Table 2). Given the unrealistic numbers of species delimited by GMYC, we choose to omit this analysis from further discussion.

ABGD and mPTP produced a concordant set of 15 species of *Oreohelix* representing a close to three-fold reduction in species given our taxonomic sampling. Eight of the delimited species are from the *O. yavapai* species group, which is distributed throughout the sky-islands of the southwestern United States and mountainous regions of western Montana (Figure 1). Several delimited species from these regions were previously considered populations of existing taxonomic units (*O. grahamensis* sp. 1, *O. grahamensis* sp. 2, *O. barbata* sp. 1) and occupy the same mountain range as their sister taxon. In addition to this cryptic diversity, a single undescribed species was also found to be distinct from the Kaibab National Forest (Figure 1).

A description of new species is beyond the scope of this study and will have to await future work. However, that we detected several cryptic and undescribed species in the *O. yavapai* species group with mPTP and ABGD, two approaches that are considered relatively conservative with respect to estimates of species diversity (Reid and Carstens 2012), indicates that there may be significant cryptic diversity within this group that remains undiscovered. Indeed, that we find several cryptic and undescribed species from the Pinaleño (e.g., *O. grahamensis* sp. 1-2) and Mogollon Mountains (*O. barbata* sp. 1) is consistent with systematic studies of other resident taxa that possess substantial genetic diversity without corresponding external morphological differences (Pinaleño Mountains: Weaver et al. 2010; Mogollon Mountains: Burbrink et al. 2011). Given the isolation and long-term stability of these regions, greater species diversity may be discovered with further sampling, and we suggest should be an aim of future exploratory conservation work.

In contrast with the aforementioned splits, our delimitation approach lumped together many recognized taxonomic species and subspecies (37 species total) into three species with the lion's share of diversity being placed in a single delimited species, the *O. strigosa* complex (29 species). It has long been recognized that this complex has the greatest degree of shell form

variation, convergence, and intergradation compared to other *Oreohelix* species complexes and among North American land snails in general (Pilsbry 1938). Given the high degree of morphological diversity associated with limestone habitats and the relatively frequent branching of the *O. strigosa* group compared to other *Oreohelix* groups (Figure 1), this complex is in a stage of recent divergence as put forward by Henderson (1918) and Pilsbry (1938) which may make detecting species boundaries difficult with our current methods and data. Reid and Carstens (2012) evaluated the ability of the PTP model family to delimit species across a wide range of simulated scenarios and found that rapid, recent radiations can lead to inaccurate results as coalescent and speciation events become indistinguishable. Similarly, any observable barcode gap should be smaller or more difficult to detect in recently diverged species, which may make it difficult for genetic distance based methods like ABGD to delimit species accurately (Kapli et al. 2017). While the current methods used in this study identified several threatened moderate – to highly diverged lineages, additional work is needed to definitively evaluate species boundaries and address the taxonomic discrepancies in the recently diverged *Oreohelix* clades (e.g., *O. strigosa* group) with richer genomic datasets and more robust genomic methods.

Moving forward, this study leaves the species status of many recently diverged *Oreohelix* unchanged while suggesting that undescribed and cryptic diversity exists in the arid southwestern United States and Western Montana. Many of the delimited ‘species’ identified in this study are composed of many morphologically distinct and geographically isolated taxonomic units, thus these delimited ‘species’ in our study possess remarkable shell form variation and population structure, which may be revealed to be species or subspecies with further investigation. If we take the results of our analyses at their face value and ignore the aforementioned possibilities - there still exists substantial localized and distinct shell form variation that may facilitate persistence in many of the threatened, delimited species we identify in this study which may warrant protection. However, approximately 35 species and subspecies would be synonymized and potentially down-listed at federal and state levels. Conversely, if we were to treat each occurrence of ornamentation evolution in the *O. strigosa* group as a species or conservation unit, we would need to develop conservation plans for 12 new units (Figure 1). Similar but smaller increases in species number would occur in the other species groups. As either extreme appears unreasonable, genomic and ecological criteria need

to be developed from future studies to apply an appropriate threshold for determining species status and resulting conservation priorities for many of the recently diverged clades identified in this study.

Devising conservation priorities for the threatened oreohelcid diversity identified in this study will require addressing three issues: 1) discerning areas where substantial genetic diversity exists when phenotype and habitat preference appears to be conserved (e.g., *O. grahamensis* and its associated delimited cryptic species); 2) identifying populations where putative local adaptation is present (e.g., *O. strigosa* group); 3) determining a threshold of morphological or genetic distinctiveness to qualify for protection and then maintaining that diversity to increase overall species viability and adaptive variation (Crandall et al. 2000). Surveying the genetic diversity of populations spanning a species' range can address the first issue (1) but demarcating and maintaining conservation units within species to help ensure species persistence (2,3) can be challenging (e.g., Mexican wolf, Geffen et al. 2004). For *Oreohelix*, this will require determining the major factors responsible for shell form variation, understanding the possible adaptive roles of such variation, and evaluating whether, if any, genomic divergence is substantial enough to warrant species/subspecies recognition. However, this task is complicated by a lack of systematic knowledge of *Oreohelix* species habitat requirements and factors responsible for shell form variation. Edaphic specialization to calcareous rock/soils may be occurring in *Oreohelix*, given the association of ornamented shell morphologies with carbonate rock/soils, but whether these morphological-geological associations reflect substantial genomic divergence that qualifies for species or subspecies recognition has yet to be determined. The methods we utilize in this study do not perform well for delimiting species in recently diverged groups (Reid and Carstens 2012), so our analyses offer limited insight for addressing this topic except to expose its relevance for the conservation of *Oreohelix* species.

The areas of greatest shell form variation and taxonomic diversity are concentrated in geologically diverse regions (Frest and Johannes 1997, Linscott and Parent in prep.). If edaphic specialization is occurring and results in substantial genomic divergence, conservation priorities should focus on protecting the soil and rock habitat requirements for edaphic specialized species, and hence, geologic diversity. It may be that future conservation plans for some *Oreohelix* species will resemble that of edaphically specialized plant species where the

focus is on protecting the underlying geologic resource (Sonter et al. 2018, Corlett and Tomlinson 2020). Indeed, disturbances to limestone outcrops from commercial industries (e.g., quarrying, Clements et al. 2006; road building, Frest and Johannes 1997; or grazing, Labaune and Magnin 2002) may have effects on the distribution of phenotypes by altering the biotic, geologic, or edaphic factors influencing shell form expression. Future studies should investigate the effects that these factors have on *Oreohelix* distribution and shell form expression so that conservation plans can be developed balancing the habitat requirements of limestone endemic *Oreohelix* and societal needs for carbonate rock

Together, our findings indicate substantial discordance between morphology-based taxonomy and genetic diversity in Oreohelicidae. We identify several possible cryptic species within existing taxonomic units and provide molecular support for the distinctiveness of 13 ecologically sensitive or threatened species. We propose that much of the phenotypic diversity within Oreohelicidae may be environmentally associated and related to calcium carbonate availability. Conserving the phenotypic and genetic variation of these calcareous rock endemic populations will require future studies on the genomic distinctiveness and habitat requirements of these taxa. The present study emphasizes the need for additional empirical studies on the genetic diversity of limestone endemic fauna in montane environments and sheds valuable light onto the management of limestone outcrops and their biodiversity conservation strategies.

CHAPTER 2: CaCO₃ availability constrains biomineralization expression and distribution of Mountainsnails (*Oreohelix*)

Abstract:

Aim: Geographic variation in macronutrients can set limits on species distributions. For species that need to produce and maintain biomineralized traits for survival, spatial variation in mineral macronutrients can constrain species' distributions by limiting the expression and function of biomineralized traits. Here, we examine whether threatened, heavily biomineralized *Oreohelix* land snail species are restricted to CaCO₃ rock regions, and whether CaCO₃ rock populations possess greater shell strength, a key component of land snail fitness.

Location: Western United States

Methods: We used Random-Forest classification models to evaluate the contribution of topographic, vegetation, climate, and geologic variables for predicting the presence of heavily biomineralized shell ornaments. We then projected the distribution of ornamented morphs at multiple spatial resolutions (90m²–1km²) across the Western United States to determine whether grain size affects any relationship between ornamentation classification and proximity to CaCO₃ rock. Shell strength and other biometric variables were measured and compared for representative ornamented and smooth forms from CaCO₃ poor and rich substrates.

Results: Proximity to CaCO₃ rock was the most important variable in all models and was highly associated local ornamentation classification and distribution. Ornamented shells were consistently stronger and heavier than smooth shells except for those smooth forms sampled from CaCO₃ rock outcrops, suggesting standardized shell strength and mass is a resource constrained response.

Conclusions: We demonstrate that biomineralization expression, trait function, and species distribution is constrained by mineral supply in a highly threatened group of land snails (*Oreohelix*). This trait-environment relationship has direct impact on the management of *Oreohelix* species and for other terrestrial biomineralizing taxa of conservation concern.

Introduction:

Spatial patterns of trait expression can provide key insights into the habitat requirements and distribution of species (Sterck et al. 2011, reviewed in Zakharova et al. 2019). For example, for functionally important traits whose expression is modulated by the concentration of a

limiting metabolic resource in the environment (e.g. greater aqueous SiO₂ concentration and larger diatom test size and thickness (Finkel and Zoe 2010); higher atmospheric O₂ availability and larger insect body size (Harrison et al. 2010)), the magnitude of trait expression may reflect a threshold of resource availability necessary for trait expression and species persistence (Kroeker et al. 2014, Harvey et al. 2018). As many functionally important traits for a variety of taxa are affected by these environmental-physiological constraints (EPC) (plants: Gutschick 1981; insects: Harrison et al. 2010; and invertebrates Finkel and Zoe 2010), understanding the distribution of these traits in the context of the spatial distribution of the limiting resource may improve estimates of the habitat requirements of populations, species, and communities across the tree of life.

A major example of a relatively well-studied EPC constrained group are aquatic organisms that produce biomineralized structures necessary for survival (e.g. shells, tests, and skeletons). Many biomineralizing aquatic species are restricted to regions with sufficient availability of the building materials used in trait biomineralization (Dillon 2000; Finkel and Zoe 2010). Similarly, the frequency of thickened or elaborate biomineralized structures is often greater among communities of aquatic species in areas of higher mineral resource availability (Finkel and Zoe 2010, Watson et al. 2012). This association of aquatic biomineralization trait expression and environmental resource availability is expected given the importance of resource availability for modulating two key aspects of aquatic biomineralization physiology: 1) the metabolic cost of mineral transport and synthesis (Rajan and Vengatesen 2020, Clark et al. 2020), and 2) the metabolic cost of maintenance to overcome constant environmental dissolution (Clark et al. 2020). These resource dependent mechanisms of aquatic biomineralization have served as the physiological underpinnings for explaining the striking disparity in biomineralization expression between areas of high and low resource availability. Species residing in regions of higher resource availability may require less energy per unit of biomineralized mass to synthesize and maintain than in resource poor regions, which may in turn enable greater available trait morphospace of biomineralized structures for lineages in resource rich regions (Vermeij and Covich 1978, Bush and Pruss 2013). Prolonged resource rich conditions may favor the specialization of morphs over many generations to different levels of resource availability and eventual habitat exclusion between morphs (Sanford and Kelly 2011, Golbuu et al. 2016, Camp et al. 2017).

For terrestrial calcifying species such as land snails, such explicit environmental-physiological mechanisms have rarely been invoked for explaining spatial patterns of biomineralization expression between or within species. However, a large number of studies have shown that land snail fitness (Crowell 1973), shell shape morphology (Alonso et al. 1985, Teshima et al. 2003), abundance (Schilthuizen et al. 2003), distribution (Clements et al. 2008), and alpha diversity (Hotopp 2002, Overton et al. 2009) often depend on the availability of calcium carbonate (CaCO_3) in the rock and soil substratum. Indeed, many land snail species are restricted to CaCO_3 resource rich regions such as limestone outcrops (Clements et al. 2008) where as much as 33% of shell CO_3^{2-} can come from limestone for resident species (Goodfriend and Stipp 1983, Yanes et al. 2008). This species distribution pattern may indicate that some limestone residents have a greater amount of resource supply for biomineralization than non-limestone populations. As limestone outcrops often harbor high levels of morphological diversity (Gittenberger 1991, Frest and Johannes 1997), the greater resource availability of CaCO_3 at these sites may permit release from metabolic constraints and allow for the expression of greatly thickened or elaborate shell morphologies.

Calcareous shell ornaments, extrusions such as a rib, keel, or spines from the outer surface of the shell, are a type of elaborate biomineralized trait that may be associated with greater CaCO_3 availability. Despite the possible physiological connection between CaCO_3 availability and land snail biomineralization expression (Goodfriend 1983), the few studies that examined the association of land snail shell ornamentation with geology using extensive surveys have been unsuccessful in finding any relationship between geology and ornamentation expression (Mesher and Welter-Schultes 2008, Welter-Schultes 2010). However, the aforementioned studies examined a single genus (*Albinaria*) where ornamented shells are often lighter size standardized weight as a smooth shell (Giokas 2008). Ornamentation in this group may not represent greater biomineralization effort given the equivalent length standardized mass to smooth shells. The coarse spatial resolution of the geologic maps (1–2km uncertainty, Welter-Schultes 2010) in these studies may have also limited the authors' ability to discriminate a CaCO_3 ornamentation relationship in *Albinaria* given the propensity of land snail morphology to vary over small spatial distances (often less than 90m, Welter-Schultes 1998). As other ornamented groups of land snails have heavier shells compared to their smooth counterparts (Quensen and Woodruff 1997) and are reported to be closely associated with limestone

(Alonso et al. 1985, Frest and Johannes 1997, Teshima et al. 2003), there is a need to reassess whether ornamentation is associated with calcareous rock in multiple land snail groups using geologic data at biologically relevant spatial resolutions. Elucidating whether ornamentation is associated with geology will enable a broader understanding of land snail biomineralization expression in the context of CaCO_3 availability, which may shed light on the habitat requirements of ornamented land snail species and the role of CaCO_3 availability in shaping land snail morphology.

As ornamentation expression often results in increased shell mass and strength, many authors have proposed that ornamentation is an anti-predator response (Palmer 1979, Quensen and Woodruff 1997). However, it remains unknown whether this is a general pattern in land snails as only a few studies have compared ornamented shell strength to smooth forms (Boettger 1932, Quensen and Woodruff 1997). While other selective pressures such as convective cooling, water retention, and insolation may also be driving ornamentation expression (Giokas 2008), quantifying the degree that ornamentation alters shell strength across taxa may provide general insight into the functional benefits of shell ornamentation as shell integrity is a necessary function for most shelled gastropods (Barker 2004).

The Mountainsnails (genus: *Oreohelix*) are a calciphilous and widely distributed montane genus of North American land snails whose members often possess thickened shell ornaments (Figure 1, Linscott et al. 2020). Many ornamented species and subspecies of *Oreohelix* are restricted to a few limestone outcrops within a given mountain range (Pilsbry 1939, Frest and Johannes 1997). The narrow range of many ornamented *Oreohelix* and ongoing threats of road and industrial development have contributed to the listing of nearly all ranked ornamented *Oreohelix* species and subspecies (Supplementary Material Table 3) as critically imperiled (G1 or S1 rank) or imperiled (G2 or S2 rank) (Linscott et al. 2020, NatureServe 2021) by NatureServe and local state governments. However, the lack of systematic knowledge of ornamented *Oreohelix* habitat requirements has limited conservation strategies for protecting *Oreohelix* diversity (Linscott et al. 2020). Conservation agencies are uncertain of which areas to prioritize for *Oreohelix* habitat, the distribution of *Oreohelix* within their district, or where to survey for new populations (Federal Register 2005, 2006, 2011). Identifying the key habitat requirements of ornamented *Oreohelix* would provide information for addressing each of these

difficulties and allow for more effective conservation planning for some of the most vulnerable and threatened *Oreohelix* species.

In this study, we test the hypothesis that calcareous rocks (e.g. limestone, marble, and dolomite) are a habitat requirement for ornamented *Oreohelix* using a presence/absence database spanning across *Oreohelix*'s range. We evaluate the importance of variables for predicting ornamentation classification across sites of known *Oreohelix* occurrence and project the distribution of morphs across Western North America using Random-Forest (Breiman 2001). We then apply our approach at multiple spatial resolutions to assess whether predictor resolution (90m²–1km²) impacts our ability to detect a relationship between ornamentation expression and calcareous rock units. Furthermore, we compared shell dimensions (i.e. weight, length, height) and shell strength of smooth and ornamented *Oreohelix* species to determine whether ornamentation expression represents greater biomineralization effort and if ornamentation impacts shell strength, a major function of the shell that is often related to land snail fitness (Quensen and Woodruff 1997, Barker 2004).

Materials and Methods:

Study area and survey data

Mountainsnail presence data were assembled from a combination of opportunistic observation datasets and dedicated field surveys from across the Western United States of America (USA) (see Supplementary Material Table 2 for number of presence and absence records and Supplementary Material Figures 1-2 for maps of presence and absence records). Absence points were taken from surveys conducted by the authors, private surveys conducted by local experts, or government surveys. Species records were classified as ornamented or smooth based on the presence of a keel or ribs on the outer surface of the shell using photographs when available or species classification (see Supplementary Material Table 4 for classifications of species). Occurrence points with greater than 500m uncertainty or that were in the same pixel (i.e. duplicates) were removed and the remaining filtered presence/absence data were used for analysis. The effect of predictors (see below) on ornamentation expression was assessed using a dataset composed only of *Oreohelix* presence locations so that any relationships between predictors and ornamentation expression are not confounded by associations with general *Oreohelix* presence or absence. Models created for projecting the

distribution of morphologies across the Western USA used all presence and absence data except that which was set aside for model evaluation.

Predictor variables

As land snails are often microhabitat specialists whose distribution may not be accurately captured using coarse resolution predictors, we evaluated ornamented and smooth *Oreohelix* species classification and distribution at predictor spatial resolutions ranging from fine to coarse (90m²–1km²; Table 1) across the continental USA (100W–125W° Longitude). We chose predictor variables known to be associated with land snail distribution, morphology, and/or physiology from other studies (Table 1, Supplementary Material Table 1): compound topographic index, elevation, slope, heat load index, global horizontal irradiance, height above nearest drainage, horizontal distance to nearest drainage, normalized difference vegetation index (NDVI), tree canopy cover, soil clay percent, soil pH, distance to developed area, and distance to CaCO₃ rock. We removed predictors that were highly correlated ($R < 0.7$) with each other across resolutions and kept the remaining variables for subsequent analysis (Table 1). Predictor variables were projected and resampled from their native resolution to the desired analytical resolution using bilinear interpolation in ArcGIS pro v.2.6.0 (see Supplementary Material Note 1 for more details). As WorldClim bioclimatic data are often the only dataset used in species distribution modelling for many conservation and biogeographical studies (e.g. Rankin et al. 2019), we made a second dataset using only the bioclimatic variables from WorldClim (Fick and Hijmans 2017) and the distance from CaCO₃ rock predictor. We retained WorldClim layers that were not highly correlated ($R < 0.7$) resulting in nine bioclimatic layers (Table 1) and the distance from CaCO₃ rock predictor being retained for analysis. To ensure we are only measuring the effect of predictor resolution and not dataset composition between resolution sets, we retained localities that were at least 1km apart resulting in 1068 smooth, 299 ornamented, and 1603 true absence localities. Sites of ornamented or smooth types were used as absences in the reciprocal classes species distribution model if the site was from a dedicated survey and if the reciprocal class was not found at the site.

Modelling relationships

We used Random-Forest (RF) classification models to determine the relative importance of predictors for *Oreohelix* classification and to generate distributional models of the two morphologies. In brief, RF is a machine learning classification and regression approach that is

capable of handling complex relationships between predictors by integrating classifications across a multitude of binary decision trees generated from random perturbations of the original dataset (Breiman 2001). This method commonly outperforms other model types for ecological classification tasks (Cutler et al. 2007) and identifying relevant variables associated with different classes (Fox et al. 2017). We created RF models through the ‘randomForest’ package (Liaw and Weiner 2002) in R v.3.6.3 (R Core Team 2020). RF models were tuned to try two variables at each split ($mtry=2$) after initial tuning using the ‘rfTune’ function (Liaw and Weiner 2002). We chose to use a high number of decision trees ($ntrees = 3000$) in our RF models as this increases reproducibility between model runs (Liaw and Weiner 2002, Kopp and Allen 2020). As class imbalance in the training data can have substantial effects on RF model outputs (Barbet-Massin et al. 2012), we sampled an equal number of localities from the minority and majority classes from the full dataset equal to 90% of the total localities of the minority class when constructing each decision tree. Variable importance of each predictor was assessed through mean decrease in accuracy (MDA) and significance of each variable was measured using the ‘rfPermute’ package (Archer 2016). ‘rfPermute’ generates null distributions of variable importance metrics for each predictor through permuting the response variable (Archer 2016). We generated variable importance metric null distributions using 100 permutations of the training dataset and measured significance according to an alpha threshold of 0.05.

We then examined how all models performed with or without the distance to CaCO_3 rock predictor by comparing model accuracy using the true-skill statistic (TSS) on a validation dataset composed of a randomly selected 20% of *Oreohelix* occurrence records withheld during training. The TSS metric quantifies a model’s ability to correctly classify presences and absences ($\text{sensitivity} + \text{specificity} - 1$) for a classification threshold that maximizes sensitivity and specificity, and has been shown to be independent of species’ prevalence (Allouche et al. 2006). TSS scores greater than 0.6 are generally considered useful for application and greater than 0.8 as excellent (Coetzee et al. 2009).

It is often difficult to interpret directly how complex machine learning methods generate classifications from predictor values (i.e. they seemingly act as a ‘black box’). To determine how predictors contribute to RF model classification, we used local interpretable model-agnostic explanation (LIME). LIME is a post-hoc interpretation method that fits a simpler local

surrogate model that is of lesser complexity but greater interpretability for a limited area of the n-dimensional space defined by the predictor variables (Ribeiro et al. 2016, Ryo et al. 2020). Through LIME, we can examine how our RF models used predictors to generate class predictions at a given locality and evaluate whether different predictors change in importance across the diverse areas that *Oreohelix* occupy (Ryo et al. 2020). LIME was applied across sites spanning subregions of *Oreohelix* ornamentation presence and absence (Rocky Mountain North, Great Basin, and Southwest USA) on RF models that included the distance from CaCO₃ predictor. We used the ‘explain’ function in the ‘lime’ package, selecting the top five features with the highest weights and the remaining parameters on default settings (Ribeiro et al. 2016). We then generated partial dependence plots of each model's relationship to distance to CaCO₃ rock to examine whether this relationship was affected by predictor resolution.

Finally, we created distribution models using RF for both morphologies using all available presence and absence data and the same predictor variables as previous RF analyses. No pseudo-absence selection or background sampling was included for any model. RF distribution models used the same model parameters as the RF classification models (i.e. mtry, ntree, and class balanced sampling). RF distributional models were evaluated using the TSS statistic on a validation dataset (randomly selected 20% of presence/absence records withheld during training) and variable importance and significance was assessed using MDA and ‘rfPermute’ (Archer 2016).

Shell measurements and crushing resistance

To measure biomineralization effort in *Oreohelix*, we measured various shell biometric variables (e.g., mass, shell length, shell volume; Supplementary Material Table 5 and Supplementary Material Table 6) of ornamented and smooth snails. We measured shell biometric variables from five species (*O. strigosa* sp. n=25, *O. strigosa goniogyra* n=33, *O. jugalis* n=23, *O. idahoensis* n=18, *O. haydeni hesperia* n=33) representing all of the major ornamentation types within *Oreohelix* (smooth, commarginal ribs, antimarginal ribs, and keel). We split *O. strigosa goniogyra* into smooth (n=18) and keeled (n=15) categories as this subspecies expresses keels on limestone outcrops and a smooth rounded morphology elsewhere. Smooth forms were split into non-limestone (n=50) and limestone resident groups (n=16) for later analyses. Live snails were collected from May to July 2020 throughout the lower Salmon and Snake River drainages, ID, USA. Snails were euthanized by drowning in

5% EtOH for 24 hours, then flash-boiled. Soft tissue was removed from the shell and the shells were left to dry for at least 48 hours. After the drying period, we measured shell biometric variables using a mass scale (Mettler Toledo: AL104) and digital calipers (Mitutoyo ABS Digimatic Calipers: Model CD-6 ASX).

Shell integrity is a necessary function of the shell for land snail survival (Barker 2004). Shell strength is closely linked to shell integrity (Barker 2004) and generally increases per unit shell mass (Quensen and Woodruff 1997). As ornamentation has been shown to increase shell strength in other land snail groups (Boettger 1932, Quensen and Woodruff 1997), ornamentation expression may lead to greater shell strength in *Oreohelix*. To investigate whether ornamentation is increasing shell strength in *Oreohelix*, we measured the force needed to crush the shell laterally as this form of crushing allowed for consistent load placement across different shell shapes and ornamentation types (Figure 3). Shells were placed on a flat metallic surface and crushed laterally on the whorl just after the aperture using a Mark-10 Force Gauge (Model M5-100) and associated test stand (Model ES20) (Figure 3). We recorded the peak compression force (N) required to break the shell.

We then used a one-way ANOVA and a post-hoc pairwise comparison of estimated marginal means using the ‘rstatix’ package (Kassambara 2020) to compare the magnitude of the difference between the mass of ornamented and smooth types after controlling for shell size as covariates (Supplementary Material Table 5 and 6). This same analysis was then repeated to compare shell strength among ornamented types using shell mass as a covariate.

Results:

Model Performance

RF classification and distributional models including the distance to CaCO₃ predictor consistently had higher TSS scores than those omitting this variable on the validation datasets but only marginally so for smooth form models (Table 2). RF classification models had TSS scores between 0.52–0.64 and ornamented distribution models had TSS scores ranging between 0.57–0.75. Smooth distribution models had TSS scores ranging from 0.55–0.67 and minimal decline in TSS when the distance to CaCO₃ rock layer was removed (Table 2). WorldClim models had consistently marginally higher TSS scores than those built using elevation or satellite predictor variables (Table 2). While higher predictor resolution slightly

Figure 1:

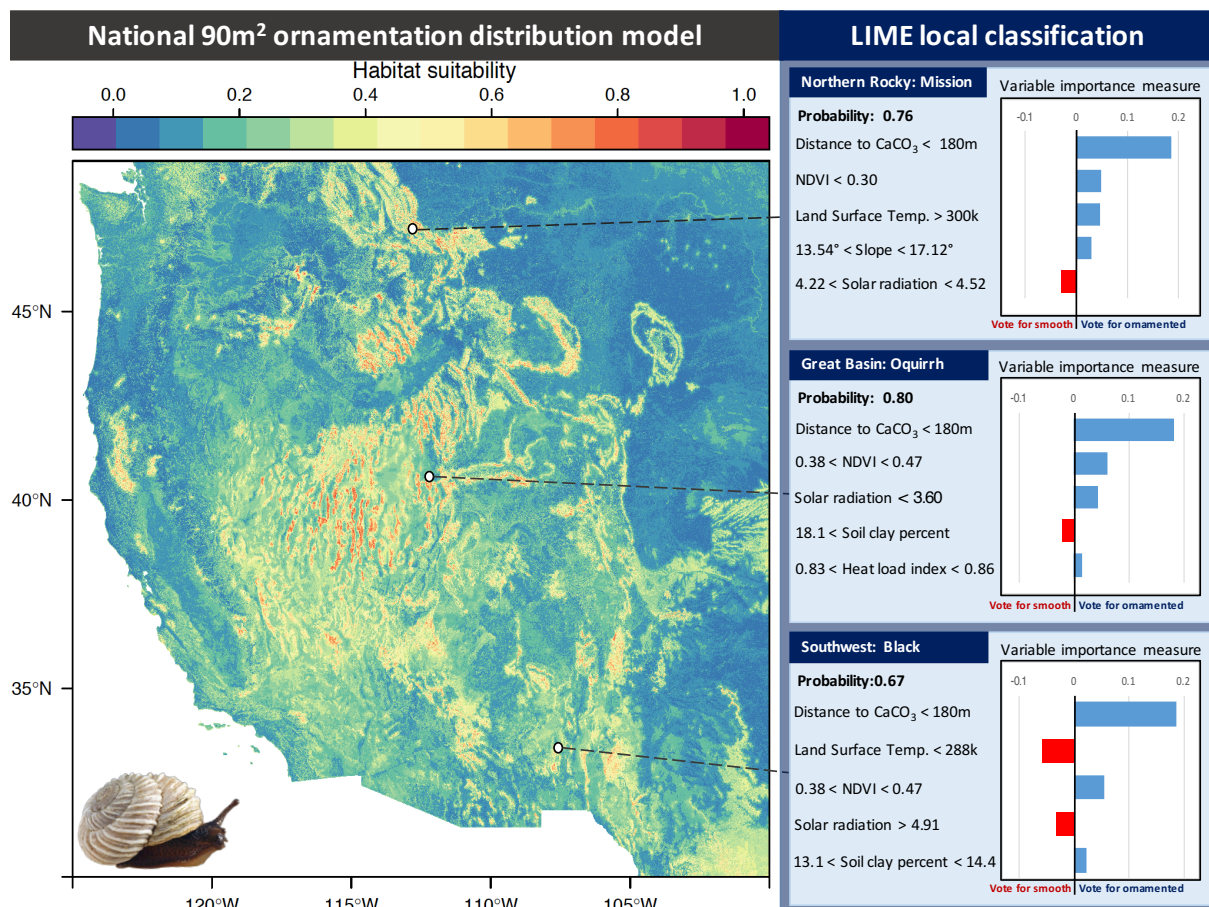


Figure 1: Ornamented Random-Forest (RF) distributional model at 90m² resolution and LIME local classifications for mountain ranges within the Rocky Mountain North, Great Basin, and Southwest regions. Local probability and variable importance metrics are derived from the ornamentation classification RF model. Photo credit: Richard Salisbury, College of Idaho.

Figure 2:

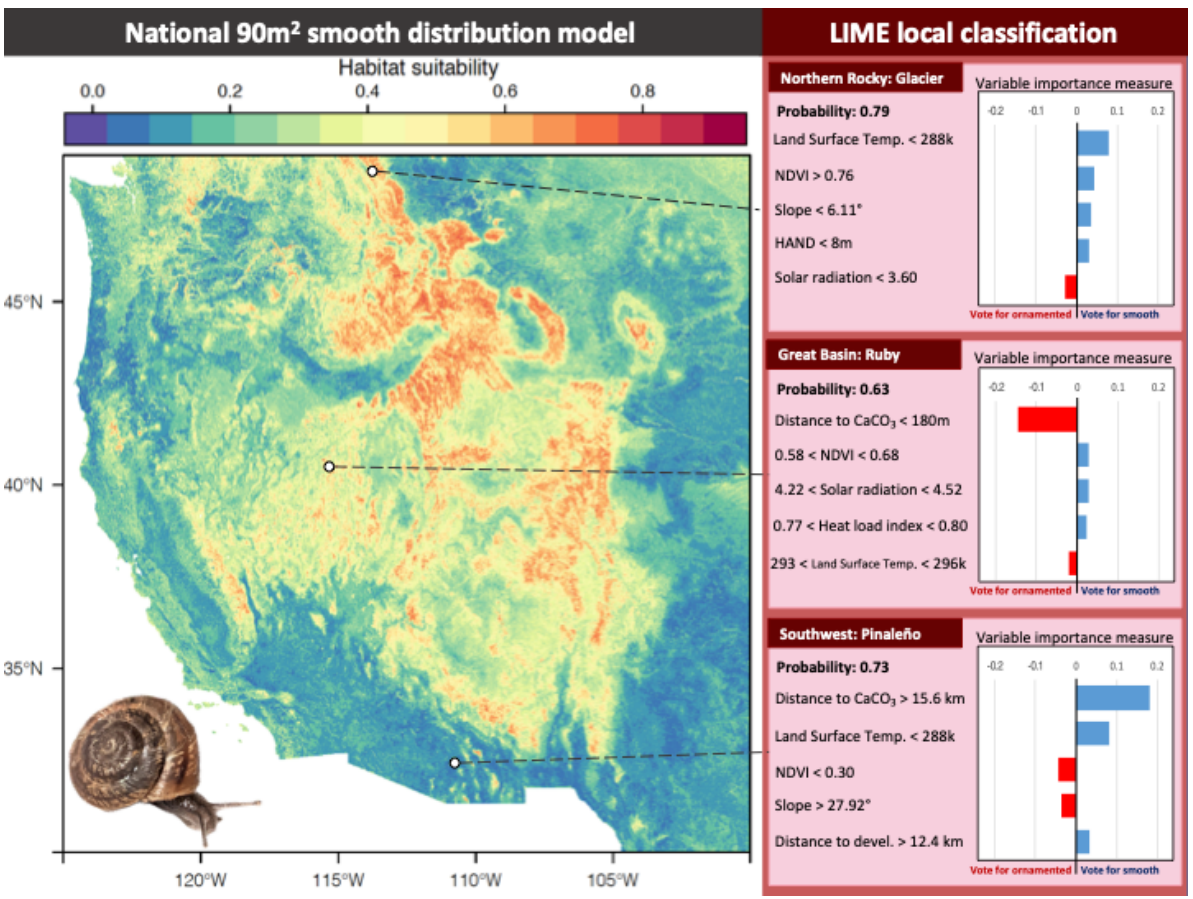


Figure 2: Smooth Random-Forest (RF) distributional model at 90m² resolution and LIME local classifications for mountain ranges within the Rocky Mountain North, Great Basin, and Southwest regions. Local probability and variable importance metrics are derived from the ornamentation classification RF model. Photo credit: Jeff Sorenson, AZ Game and Fish.

increased model accuracy for classification models, there was no clear pattern of predictor resolution on distribution model performance (Table 2).

Variable importance and partial dependence plots

For all dataset resolutions, study areas, and models of ornamented *Oreohelix* expression (classification or distribution models), distance from CaCO₃ rock was the most important predictor (Table 2, Figure 3). This pattern was consistent across permutations of the RF model and significant (Table 2). Partial dependence plots of the RF ornamentation classification model showed a declining ornamentation probability with greater distance from CaCO₃ rock but a reduction in the slope of decline as resolution increased (Figure 4). Ornamented distributional model partial dependence plots mirrored the classification model plots with decreasing ornamentation probability as distance to CaCO₃ rock increased. Resolution appeared to have minimal effect on variable importance.

Distance to CaCO₃ rock was also an important and significant variable for classification (Table 3) and distribution models (Supplementary Material Table 3) of smooth *Oreohelix* but less so than elevation (Supplemental 3) for smooth form distributional models. Distance to CaCO₃ rock was also the most important variable for smooth WorldClim distribution models (Supplementary Material Table 3). Smooth *Oreohelix* partial dependence plots indicated that smooth form classification probability increased with increasing distance to CaCO₃ rock but increased with closer proximity to CaCO₃ rock for distributional models (Figure 4). However, the declining probability of smooth form with increasing distance to CaCO₃ rock was minimal compared to ornamented species distribution models except for WorldClim models (Figure 4). This pattern was consistent across resolution sets.

All other predictors significantly contributed to classification or distributional models. The top five predictors changed across models but distance to CaCO₃ rock, NDVI, July mean surface temperature, and elevation were consistently in the top five (Table 1) for ornamentation or smooth form distributional or classification models. Variables important for ornamentation classification were generally also important in smooth form and ornamented distribution models (Supplementary Material Table 1).

Local classification of *Oreohelix* sites by LIME (Figures 1 and 2) revealed that distance to CaCO₃ rock is the most important variable for local classification of *Oreohelix* sites and that decreased distance leads to greater probability of ornamentation classification across

Predictor	Variable Importance			
	90m ²	250m ²	1km ²	1km ² WC
Soil ph	26.38	20.84	17.45	-
Soil clay content	18.31	19.79	18.16	-
Horizontal distance to nearest drainage	24.53	24.92	16.59	-
Height above nearest drainage	19.27	22.59	16.39	-
Compound topographic index	5.17	14.04	9.17	-
Global Horizontal Irradiance	33.66	34.59	37.45	-
Heat load index	-1.34	0.14	2.96	-
Slope	22.60	15.83	19.44	-
Elevation	28.92	31.87	27.66	-
Normalized Difference Vegetation Index	34.06	33.49	31.90	-
July Mean Land Surface Temperature	23.54	30.46	23.86	-
Distance to developed area	8.19	12.69	8.25	-
Distance to calcareous rock	52.61	55.85	55.83	69.33
WorldClim Annual Mean Temperature	-	-	-	44.36
WorldClim Isothermality	-	-	-	43.81
WorldClim Temperature Annual Range	-	-	-	49.82
WorldClim Mean Annual Precipitation	-	-	-	31.62
WorldClim Mean Temperature of Wettest Quarter	-	-	-	38.71
WorldClim Mean Temperature of Driest Quarter	-	-	-	62.07
WorldClim Precipitation Seasonality	-	-	-	36.26
WorldClim Precipitation of Driest Quarter	-	-	-	36.66
WorldClim Precipitation of Warmest Quarter	-	-	-	43.25

Table 1: MDA variable importance measures for Random-Forest classification models at different predictor resolutions. Predictors in bold are the most important predictors for that classification set.

Model	Model Accuracy (TSS)			
	90m²	250m²	1km²	1km² WC
RF classification	0.62 / 0.52	0.60 / 0.59	0.59 / 0.55	0.64 / 0.58
RF ornamented distribution	0.66 / 0.57	0.66 / 0.65	0.69 / 0.65	0.75 / 0.72
RF smooth distribution	0.58 / 0.55	0.58 / 0.59	0.58 / 0.57	0.67 / 0.66

Table 2: True-skill statistic accuracy for Random-Forest classification and distributional models at different predictor resolutions. Models including the distance to CaCO₃ rock layer are the first value in the row followed by models that omitted this predictor.

subregions. Ornamentation also appeared to be mildly associated with warmer surface temperatures, moderate solar radiation, and less claylike soils at local sites, though these contributed relatively little to local classification compared to distance to CaCO₃ rock (Figure 1).

Ornamentation expression, biomineralization effort, and shell strength

Size standardized mass was significantly greater for all ornamented types except the keeled form when compared to smooth forms residing on non-limestone rock (Figure 3, Supplementary Material Table 5). Size standardized mass was also greater for smooth limestone populations compared to non-limestone smooth populations (Figure 3, Supplementary Material Table 5). Mass standardized shell strength was greater for all ornamented types than smooth forms except those smooth forms that were limestone residents (Figure 3, Supplementary Material Table 6).

Discussion:

In this study, we examined whether access to calcareous rock was associated with shell ornaments in the Mountainsnails (*Oreohelix*) and if shell ornaments represent greater biomineralization investment compared to smooth forms. We found that, across all models and spatial resolutions (90m²–1km²), ornamentation was associated with proximity to CaCO₃ rock and that distance to CaCO₃ rock was the most important variable for either classification or distributional models. The ornamented forms in this study were also found to have greater size standardized shell mass compared to smooth forms (except for keeled forms), indicating that most ornamented shells were thicker and required more material to produce than a smooth form of the same size. All of these results support the hypothesis that greater biomineralization effort in *Oreohelix* is associated with CaCO₃ rich regions and indicate a possible physiological connection of CaCO₃ availability and *Oreohelix* shell biomineralization.

Previous studies of land snail ornamentation and geology have either found no association with geology (Welter-Schultes 2010), or largely focused on the preponderance of keeled forms at karst sites and the possible functional benefit that a slimmer profile may have for accessing narrow refuge sites common in karst landscapes (Alonso et al. 1985, Teshima et al. 2003). In *Oreohelix*, ornamented forms can be of a variety of shell shapes and are all commonly associated with CaCO₃ rock sites (median distance to CaCO₃ rock = 0 for ornamented forms in our dataset, Supplementary Material Table 7). This pattern indicates an association of

Figure 3:

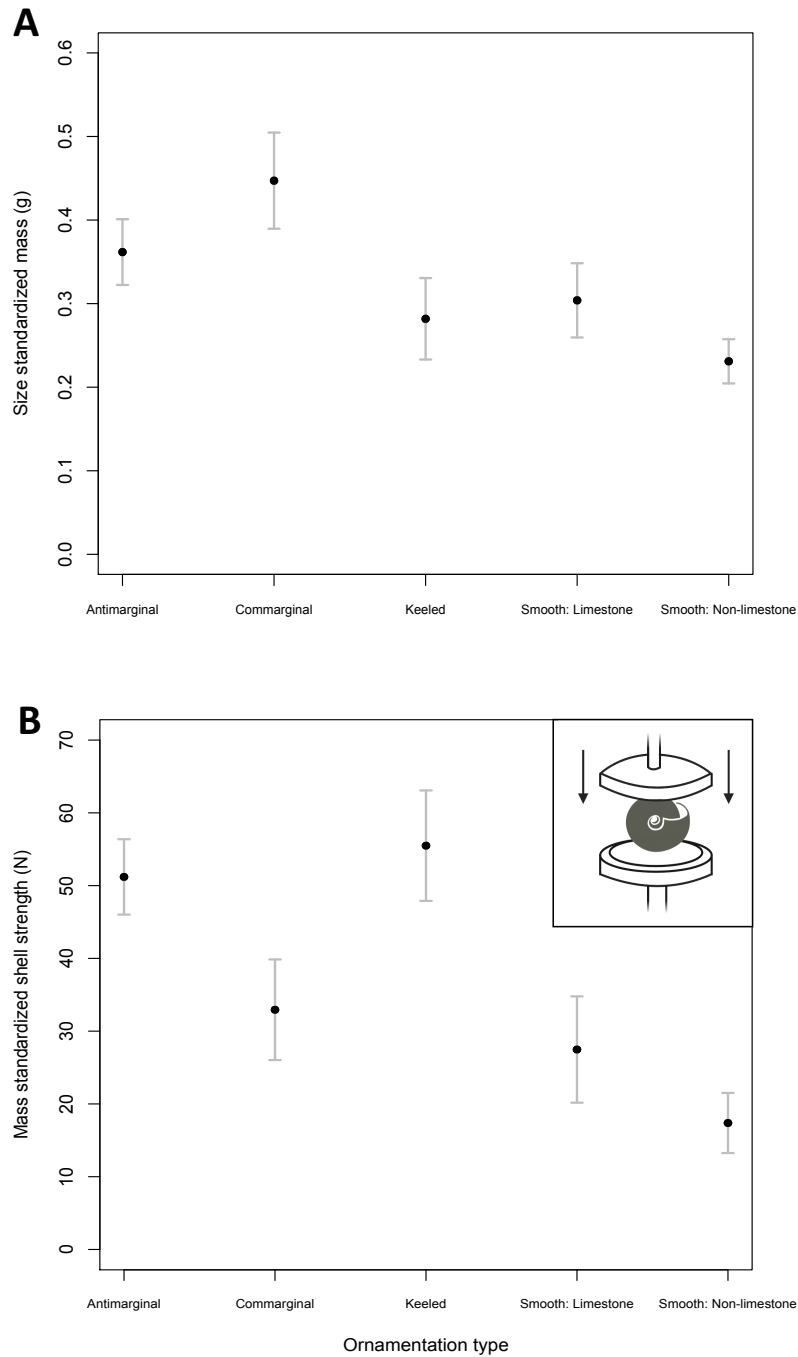


Figure 3: Standardized biometric and peak force measurements for major ornamented shell types. A: Mean and 95% confidence intervals of size standardized shell mass after effects of shell height and width were removed. B: Mean and 95% confidence intervals of mass standardized force required for crushing after the effect of shell mass was removed. Inset depicts orientation of shell and direction of load applied during crushing.

Figure 4:

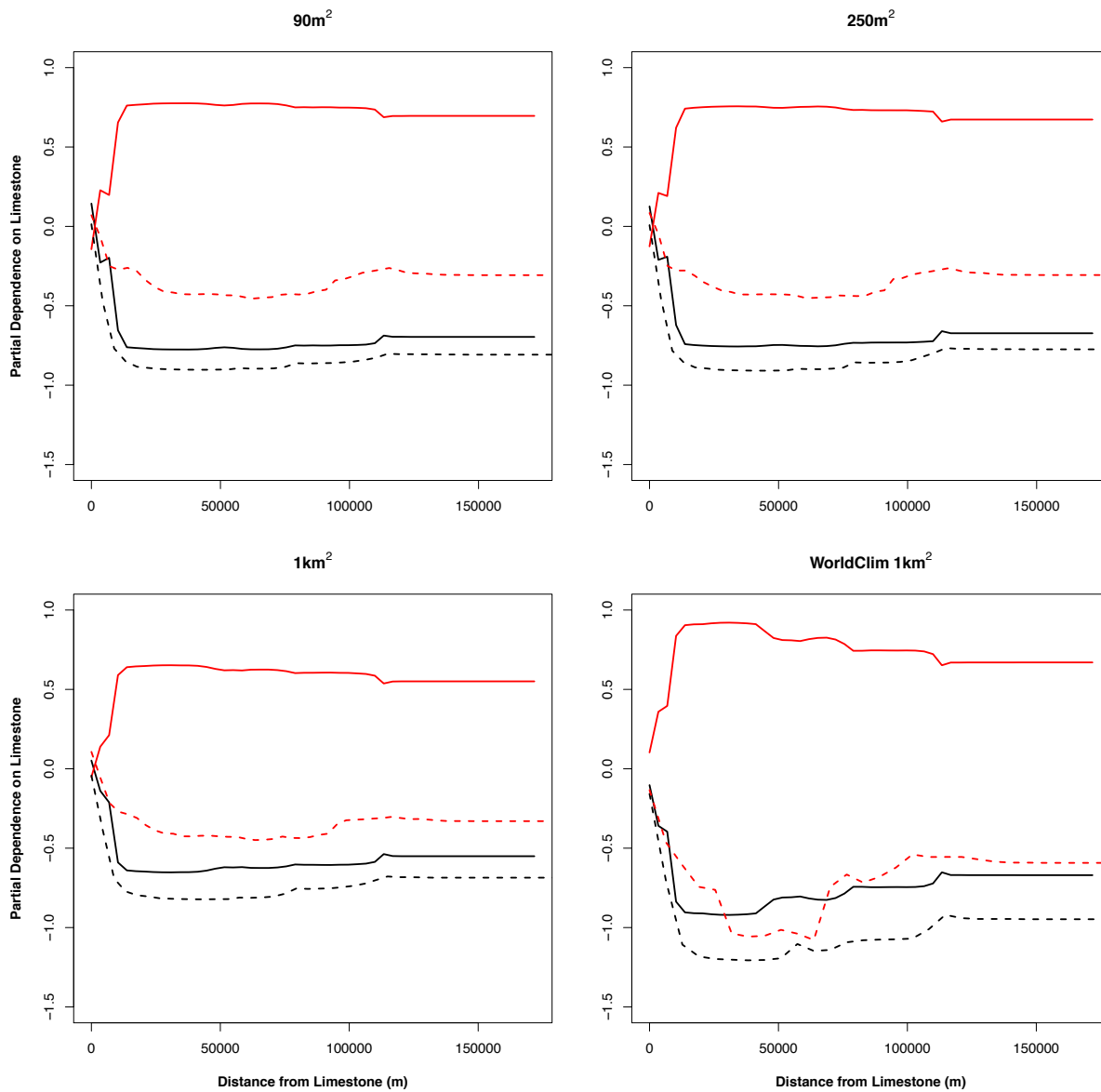


Figure 4: Partial dependence plot of distance to CaCO₃ rock on ornamented classification and distribution models. Negative values indicate classification probability of the focal class decreases vice versa for positive values. Solid lines denote ornamentation classification models and dotted lines distributional models. Black lines depict ornamented classification or presence response with distance to CaCO₃ rock and red lines indicate smooth classification or presence.

ornamentation with other qualities of CaCO₃ rock sites across Western North America besides topography. Given the relationship of CaCO₃ availability and biomineralization effort in aquatic molluscs (Waldbusser 2010, Watson et al. 2012), and the higher biomineralization effort and strong association of ornamentation with CaCO₃ rock in *Oreohelix*, we propose that CaCO₃ availability generally constrains biomineralization effort in *Oreohelix*. We also suggest that spatial variation in CaCO₃ availability may play a larger role in shaping patterns of land snail biomineralization expression than has been previously recognized.

Ornamented forms were also generally stronger per unit mass when crushed laterally, which suggests that ornamentation has a distinct functional benefit whose importance remains to be assessed in natural populations. Many *Oreohelix* populations have noticeable frequencies of repair scars from shell breakage (Pilsbry 1939, Frest and Johannes 1997), which indicates crushing may be a substantial agent of selection for some members of this group. Other functional benefits of ornamentation expression that have been identified in other semi-arid land snail groups, such as increased convective cooling and water retention (Giokas 2008), may also be at play in *Oreohelix*. When taken in the context of the spatial patterns of ornamentation expression identified in this study, ornamentation in *Oreohelix* appears to represent a resource constrained trait which may be a response to a variety of selective pressures.

An unexpected finding of this study is that keeled forms, while associated with proximity to CaCO₃ rock, do not appear to require significantly greater biomineralization effort for expression compared to smooth forms (Figure 4). This may be partly explained by selection for narrow refuges at karst sites (Alonso et al. 1985). However, that these forms are also the strongest when crushed laterally suggests it is possible to generate substantial increases in shell strength without commensurate biomineralization investment. This may partly explain the anecdotally reported higher frequency of keeled forms in land snails compared to other ornamented types (Goodfriend 1986), as the possible functional benefits and lower CaCO₃ requirements of keeled forms may facilitate the evolution of this form in weakly or non-calcareous environments (e.g. Stankowski 2013). Alternatively, the lower internal shell volume of keeled forms may limit body volume and represent a substantial cost (Graus 1974), a hypothesis worth evaluating but beyond the scope of this study.

The apparent exclusivity of ornamented forms to CaCO₃ rock areas and slight association of smooth forms to CaCO₃ rock areas suggest that ornamented forms are likely locally adapted to CaCO₃ rock areas and smooth forms have a more general preference. This finding has immediate applications for conservation agencies as threatened ornamented *Oreohelix* populations likely require access to CaCO₃ rock to persist. Limestone outcrops are some of the most at-risk sites from industrial mineral development for aggregate, cement, and agricultural applications (Che-Castaldo and Neel 2016). Disturbances to these sites from commercial industries (e.g., quarrying: Clements et al. 2006, road building: Frest and Johannes 1997, or grazing: Labaune and Magnin 2002) may change CaCO₃ dynamics locally by altering the biotic, geologic, or edaphic factors influencing shell form expression. Future conservation plans of ornamented *Oreohelix* need to factor in the habitat requirements identified in this study to better balance the requirements of these species with societal demands for carbonate rock.

A previous study highlighted that ornamented *Oreohelix* species are recently diverged from the closest geographic smooth form (Linscott et al. 2020). This pattern appears to be fairly common as many ornamented land snail and riverine species associated with CaCO₃ rock areas are often recently diverged from their sister smooth form species (Glaubrecht and Köhler 2004, Elejalde et al. 2008, Greve et al. 2010). Whether this is the result of phenotypic plasticity remains to be explored in many ornamented groups, but so far those examined have shown that ornamented species breed true to form in common garden conditions and ornamentation is heritable (Woodruff and Gould 1987, Elejalde et al. 2006). Future common garden and genomic studies of ornamented and smooth form species pairs are needed to determine whether ornamentation is heritable and if substantial genomic divergence accompanies ornamentation expression.

This is the first study, to the authors' knowledge, to propose that CaCO₃ availability modulates shell ornamentation expression in land snails. While it is likely that similar relationships exist in other land snail species, differences in land snail physiology and environmental conditions in species distributions may limit the applicability of our approach to other systems. For example, ornamentation expression in *Albinaria* does not always represent an increased investment in biomineralization (Giokas 2008) and may not require access to sites with higher CaCO₃ availability. CaCO₃ can also be deposited through aeolian sediments (Oerter and Amundson 2016), sea spray (Whipkey et al. 2002), or biotic processes

(Cailleau et al. 2011) which require in-situ field measurements and greater effort to interpolate and project spatially than the geologic maps used here. Species may also primarily meet their CaCO_3 requirements through either dietary (Fournie and Chetail 1984), soil (Charrier et al. 2013), or dissolved carbonate rock/shell absorption (Kado 1960, Appleton and Heeg 1999) which may vary in relative availability across sites. A final consideration is that strong selection for heavily biomineralized or ornamented forms (e.g. due to predation or insolation) may drive ornamentation expression without high levels of CaCO_3 availability, though this may require increased energy assimilation or reduced shell growth rate (Bourdeau 2010). Future studies should focus on determining how CaCO_3 dynamics influence biomineralization expression across ecosystems and clades so that we can understand how this resource contributes to the habitat requirements and morphological evolution of other biomineralizing species.

CHAPTER 3: Recognizing and predicting global patterns of mollusc ornamentation expression through machine-learning

Abstract:

Anthropogenic CO₂ emissions have caused a global decline of the saturation level of calcium carbonate (CaCO₃) minerals in marine environments, which has resulted in increased dissolution rates and calcification costs for biomineralizing organisms. A keystone group in almost all marine ecosystems, molluscs generally respond negatively to experimental ocean acidification manipulation but also demonstrate varying levels of tolerance for acidified conditions. One major axis of phenotypic variation that may be shaping mollusc species vulnerability to ocean acidification is the presence of elaborate shell sculpture that increases shell surface area and dissolution rates. However, there has been no broad-scale analysis of shell sculpture or ornamentation distribution in the context of carbonate chemistry at the species level. Here, we assess the extent that ornamented, smooth, and sea slug gastropods may be affected by ocean acidification using machine-vision models to morphotype all marine gastropod species images in the Global Biodiversity Information Facility database and comparing the projected distribution of classified species using Random-Forest species distribution models for current and future conditions under the RCP8.5 emission scenario. Accurate morphological classifications were generated for 16,897 gastropod species of which 658 had sufficient marine records for distribution modelling. All species were projected to experience suitability decline at observed sites and approximately 66% of all species were projected to lose 20% of their total projected area. Mean CaCO₃ mineral saturation state was the most important variable on average for ornamented species distribution model but had equal importance compared to smooth or slug gastropod morphotypes. Our findings place emphasis on the role of the carbon cycle in shaping mollusc species distribution and trait expression, and are consequential for predicting the fate of marine mollusc species under ocean acidification.

Introduction:

Anthropogenic CO₂ emissions have caused a global decline of calcium carbonate (CaCO₃) mineral saturation in marine environments, which has resulted in increased dissolution rates and calcification costs for biomineralizing organisms (Hurd et al. 2020, Figuerola et al. 2021). Range shifts (Simon-Nutbrown et al. 2020), population declines (Bednaršek et al.

2017), and morphological change (Barclay et al. 2019; Teixidó et al. 2020) has already been observed for many calcifying species in response to rapid ocean acidification, particularly in polar environments (Byrne et al. 2013; Mekkes et al. 2021; Neimi et al. 2021). At the current rate of ocean acidification, environmental conditions in the next century (ca. 2100) will be significantly harsher for marine calcifiers and may result in the extirpation or distributional shift of many keystone calcifying species (Terhaar et al. 2020). However, calcifying species response to ocean acidification is not uniform (Clark et al. 2020). Species vulnerability to ocean acidification is a result of a complex set of physiological, life-history, and morphological traits which may lead to a gamut of responses to ocean acidification (Clark et al. 2020; Figuerola et al. 2021). Despite their importance, we still do not fully understand how traits shape species vulnerability in different groups (Figuerola et al. 2021) - there is a need to quantify how different calcifying species traits may increase or decrease species vulnerability to ocean acidification to anticipate future climate impacts on species persistence.

A set of traits that are likely to impact calcifying species survival in acidified conditions are those that modify the available surface area available for dissolution (Barner et al. 2017). The amount of biomineralized surface area along with CaCO_3 saturation state of the environment (either in the form aragonite or calcite) are the primary parameters governing dissolution rate of calcified structures (Ries et al. 2016). CaCO_3 saturation state is modulated in marine environments by the availability of carbonate (CO_3^{2-}). In cooler waters such as the arctic or deep ocean, carbonate dissolves more easily which decreases the saturation state of CaCO_3 and increases shell dissolution rate (Clark et al. 2020). Conversely, carbonate does not dissolve as readily in warm waters resulting in greater CaCO_3 saturation state and greatly diminished shell dissolution. Given this pattern of CaCO_3 saturation state, it is not surprising that many calcifying taxa (e.g. molluscs (Watson et al. 2012), foraminifera (Boersma 1992), echinoderms (Watson et al. 2012); and brachiopods (Watson et al. 2012)) have evolved more elaborate and thickened biomineralized structures in highly supersaturated CaCO_3 regions and lower surface area to volume ratio structures in weakly saturated or undersaturated CaCO_3 habitats (Graus 1974). However, these spatial patterns of trait expression and resource availability have evolved over relatively long time frames compared to the rapid forecasted changes CaCO_3 saturation state predicted for the near future (Pelejero

et al. 2010). Species with higher calcified structure surface in warm water regions area may not have sufficient time to adapt to ongoing acidification compared to cold-water species that may be pre-adapted to low mineral availability and optimized for minimizing dissolution costs (Clarke 1993). Alternatively, cold water species may exist already at the lower end of tolerable conditions for marine calcifiers and may be pushed past the brink of suitable conditions under ocean acidification (Neime et al. 2021).

Molluscs, a keystone group in almost all marine ecosystems, generally respond negatively to experimental ocean acidification manipulation but also demonstrate varying levels of tolerance to acidified conditions (Rajan and Vengatesen 2020). While much of the variation in ocean acidification vulnerability between mollusc species is due in large part to different cellular and tissue physiological mechanisms underlying the calcification process between species (Clark 2020), a major component of phenotypic variation that may determine species vulnerability to ocean acidification is the presence of elaborate shell sculpture (e.g. external biomineralized extrusions of the shell such as spines, ribs, varices, and nodules) that increases shell surface area and dissolution rates (Flessa and Brown 1983). Past biogeographical studies have documented that the proportion of ornamented species depends on latitude and depth, with a higher proportion of ornamented species being associated with warm equatorial and shallower regions than cooler arctic and deep areas (Graus 1974, Clarke 1993, Watson et al. 2012). The close association between the spatial distribution of ornamentation expression and saturation state of CaCO_3 minerals has led past investigators to propose that ornamentation expression may be limited by CaCO_3 availability (Graus 1974, Watson et al. 2012). However, these studies have been limited either by sampling only a few sites or by studying only a single taxonomic group of molluscs across a wide range.

To quantify how shell ornamentation may contribute to mollusc species vulnerability to ocean acidification, we need to quantify how species with or without shell ornamentation are projected to respond to ocean acidification for as many species as possible across a global range. Here, we assess the extent that shell ornamentation influences mollusc vulnerability to ocean acidification in marine gastropods globally. We used machine-vision models to morphotype all marine gastropod species images in the Global Biodiversity Information Facility (GBIF) database and compared the projected distribution of classified species using Random-Forest species distribution models for current and future conditions under the RCP8.5

emission scenario (Assis et al. 2018). Our approach enabled us to identify: (1) the distribution of ornamentation across taxonomic groups; (2) habitat variables associated with ornamented, smooth, and sea slug species distribution; (3) any differences in climate vulnerability between ornamented and non-ornamented gastropods; and (4) regions likely to experience significant gastropod species decline. Together, we synthesize this information to understand how ornamentation expression may contribute to gastropod species vulnerability to ocean acidification.

Materials and Methods:

Machine vision approach and morphological classification

Images used for developing and applying machine-vision models came from publicly available biological repositories and machine-vision image datasets. To develop machine-vision models, it is best practice to have a diverse set of annotated target images to train for positive detections and a number of background images of non-target objects to train the model to avoid false positive detections (Bochkovski et al. 2020). The training dataset images used for developing machine-vision models were taken randomly from the Global Biodiversity Information Facility (GBIF) images available for gastropods along with an equal number of non-gastropods images for background images (gastropod doi: 10.15468/dl.6nr29f; non-gastropods doi: 10.15468/dl.ejnwzr). Coral and rocks images without gastropods were also taken from the ImageNet database to supplement sampled GBIF background images (Deng et al. 2009). Images containing gastropods were annotated by malacological experts into slug, smooth, and ornamented types using DarkMark (<https://www.coderun.ca/darkmark/>) in YOLOv4 format for training. Any land or sea slug were classified as a slug while any sculptured gastropod were classified as ornamented based on expert knowledge (Figure 1). A total of 17,220 images which contained 2278 slugs, 4105 ornamented, 5182 smooth form gastropods and 8,829 non-gastropod background images were then used for machine-vision model development. Twenty percent of all images were withheld during training (3,444) and used for evaluating model performance.

We utilized the YOLOv4 framework for detecting and classifying gastropods in images (Bochkovski et al. 2020). YOLOv4 is a single-shot object detector which has been shown to achieve the highest performance in terms of accuracy and speed on the benchmark COCO image dataset (Wang et al. 2020). Parameters were then chosen to train YOLOv4 models on a

Nvidia Titan RTX using the following modified settings in addition to default anchors and image augmentations: filters size of 24, batch size of 64, subdivisions number of 16, and non-maximal suppression calibrated using distance intersect-over-union (Zheng et al. 2020). Training was performed over sufficient iterations to maximize mean average precision (mAP) and F1-scores of the validation dataset to avoid overtraining (Bochkovskiy et al. 2020). Precision measures the proportion of true-positives over the true-positives plus false-positives and recall is the proportion of true-positives over true-positives plus false-negatives. Average precision summarizes the precision-recall curve for each class by taking the average of precision values measured over a series of recall values (0.1, 0.2, ... 1). mAP is the mean of average precision values across all object classes. A true-positive was scored only if the training bounding-box had at least 0.5 intersect-over-union (IoU) with the detection bounding box. The F1-score is the harmonic mean between precision and recall and is commonly reported along with mAP. The best performing model in terms of mAP and F1-scores on the whole evaluation was then used to detect and classify gastropod images in subsequent analyses. Museum type images and citizen-science images were also evaluated separately to determine how the detector performs on these two different types of data.

We applied the gastropod object detector on a combined image dataset composed of all imaged gastropod molluscs on GBIF (accessed on March 2, 2021; doi: 10.15468/dl.6nr29f), the Academy of Natural Sciences (<http://clade.ansp.org/malacology>) type image dataset, and the Mollusca Types in Great Britain (<https://gbmolluscatypes.ac.uk/>) type image collection, the latter two are only partially available on GBIF at the time of this study. Detections were counted at the species level for type images and non-type images separately for each of the three classes (slug, ornamented, smooth) if the detector had a confidence score greater than 70%. Species with a minimum of three detections and a majority of type images with detections into one category were classified as the majority type. For species without type images, species were classified only if more than 70% of the detections were in one category and if at least seven detections were present for that species. We chose a minimum of three detections for type images as many mollusc shells are often only photographed in three perspectives (aperture facing, apex, basal). A more stringent threshold was chosen for citizen-science images based on differences in object detector performance between type images and citizen-science images (see Results section below).

Distribution data and predictor variables

All classified species were mined for occurrence data from GBIF (accessed on April 4, 2021; doi:). Records were filtered using CoordinateCleaner (Zizka et al. 2019) in R v.4.0.5 (R core team 2021) to remove records associated with capitals, country and province centroids, biodiversity institutions localities, identical latitude and longitude, geographic outlier coordinates, and only keeping those found in the ocean. Duplicate species records within 5 arc-minutes of each other were removed to match predictor variable resolution. Species with a minimum of 25 occurrence records were retained for distribution modelling as this is the minimum number of records for highly prevalent species (van Proosdij et al. 2016) and species prevalence is unknown for many of the mollusc species in this study. A random sampling of background points equal to 10 times the number of occurrence records were used in distribution models.

Predictor variables were chosen based on their known association with gastropod species distributions and whether projections were available for future conditions (Table 3). Bathymetry was taken from the GEBCO global bathymetric layer and used to generate roughness, northness, eastness, and slope using ArcGIS Pro 2.7.0 (gebcoscientists.com/data_and_products/gridded_bathymetry_data/). Seafloor temperature, current velocity, salinity, and oxygen were taken from Bio-ORACLE v.2.0 (Assis et al. 2018) for current and future conditions under the RCP8.5 climate emission scenario. Seafloor aragonite saturation state was taken from the Marine Conservation Institute (Davies and Guinotte 2011) for current conditions and projected for future conditions by combining seafloor aragonite saturation state changes from 2000 - 2100 using the projected aragonite saturation state changes under the RCP8.5 emission scenario (<https://github.com/chiulinwei/SCC85/>). Predictors with greater than 0.7 Pearson correlation coefficient at present localities were dropped so that only one correlated predictor was present in the final dataset. This resulted in eight layers being retained for species distribution modelling: aragonite saturation state, current velocity, salinity, oxygen, depth, slope, eastness, and northness.

Species distribution models were constructed for all species using Random-forest classification (RF) in R (Breiman 2001). We chose to use RF as it can handle complex relationships between predictor variables and models can be generated quickly for a large number of species. RF models were tuned to try two variables at each split ($mtry=2$,

ntrees=500) after initial tuning using the 'rfTune' function (Liaw and Weiner 2002) subset of 50 species. As class imbalance in the training data can have substantial effects on RF model outputs (Barbet-Massin et al. 2012), we sampled an equal number of localities from the minority and majority classes from the full dataset equal to the total number of localities of the minority class when constructing each decision tree. Variable importance of each predictor was assessed through mean decrease in accuracy (MDA) and mean variable importance was compared across morphotypes using a one-way ANOVA. We measured out-of-bag error estimates for each species distribution model and retained all models with less than 10% out of bag error estimates for future projections.

Species distributions were then projected for current conditions and predicted conditions under the RCP8.5 climate emission scenario. To compare how species will respond to future climate change, we first measured home range suitability change by measuring the difference between predicted habitat suitability values for known occurrence points under current and future conditions. Current and future species ranges were then constructed using one standard deviation from the mean of the suitability values for occurrence points as a cut-off (Choe et al. 2016) for presence points. Differences in range size were assessed by dividing the total number of predicted present pixels under current conditions by the total number of present pixels predicted for future conditions. Home range suitability change and range size change were then compared across groups using a one-way ANOVA between groups and a linear model of habitat suitability/range change as a response variable and mean values of habitat variables morphotype groupings as categorical variables. In addition to the previous habitat variables used for species distribution models, we included latitude as a predictor variable for linear models of suitability/range change as most projected environmental differences are anticipated to affect higher latitudinal areas (Mekkes et al. 2021).

Results:

Morphological classification and occurrence data

The highest mAP on the validation dataset was achieved after 6400 iterations of training (84.13% for non-type images; 98.63% for type-images). F1-scores were 0.80 for non-type images and 0.94 for type images on the validation set. After 6400 iterations, mAP and F1-scores plateaued and began to decline which indicates overfitting, so the 6400 weights were used for gastropod classification. The difference in performance between data sources is likely

due to greater variation in lighting, focus, and specimen angle for non-type images compared to standardized photographic conditions for type-images. For this reason, type-image species classifications took precedence over non-type images for species classification.

Our approach resulted in the morphotyping of 837,158 images of 16,897 marine and non-marine gastropod species. Almost all species retained had detections entirely classified into one class (mean class detection ratio: 0.9507). Occurrence points were used to filter the classified species list to marine species by only retaining GBIF occurrences in the ocean, which resulted in 6,204 marine species from 329,551 localities. Further filtering by removing duplicated localities, those with missing data, and keeping only species with 25 or more occurrence points resulted in 658 species found at 58,624 localities.

Ornamentation was found to be widespread among marine gastropod families with 56% of all classified families having at least one ornamented member. Approximately 11.6% of all classified marine species were sea slugs, 25.3% were classified as smooth, and 63.1% as ornamented. This finding is consistent with previous broad scale studies that have found that ornamentation is common in marine environments (Vermeij 2015). The final filtered distribution dataset was composed of 153 slug species, 166 smooth species, and 339 ornamented species when available. Ornamentation occurrence points on average had significantly higher aragonite saturation state values than smooth forms (pairwise t-test; $p < 0.0001$, mean ornamented = 2.674, mean smooth = 2.338).

Distribution model performance and predictor importance

All species distribution models had lower than 10% out of bag error estimates (maximum 7.1%; mean 1.7%) and were used to project for current and future conditions. The predictor with the highest variable importance across all species distribution models was aragonite saturation state followed by oxygen availability and depth (Table 1). There were no significant differences in variable importance values between all morphotypes for aragonite saturation

Figure 1:

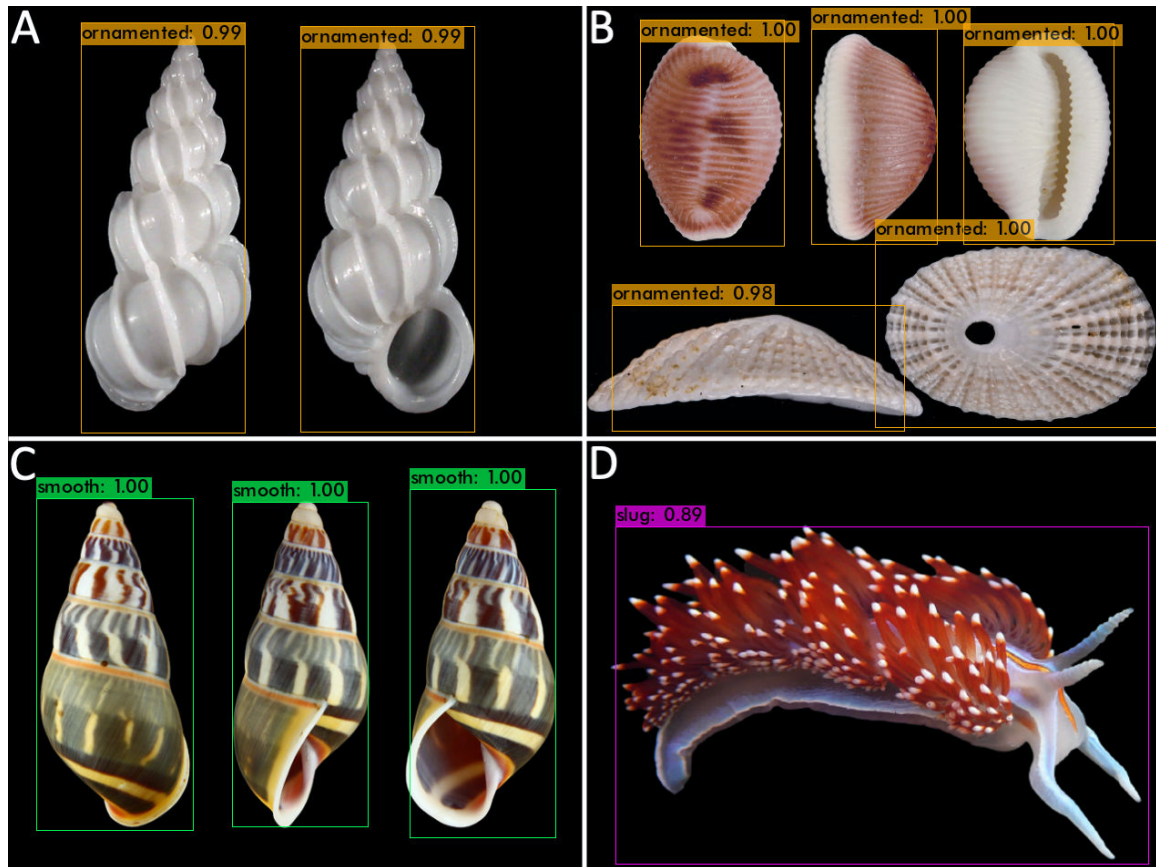


Figure 1: Example ornamented categories and detections by YOLOv4 object detector. A: The angled wentletrap (*Epitonium angulatum*), an example of an ornamented coiled gastropod. B: Weakly coiling ornamented limpets and cowrie forms. C: Representative smooth shelled species *Amphidromus everetti*. D: Example classification of a sea slug, *Hermisenda opalescens*. All photos were taken from Wikipedia commons and the Bailey Shell Musuem (Creative Commons License v. 4.0).

Table 1:

Variable	Ornamented	Slug	Smooth
Aragonite saturation state	21.24632	22.46859	22.93887
Depth	19.49906	18.48978	20.90301
Eastness	5.912727	6.612432	6.1414
Northness	6.398675	7.02695	7.03273
Oxygen	20.22003	21.06699	20.94406
Current velocity	9.254527	7.794025	9.742367
Salinity	15.50754	14.19834	15.52407
Slope	14.2649	12.91055	14.3656

Table 1: Random Forest Variable Importance of Gastropod Morphotypes.

Table 2:

Suitability Change Model	Estimate	SE	p
Intercept	5.50E-01	9.77E-02	2.64E-08
Aragonite Saturation State	-6.01E-02	1.69E-02	4.14E-04
Depth	6.86E-05	2.93E-05	1.94E-02
Oxygen	-2.08E+00	1.17E-01	< 2.00E-16
Current Velocity	1.24E+00	1.82E-01	2.70E-11
Salinity	-8.72E-03	2.73E-03	1.45E-03
Slope	1.76E-02	1.09E-02	1.00E-02
Morphotype(slug)	-3.17E-03	1.27E-02	7.10E-03
Morphotype(smooth)	-2.57E-02	1.17E-02	6.00E-02
Latitude	3.48E-03	6.14E-04	2.15E-08

Total Range Change Model	Estimate	SE	p
Intercept	6.65E-01	1.48E-01	6.55E-06
Aragonite Saturation State	-1.88E-01	2.56E-02	8.12E-13
Depth	2.19E-04	4.45E-05	1.09E-06
Oxygen	-3.55E+00	1.78E-01	< 2.00E-16
Current Velocity	1.48E+00	2.77E-02	1.24E-07
Salinity	-2.67E-03	4.14E-03	5.19E-03
Slope	2.75E-02	1.65E-02	9.60E-03
Morphotype(slug)	-4.36E-03	1.92E-02	9.81E-01
Morphotype(smooth)	-4.06E-02	1.77E-02	9.00E-02
Latitude	-6.73E-03	9.32E-04	1.16E-12

Table 2: Regression model outputs for habitat suitability and range change models. Bold values correspond to significant predictors at an alpha values of 0.05.

state (Table 1). Partial dependence plots of aragonite saturation state were highly similar with increased presence classification probability plateauing over ~ 2.0 state and significantly declining below this value (Figure 2). Oxygen and bathymetry partial dependence plots were also highly similar across morphotypes with increased presence classification probability with shallower depth and increased oxygen availability (Supplemental Figures 1 and 2).

All species were projected to experience a mean decline in suitability across their known presence points under future ocean acidification conditions (mean suitability change = -0.27, minimum suitability decline = -0.01). Smooth species had much greater mean suitability decline compared to ornamented or slug species (smooth mean suitability change = -0.31, ornamented mean suitability change = -0.25, slug mean suitability change = -0.27). Smooth species were also projected to experience greater range declines than ornamented and slug species (smooth range mean range change = -53%, ornamented mean range change = -42%, slug range change = -43%).

Linear models of habitat suitability and range change indicated aragonite saturation state, salinity, current velocity, slope, depth, and latitude were significant predictors. Morphotypes were not significantly related to suitability or range decline when latitude was included in the model (Table 3). When latitude is removed as a predictor, smooth formed species have significantly greater negative regression coefficients than ornamented and slug gastropods, indicating greater suitability/range decline. As smooth form species generally occur at higher latitudes than slugs and ornamented marine gastropods (Table 1), latitude may be primarily responsible for any differences in suitability/range change between morphotypes and can be seen when we look at the spatial distribution of smooth form species decline (Figure 3).

Figure 2:

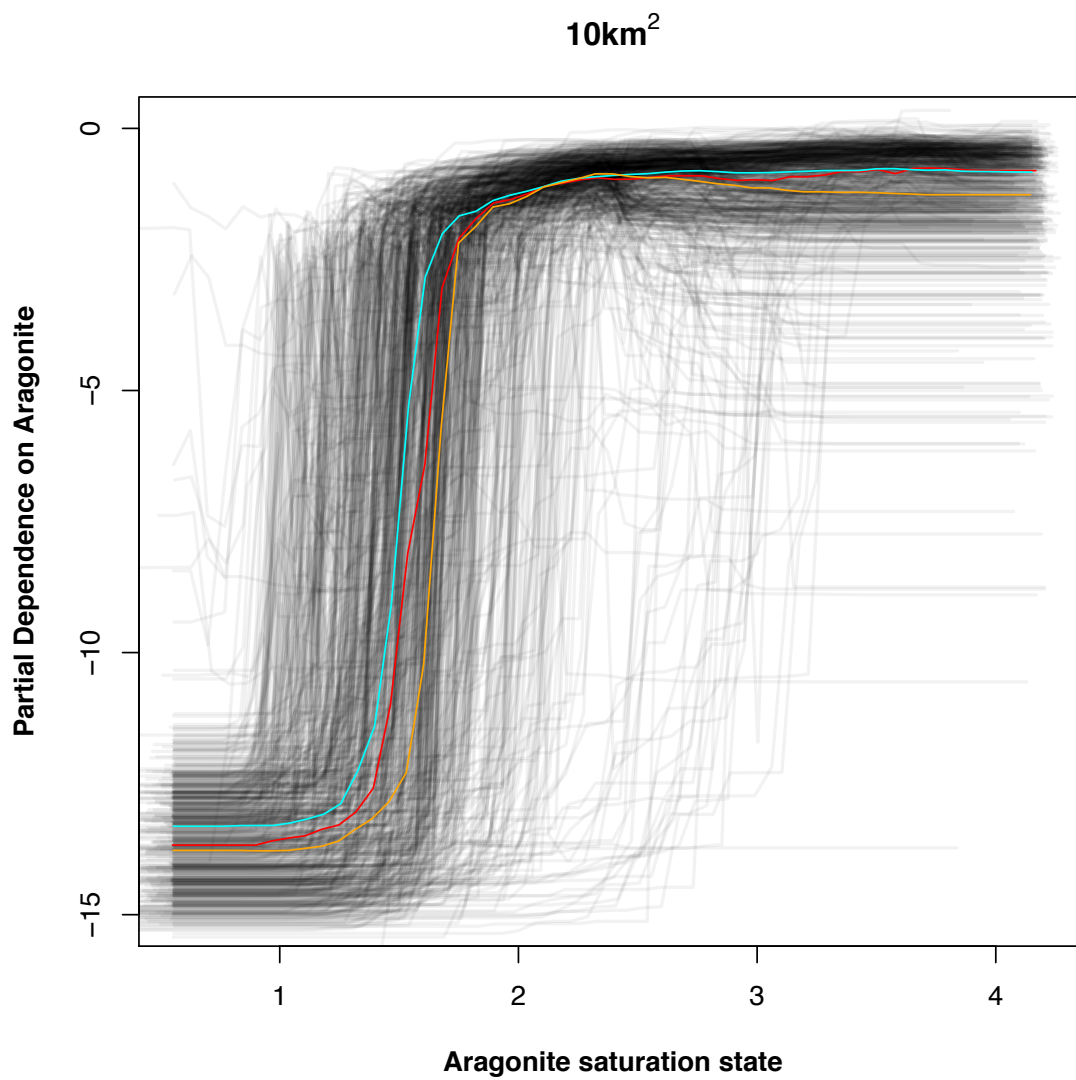


Figure 2: Partial dependence plot of aragonite saturation state and gastropod morphotype presence. Higher partial dependence values indicate higher likelihood for ornamentation classification. Colored lines depict median partial dependence lines for morphotype groups and black lines denote species. Cyan: ornamented; Red: smooth; Orange: sea slug.

Figure 3:

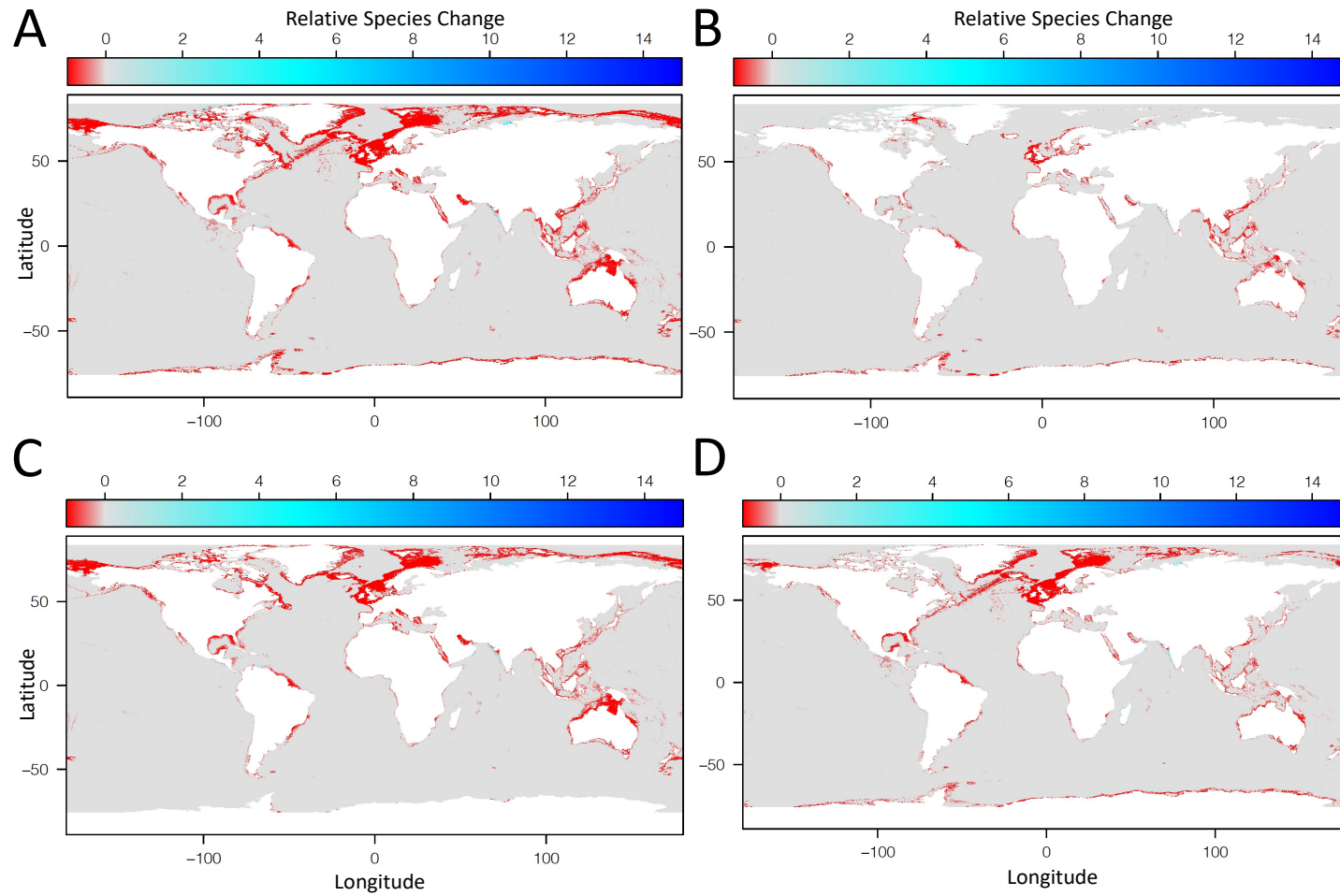


Figure 3: Relative species richness change from current to projected ocean acidification conditions. A: All species. B: Slug species. C: Ornamented species; D. Smooth species. Negative values correspond to fold change with -1 representing complete loss and 0 representing no change at a given pixel. Positive values corresponding to species richness gains for each fold.

Discussion:

Marine gastropods are a highly diverse group of species that display remarkable variation in their tolerance to experimental acidification (Rajan and Vengatesen 2020). Using machine-vision classification, we found that ornamentation is broadly distributed across marine gastropod families and are associated with higher CaCO_3 saturation states compared to smooth or slug species. We also found that CaCO_3 saturation state is the most important variable for explaining all morphotype distributions followed by oxygen content and bathymetry. Our global scale models predict very similar response curves across morphotypes, with no significant differences in variable importance between species groups.

Gastropod species are generally projected to decline severely under future ocean acidification with the greatest declines being observed for polar species. We also find that ornamented species are not predicted to experience any more severe decline in their ancestral range or in their total projected area than smooth or sea slug gastropod species. Overall, our global scale model suggests that latitudinal position, and not morphology, is the primary driver of species decline under the RCP 8.5 emission scenario.

Classification of gastropod species

Our machine-vision model was highly accurate and performed well across a range of image types and photographic settings. Ornamentation was found to be widespread among marine gastropod families and composed the vast majority of marine species classified by the machine vision model. The high percentage (63.1%) of ornamented marine species is in line with other studies that have documented that sculpture is common to marine gastropods (Vermeij 2015). Our approach may even have underestimated the true number of ornamented species on GBIF as species that are polymorphic for ornamentation are generally excluded due to our filtering threshold for species morphotype classification. Species numbers for sea slugs are also likely underestimated as these species are not well represented in museum collections as they are in citizen-science images, which the machine-vision model does not perform as well on. Overall, our approach represents a significant step forward for phenomic dataset generation for gastropods and can serve as a future starting point for future ornamentation classification by ornamentation types (e.g. spined, ribs, varices).

CaCO_3 saturation and ornamentation expression

Many regional and taxonomically focused studies have documented clines in ornamentation frequency from regions of elevated to lower CaCO_3 saturation (Graus 1974). Similarly, small-scale studies covering the breadth of single shelves have found that ornamentation is expressed at higher frequency in the 0 – 200 meter depth range but swiftly declines thereafter (Etter and Rex 1990). These patterns suggest that ornamentation expression can change quickly over relatively small areas and between regional environments.

In this study, we find ornamentation occurrence points on average have significantly higher aragonite saturation state values than smooth forms. However, this pattern does not translate to differences in aragonite saturation state response curves in our species distribution models or greater aragonite saturation state variable importance compared to smooth form species distribution models. This pattern could be interpreted as ornamented species distributions not being primarily limited by CaCO_3 saturation state and may be primarily determined by another factor not sampled in this study. Two major alternative hypotheses is that ornamentation expression is primarily driven by increased interactions with shell crushing predators (Vermeij 1978; Vermeij 1995) or by temperature constraints of metabolism (Clarke 1993; Watson et al. 2012). Testing these hypotheses is beyond the scope of this study and should be a focus of future work.

Another reason for the differences between the aforementioned small scale studies and the global scale model of this study is that our approach may not be appropriate for addressing fine scale patterns which may dominate ornamented species distributions. As our study is limited in resolution to $\sim 10\text{km}^2$ pixels, we may not be fully capturing the small-scale differences in species distributions which are common to previous ornamentation distribution studies. Furthermore, the restriction of only creating species distribution models of species with a minimum of 25 non-overlapping occurrences may bias our sampling to species of relatively large species distribution ranges (minimum 250km^2). This number could be relaxed as very few marine gastropod species are likely to have high prevalence globally and is more likely that any highly prevalent species would possess at least 25 occurrences in the final dataset. Future studies should focus on testing whether ornamented species distribution models have different response curves from smooth distribution models using higher resolution predictor datasets, possibly for smaller subregions where existing datasets may be available (e.g. Rodríguez-Basalo et al. 2021).

Future distributional changes and home range suitability

Under the RCP 8.5 climate emission scenario, almost all species were projected to decline in suitable area with more than 66% of species projected to lose more than 20% suitable area by the year 2100. Additionally, more than 43% of species were projected to experience mean suitability declines over 20% **over** known occurrence sites by the year 2100. Species richness decline appears to be concentrated in polar environments for shelled gastropods but is also prevalent in other latitudinal regions (Figure 3). Overall, our models depict a bleak outlook for gastropod species distribution and indicate that they may decline severely globally if they do not adapt to new conditions or if there are no curbs to anthropogenic emissions as has been indicated for another biomineralizing groups (Simon-Nutbrown et al. 2020) .

The species most affected by ocean acidification were those currently located in polar environments (see Results). Higher declines of smooth species compared to other morphotype categories was revealed in our regression analyses to be primarily the result of latitudinal differences between ornamented/slugs and smooth morphotypes. Once latitude was included in the model for habitat suitability or range change, no differences in decline between morphotypes could be established. This result is in agreement with other studies of climate change on marine species which have documented that the most affected regions are those with the greatest magnitude of change (i.e. polar environments). However, that there are no differences in habitat suitability decline or projected range change between ornamented, smooth, and sea slug morphotypes is surprising given the purported specialization of ornamented gastropods to areas with high CaCO_3 saturation state or a high density of predators and the relatively narrower ecological breadth of sea slugs compared to gastropods in general (Wägele and Klusmann-Kolb 2005). This may indicate the full suite of environmental variation present in small-scale studies is not covered at the grain-size of our distribution models (see above) or that gastropod morphotypes share common environmental constraints on their distributions which are altered under future ocean acidification conditions. Together, our results suggest that latitude is the primary determinant of species vulnerability to ocean acidification and not species traits.

References:

1. Allouche O, Tsoar A, Kadmon R (2006) Assessing the accuracy of species distribution models: prevalence, kappa and the true skill statistic (TSS). *Journal of Applied Ecology* 43:1223–1232. <https://doi.org/10.1111/j.1365-2664.2006.01214.x>
2. Alonso MR, López-Alcántara A, Rivas P, Ibáñez M (1985) A biogeographic study of *Iberus gualtierianus* (L.)(Pulmonata: Helicidae). *Soosiana* 13:1–10
3. Alonso MR, López-Alcántara A, Rivas P, Ibáñez M (1985) A biogeographic study of *Iberus gualtierianus* (L.)(Pulmonata: Helicidae). *Soosiana* 13:1–10.
4. Assis J, Tyberghein L, Bosch S, et al (2018) Bio-ORACLE v2.0: Extending marine data layers for bioclimatic modelling. *Global Ecology and Biogeography* 27:277–284. <https://doi.org/10.1111/geb.12693>
5. Barbet-Massin M, Jiguet F, Albert CH, Thuiller W (2012) Selecting pseudo-absences for species distribution models: how, where and how many? *Methods in Ecology and Evolution* 3:327–338. <https://doi.org/10.1111/j.2041-210X.2011.00172.x>
6. Barclay K, Gaylord B, Jellison B, et al (2019) Variation in the effects of ocean acidification on shell growth and strength in two intertidal gastropods. *Mar Ecol Prog Ser* 626:109–121. <https://doi.org/10.3354/meps13056>
7. Barker GM (2004) *Natural Enemies of Terrestrial Molluscs*. CABI
8. Barner AK, Chan F, Hettlinger A, et al (2018) Generality in multispecies responses to ocean acidification revealed through multiple hypothesis testing. *Global Change Biology* 24:4464–4477. <https://doi.org/10.1111/gcb.14372>
9. Baskin JM, Baskin CC (1988) Endemism in Rock Outcrop Plant Communities of Unglaciated Eastern United States: An Evaluation of the Roles of the Edaphic, Genetic and Light Factors. *Journal of Biogeography* 15:829. doi: 10.2307/2845343
10. Bauer LJ (1989) Moorland Beetle Communities on Limestone `Habitat Islands. I. Isolation, Invasion and Local Species Diversity in Carabids and Staphylinids. *The Journal of Animal Ecology* 58:1077. doi: 10.2307/5143
11. Bednaršek N, Feely RA, Tolimieri N, et al (2017) Exposure history determines pteropod vulnerability to ocean acidification along the US West Coast. *Sci Rep* 7:4526. <https://doi.org/10.1038/s41598-017-03934-z>

12. Bochkovskiy A, Wang C-Y, Liao H-YM (2020) YOLOv4: Optimal Speed and Accuracy of Object Detection. arXiv:200410934 [cs, eess]
13. Boersma A (1998) 2 - Foraminifera. In: Haq BU, Boersma A (eds) Introduction to Marine Micropaleontology (Second Edition). Elsevier Science B.V., Amsterdam, pp 19–77
14. Boettger (1932) Die funktionelle Bedeutung der Rippung bei Landschneckengehäusen. Zoologischer Anzeiger 98:209–213
15. Bourdeau PE (2010) An inducible morphological defence is a passive by-product of behaviour in a marine snail. Proc R Soc B 277:455–462.
<https://doi.org/10.1098/rspb.2009.1295>
16. Breiman L (2001) Random Forests. Machine Learning 45:5–32.
<https://doi.org/10.1023/A:1010933404324>
17. Brunfeldt SJ, Sullivan J, Soltis DE, Soltis PS (2001) Comparative phylogeography of northwestern North America: a synthesis. Special Publication-British Ecological Society, 14, 319-340.
18. Burbrink FT, Yao H, Ingrasci M, Bryson Jr RW, Guiher TJ, Ruane S (2011) Speciation at the Mogollon Rim in the Arizona Mountain Kingsnake (*Lampropeltis pyromelana*). Molecular Phylogenetics and Evolution, 60(3), 445-454.
[doi:10.1016/j.ympev.2011.05.009](https://doi.org/10.1016/j.ympev.2011.05.009)
19. Burke TE, Leonard WP (2013) Land snails and slugs of the Pacific Northwest. Oregon State University Press, Corvallis, OR.
20. Bush AM, Pruss SB (2013) Theoretical Ecospace for Ecosystem Paleobiology: Energy, Nutrients, Biominerals, and Macroevolution. The Paleontological Society Papers 19:1–20. <https://doi.org/10.1017/S1089332600002667>
21. Byrne M, Lamare M, Winter D, et al (2013) The stunting effect of a high CO₂ ocean on calcification and development in sea urchin larvae, a synthesis from the tropics to the poles. Philosophical Transactions of the Royal Society B: Biological Sciences 368:20120439. <https://doi.org/10.1098/rstb.2012.0439>
22. Cailleau G, Braissant O, Verrecchia EP (2011) Turning sunlight into stone: the oxalate-carbonate pathway in a tropical tree ecosystem. Biogeosciences 8:1755–1767.
<https://doi.org/10.5194/bg-8-1755-2011>

23. Camp EF, Nitschke MR, Rodolfo-Metalpa R, et al (2017) Reef-building corals thrive within hot-acidified and deoxygenated waters. *Scientific reports* 7:1–9
24. Cardinale BJ, Hillebrand H, Harpole WS, et al (2009) Separating the influence of resource ‘availability’ from resource ‘imbalance’ on productivity-diversity relationships. *Ecology Letters* 12:475–487. doi: 10.1111/j.1461-0248.2009.01317.x
25. Chandra Rajan K, Vengatesen T (2020) Molecular adaptation of molluscan biomineralisation to high-CO₂ oceans – The known and the unknown. *Marine Environmental Research* 155:104883.
<https://doi.org/10.1016/j.marenvres.2020.104883>
26. Charrier M, Marie A, Guillaume D, et al (2013) Soil Calcium Availability Influences Shell Ecophenotype Formation in the Sub-Antarctic Land Snail, *Notodiscus hookeri*. *PLOS ONE* 8:11
27. Che-Castaldo JP, Neel MC (2016) Species-level persistence probabilities for recovery and conservation status assessment. *Conservation Biology* 30:1297–1306. doi: 10.1111/cobi.12728
28. Choe H, Thorne JH, Seo C (2016) Mapping National Plant Biodiversity Patterns in South Korea with the MARS Species Distribution Model. *PLOS ONE* 11:e0149511.
<https://doi.org/10.1371/journal.pone.0149511>
29. Clark MS (2020) Molecular mechanisms of biomineralization in marine invertebrates. *Journal of Experimental Biology* 223:. <https://doi.org/10.1242/jeb.206961>
30. Clark MS, Peck LS, Arivalagan J, et al (2020) Deciphering mollusc shell production: the roles of genetic mechanisms through to ecology, aquaculture and biomimetics. *Biological Reviews* 95:1812–1837. <https://doi.org/10.1111/brv.12640>
31. Clarke A (1993) Temperature and Extinction in the Sea: A Physiologist’s View. *Paleobiology* 19:499–518
32. Clements R, Ng PK, Lu XX, et al (2008) Using biogeographical patterns of endemic land snails to improve conservation planning for limestone karsts. *Biological conservation* 141:2751–2764
33. Clements R, Sodhi NS, Schilthuizen M, Ng PK (2006) Limestone Karsts of Southeast Asia: Imperiled Arks of Biodiversity. *BioScience*, 56(9), 733. doi:10.1641/0006-3568(2006)56[733:lksai]2.0.co;2

34. Cline LC, Hobbie SE, Madritch MD, Buyarski CR, Tilman D, Cavender-Bares JM (2018) Resource availability underlies the plant-fungal diversity relationship in a grassland ecosystem. *Ecology* 99:204–216. doi: 10.1002/ecy.2075
35. Coetzee BWT, Robertson MP, Erasmus BFN, et al (2009) Ensemble models predict Important Bird Areas in southern Africa will become less effective for conserving endemic birds under climate change. *Global Ecology and Biogeography* 18:701–710. <https://doi.org/10.1111/j.1466-8238.2009.00485.x>
36. Conti E, Soltis DE, Hardig TM, Schneider J (1999) Phylogenetic Relationships of the Silver Saxifrages (*Saxifraga*, Sect. *Ligulatae* Haworth): Implications for the Evolution of Substrate Specificity, Life Histories, and Biogeography. *Molecular Phylogenetics and Evolution* 13:536–555. doi: 10.1006/mpev.1999.0673
37. Corlett RT, Tomlinson KW (2020) Climate Change and Edaphic Specialists: Irresistible Force Meets Immovable Object? *Trends in Ecology & Evolution*, 35(4), 367-376. doi:10.1016/j.tree.2019.12.007
38. Crandall KA, Bininda-Emonds OR, Mace GM, Wayne RK (2000) Considering evolutionary processes in conservation biology. *Trends in Ecology & Evolution*, 15(7), 290-295. doi:10.1016/s0169-5347(00)01876-0
39. Crowell HH (1973) Laboratory study of calcium requirements of the brown garden snail, *Helix aspersa* Müller. *Journal of Molluscan Studies* 40:491–503
40. Cutler DR, Edwards Jr TC, Beard KH, et al (2007) Random forests for classification in ecology. *Ecology* 88:2783–2792
41. Davies AJ, Guinotte JM (2011) Global Habitat Suitability for Framework-Forming Cold-Water Corals. *PLOS ONE* 6:e18483. <https://doi.org/10.1371/journal.pone.0018483>
42. Deng J, Dong W, Socher R, et al (2009) ImageNet: A large-scale hierarchical image database. In: 2009 IEEE Conference on Computer Vision and Pattern Recognition. pp 248–255
43. Dillon RT (2000) The ecology of freshwater molluscs
44. Elejalde MA, Madeira MJ, Arrebola JR, Munoz B, Gómez-Moliner BJ (2008) Molecular phylogeny, taxonomy and evolution of the land snail genus *Iberus*

- (Pulmonata: Helicidae). *Journal of Zoological Systematics and Evolutionary Research* 46:193–202. doi: 10.1111/j.1439-0469.2008.00468.x
45. Elejalde MA, Muñoz B, Arrébola JR, Gómez-Moliner BJ (2005) Phylogenetic relationships of *Iberus gualtieranus* and *I. alonensis* (Gastropoda: Helicidae) based on partial mitochondrial 16S rRNA and COI gene sequences. *Journal of Molluscan Studies* 71:349–355
 46. Emberton, K. C. (1991). Polygyrid relations: A phylogenetic analysis of 17 subfamilies of land snails (Mollusca: Gastropoda: Stylommatophora). *Zoological Journal of the Linnean Society*, 103(3), 207-224. doi:10.1111/j.1096-3642.1991.tb00903.x
 47. Erskine P, Ent AVD, Fletcher A (2012) Sustaining Metal-Loving Plants in Mining Regions. *Science* 337:1172–1173. doi: 10.1126/science.337.6099.1172-b
 48. Etter RJ, Rex MA (1990) Population differentiation decreases with depth in deep-sea gastropods. *Deep Sea Research Part A Oceanographic Research Papers* 37:1251–1261. [https://doi.org/10.1016/0198-0149\(90\)90041-S](https://doi.org/10.1016/0198-0149(90)90041-S)
 49. Fairbanks HL (1975) A taxonomic study of *Oreohelix haydeni* in western Montana. Masters Thesis, University of Montana, Montana, USA.
 50. Federal Register (2005) Endangered and Threatened Wildlife and Plants; 90-Day Finding on a Petition To List the Uinta Mountainsnail as Endangered. *Federal Register* 69303–69305
 51. Federal Register (2006) Endangered and Threatened Wildlife and Plants; 90-Day Finding on a Petition To List the Black Hills Mountainsnail as Threatened or Endangered. *Federal Register* 9988–9999
 52. Federal Register (2011) Endangered and Threatened Wildlife and Plants; 12-Month Finding on a Petition To List the Bearmouth Mountainsnail, Byrne Resort Mountainsnail, and Meltwater Lednian Stonefly as Endangered or Threatened. *Federal Register* 76:18684–18701
 53. Felsenstein J (1988) Phylogenies From Molecular Sequences: Inference And Reliability. *Annual Review of Genetics* 22:521–565. doi: 10.1146/annurev.genet.22.1.521

54. Fick SE, Hijmans RJ (2017) WorldClim 2: new 1-km spatial resolution climate surfaces for global land areas. *International journal of climatology* 37:4302–4315
55. Figuerola B, Hancock AM, Bax N, et al (2021) A Review and Meta-Analysis of Potential Impacts of Ocean Acidification on Marine Calcifiers From the Southern Ocean. *Front Mar Sci* 8:. <https://doi.org/10.3389/fmars.2021.584445>
56. Finkel ZV, Kotrc B (2010) Silica use through time: macroevolutionary change in the morphology of the diatom fustule. *Geomicrobiology Journal* 27:596–608
57. Flessa KW, Brown TJ (1983) Selective solution of macroinvertebrate calcareous hard parts: a laboratory study. *Lethaia* 16:193–205. <https://doi.org/10.1111/j.1502-3931.1983.tb00654.x>
58. Folmer O (1994) DNA primers for amplification of mitochondrial cytochrome c oxidase subunit I from diverse metazoan invertebrates. *Molecular Marine Biology and Biotechnology* 3:294–299.
59. Fournié J, Chétail M (1984) Calcium Dynamics in Land Gastropods. *Am Zool* 24:857–870. <https://doi.org/10.1093/icb/24.4.857>
60. Fox EW, Hill RA, Leibowitz SG, et al (2017) Assessing the accuracy and stability of variable selection methods for random forest modeling in ecology. *Environmental monitoring and assessment* 189:1–20
61. Frankham R, Ballou JD, Dudash MR, Eldridge MD, Fenster CB, Lacy RC, Mendelson III JR, Porton IJ, Ralls K, Ryder OA (2012) Implications of different species concepts for conserving biodiversity. *Biological Conservation* 153:25–31. doi: 10.1016/j.biocon.2012.04.034
62. Frest TJ, Johannes EJ (1997) Land snail survey of the lower Salmon River drainage, Idaho. Bureau of Land Management, Idaho State Office. doi: 10.5962/bhl.title.62859
63. Geffen E, Anderson MJ, Wayne RK (2004) Climate and habitat barriers to dispersal in the highly mobile grey wolf. *Molecular Ecology* 13:2481–2490. doi: 10.1111/j.1365-294x.2004.02244.x
64. Gilman RT, Behm JE (2011) Hybridization, Species Collapse, And Species Reemergence After Disturbance To Premating Mechanisms Of Reproductive Isolation. *Evolution* 65:2592–2605. doi: 10.1111/j.1558-5646.2011.01320.x

65. Giokas S (2000) Congruence and conflict in Albinaria (Gastropoda, Clausiliidae). A review of morphological and molecular phylogenetic approaches. *Belgian Journal of Zoology* 130:93–100.
66. Giokas S (2008) Shell surface adaptations in relation to water management in rock-dwelling land snails, Albinaria (Pulmonata: Clausiliidae). *Journal of Natural History* 42:451–465. doi: 10.1080/00222930701835407
67. Gittenberger E (1991) What about non-adaptive radiation? *Biological Journal of the Linnean Society* 43:263–272. <https://doi.org/10.1111/j.1095-8312.1991.tb00598.x>
68. Glaubrecht M, Köhler F (2004) Radiating in a river: systematics, molecular genetics and morphological differentiation of viviparous freshwater gastropods endemic to the Kaek River, central Thailand (Cerithioidea, Pachychilidae): KAEK RIVER RADIATION. *Biological Journal of the Linnean Society* 82:275–311. <https://doi.org/10.1111/j.1095-8312.2004.00361.x>
69. Goodfriend GA (1986) VARIATION IN LAND-SNAIL SHELL FORM AND SIZE AND ITS CAUSES: A REVIEW. *SYSTEMATIC ZOOLOGY* 35:204–223
70. Goodfriend GA, Stipp JJ (1983) Limestone and the problem of radiocarbon dating of land-snail shell carbonate. 575–577
71. Grabenstein KC, Taylor SA (2018) Breaking Barriers: Causes, Consequences, and Experimental Utility of Human-Mediated Hybridization. *Trends in Ecology & Evolution* 33:198–212. doi: 10.1016/j.tree.2017.12.008
72. Graus RR (1974) Latitudinal trends in the shell characteristics of marine gastropods. *Lethaia* 7:303–314. <https://doi.org/10.1111/j.1502-3931.1974.tb00906.x>
73. Greve C, Hutterer R, Groh K, et al (2010) Evolutionary diversification of the genus Theba (Gastropoda: Helicidae) in space and time: A land snail conquering islands and continents. *Molecular Phylogenetics and Evolution* 57:572–584. <https://doi.org/10.1016/j.ympev.2010.08.021>
74. Gutschick VP (1981) Evolved strategies in nitrogen acquisition by plants. *The American Naturalist* 118:607–637
75. Harrison JF, Kaiser A, VandenBrooks JM (2010) Atmospheric oxygen level and the evolution of insect body size. *Proceedings of the Royal Society B: Biological Sciences* 277:1937–1946

76. Harvey BP, Agostini S, Wada S, et al (2018) Dissolution: the Achilles' heel of the triton shell in an acidifying ocean. *Frontiers in Marine Science* 5:371
77. Haskell DG, Pan JW (2013) Phylogenetic analysis of threatened and range-restricted limestone specialists in the land snail genus *Anguispira*. *Conservation Genetics* 14:671–682. doi: 10.1007/s10592-013-0460-4
78. Heled J, Drummond AJ (2009) Bayesian Inference of Species Trees from Multilocus Data. *Molecular Biology and Evolution* 27:570–580. doi: 10.1093/molbev/msp274
79. Henderson J (1918) On The North American Genus *Oreohelix*. *Journal of Molluscan Studies* 13:21–24. doi: 10.1093/oxfordjournals.mollus.a063671
80. Hotopp KP (2002) Land Snails And Soil Calcium In Central Appalachian Mountain Forest. *Southeastern Naturalist* 1:27–44. doi: 10.1656/1528-7092(2002)001[0027:lsasci]2.0.co;2
81. Hurd CL, Beardall J, Comeau S, et al (2019) Ocean acidification as a multiple driver: how interactions between changing seawater carbonate parameters affect marine life. *Mar Freshwater Res* 71:263–274. <https://doi.org/10.1071/MF19267>
82. Kado Y (1960) Studies on shell formation in molluscs. *Journal of science of the Hiroshima University Ser B-1 Zoology* ????
83. Kassambara A (2021) [kassambara/rstatix](https://www.kassambara.com/rstatix/)
84. Katoh K, Rozewicki J, Yamada KD (2019) MAFFT online service: multiple sequence alignment, interactive sequence choice and visualization. *Briefings in Bioinformatics* 20:1160–1166. doi: 10.1093/bib/bbx108
85. Kopp D, Allen D (2021) Trait–environment relationships could alter the spatial and temporal characteristics of aquatic insect subsidies at the macrospatial scale. *Ecography* 44:391–402
86. Kroeker KJ, Sanford E, Jellison BM, Gaylord B (2014) Predicting the effects of ocean acidification on predator-prey interactions: a conceptual framework based on coastal molluscs. *The Biological Bulletin* 226:211–222
87. Kruckeberg AR (1986) An Essay: The Stimulus of Unusual Geologies for Plant Speciation. *Systematic Botany* 11:455. doi: 10.2307/2419082

88. Labaune C, Magnin F (2002) Pastoral management vs. land abandonment in Mediterranean uplands: Impact on land snail communities. *Global Ecology and Biogeography*, 11(3), 237-245. doi:10.1046/j.1466-822x.2002.00280.x
89. Leaché AD, Fujita MK, Minin VN, Bouckaert RR (2014) Species Delimitation using Genome-Wide SNP Data. *Systematic Biology* 63:534–542. doi: 10.1093/sysbio/syu018
90. Liaw A, Wiener M (2001) Classification and Regression by RandomForest. *Forest* 23:
91. Linscott TM, Weaver K, Morales V, Parent CE (2020) Assessing species number and genetic diversity of the Mountainsnails (Oreohelicidae). *Conservation Genetics* 21:971–985
92. Love JD. Names and descriptions of new and reclassified formations in northwestern Wyoming. U. S. Geological Survey Professional Paper 932-C
93. Mace GM (2004) The role of taxonomy in species conservation. *Philosophical Transactions of the Royal Society of London Series B: Biological Sciences* 711–719.
94. Mekkes L, Sepúlveda-Rodríguez G, Bielkinité G, et al (2021) Effects of Ocean Acidification on Calcification of the Sub-Antarctic Pteropod *Limacina retroversa*. *Front Mar Sci* 8:. <https://doi.org/10.3389/fmars.2021.581432>
95. Mesher CS, Welter-Schultes FW (2008) Studies on range expansion, predation pressure, and insolation in *Albinaria* on the island of Dia (Greece), focused on a recently introduced species (Gastropoda: Clausiliidae). *Species Phyl Evol* 1:129–140
96. Minin V, Abdo Z, Joyce P, Sullivan J (2003) Performance-Based Selection of Likelihood Models for Phylogeny Estimation. *Systematic Biology* 52:674–683. doi: 10.1080/10635150390235494
97. Miranda M (2003) Mining and critical ecosystems: mapping the risks. World Resources Institute, Washington, D.C.
98. Monaghan MT, Wild R, Elliot M, Fujisawa T, Balke M, Inward DJ, Vogler AP (2009) Accelerated Species Inventory on Madagascar Using Coalescent-Based Models of Species Delineation. *Systematic Biology*, 58(3), 298-311. doi:10.1093/sysbio/syp027

99. Moreno-Rueda G (2009) Disruptive selection by predation offsets stabilizing selection on shell morphology in the land snail *Iberus g. gualtieranus*. *Evol Ecol* 23:463–471. <https://doi.org/10.1007/s10682-008-9245-5>
100. Murguía DI, Bringezu S, Schaldach R (2016) Global direct pressures on biodiversity by large-scale metal mining: Spatial distribution and implications for conservation. *Journal of Environmental Management* 180:409–420. doi: 10.1016/j.jenvman.2016.05.040
101. NatureServe (2021) NatureServe Explorer [web application].
102. Natureserve. 2019. NatureServe Explorer: An online encyclopedia of life [web application]. Version 7.0. NatureServe, Arlington, VA. U.S.A. Available
103. Nekola JC (2014) Overview of the North American Terrestrial Gastropod Fauna. *American Malacological Bulletin* 32:225. doi: 10.4003/006.032.0203
104. Niemi A, Bednaršek N, Michel C, et al (2021) Biological Impact of Ocean Acidification in the Canadian Arctic: Widespread Severe Pteropod Shell Dissolution in Amundsen Gulf. *Front Mar Sci* 8:600184. <https://doi.org/10.3389/fmars.2021.600184>
105. Oerter EJ, Amundson R (2016) Climate controls on spatial and temporal variations in the formation of pedogenic carbonate in the western Great Basin of North America. *Geological Society of America Bulletin* 128:1095–1104. <https://doi.org/10.1130/B31367.1>
106. Palmer AR (1979) Fish predation and the evolution of gastropod shell sculpture: experimental and geographic evidence. *Evolution* 697–713
107. Paradis E, Schliep K (2018) ape 5.0: an environment for modern phylogenetics and evolutionary analyses in R. *Bioinformatics* 35:526–528. doi: 10.1093/bioinformatics/bty633
108. Paridon BJV, Gilleard JS, Colwell DD, Goater CP (2017) Life Cycle, Host Utilization, and Ecological Fitting for Invasive Lancet Liver Fluke, *Dicrocoelium dendriticum*, Emerging in Southern Alberta, Canada. *Journal of Parasitology* 103:207–212. doi: 10.1645/16-140

109. Pelejero C, Calvo E, Hoegh-Guldberg O (2010) Paleo-perspectives on ocean acidification. *Trends in Ecology & Evolution* 25:332–344.
<https://doi.org/10.1016/j.tree.2010.02.002>
110. Pierce HG, Constenius KN (2001) Late Eocene-Oligocene nonmarine mollusks of the northern Kishenehn Basin, Montana and British Columbia. *Annals of the Carnegie Museum* 70.1:1-112.
111. Pilsbry HA (1939) Land mollusca of North America. Academy of Natural Sciences., Philadelphia, PA
112. Proosdij ASJ van, Sosef MSM, Wieringa JJ, Raes N (2016) Minimum required number of specimen records to develop accurate species distribution models. *Ecography* 39:542–552. <https://doi.org/10.1111/ecog.01509>
113. QUENSEN III J, S WOODRUFF D (1997) Associations between shell morphology and land crab predation in the land snail *Cerion*. *Functional Ecology* 11:464–471
114. R Core Team (2019) R: A language and environment for statistical computing, version 3.3. 1. Vienna, Austria: R Foundation for Statistical Computing.
115. R Core Team (2021) R: A language and environment for statistical computing.
116. Rajakaruna N (2004) The Edaphic Factor in the Origin of Plant Species. *International Geology Review* 46:471–478. doi: 10.2747/0020-6814.46.5.471
117. Rajakaruna N (2017) Lessons on Evolution from the Study of Edaphic Specialization. *The Botanical Review* 84:39–78. doi: 10.1007/s12229-017-9193-2
118. Rajan KC, Vengatesen T (2020) Molecular adaptation of molluscan biomineralisation to high-CO₂ oceans–The known and the unknown. *Marine environmental research* 155:104883
119. Rambaut A, Drummond AJ, Xie D, Baele G, Suchard MA (2018) Posterior Summarization in Bayesian Phylogenetics Using Tracer 1.7. *Systematic Biology* 67:901–904. doi: 10.1093/sysbio/syy032
120. Rankin AM, Wilke T, Lucid M, et al (2019) Complex interplay of ancient vicariance and recent patterns of geographical speciation in north-western North American temperate rainforests explains the phylogeny of jumping slugs (*Hemphillia* spp.). *Biological Journal of the Linnean Society* 127:876–889

121. Rannala B, Yang Z (2017) Efficient Bayesian species tree inference under the multispecies coalescent. *Systematic Biology*. doi: 10.1093/sysbio/syw119
122. Reid NM, Carstens BC (2012) Phylogenetic estimation error can decrease the accuracy of species delimitation: a Bayesian implementation of the general mixed Yule-coalescent model. *BMC Evolutionary Biology* 12:196. doi: 10.1186/1471-2148-12-196
123. Ribeiro MT, Singh S, Guestrin C (2016) Model-Agnostic Interpretability of Machine Learning. arXiv:160605386 [cs, stat]
124. Ries JB, Ghazaleh MN, Connolly B, et al (2016) Impacts of seawater saturation state ($\Omega_A=0.4-4.6$) and temperature (10, 25°C) on the dissolution kinetics of whole-shell biogenic carbonates. *Geochimica et Cosmochimica Acta* 192:318–337.
<https://doi.org/10.1016/j.gca.2016.07.001>
125. Rodríguez-Basalo A, Prado E, Sánchez F, et al (2021) High Resolution Spatial Distribution for the Hexactinellid Sponges *Asconema setubalense* and *Pheronema carpenteri* in the Central Cantabrian Sea. *Front Mar Sci* 8:.
<https://doi.org/10.3389/fmars.2021.612761>
126. Roth B, Emberton KC (1994) "Extralimital" Land Mollusks (Gastropoda) from the Deep River Formation, Montana: Evidence for Mesic Medial Tertiary Climate. *Proceedings of the Academy of Natural Sciences of Philadelphia* 93–106.
127. Roth B, Land Mollusks (Gastropoda, Pulmonata) from Early Tertiary Bozeman Group, Montana. *Proceedings of the California Academy of Sciences* 44:237–267.
128. Ryo M, Angelov B, Mammola S, et al (2021) Explainable artificial intelligence enhances the ecological interpretability of black-box species distribution models. *Ecography* 44:199–205
129. Sanford E, Kelly MW (2011) Local adaptation in marine invertebrates. *Annual review of marine science* 3:509–535
130. Schilthuizen M (1994) Reproductive isolation in snails of the genus *Albinaria* (Gastropoda: Clausiliidae). *Biological Journal of the Linnean Society* 52:317–324.
doi: 10.1111/j.1095-8312.1994.tb00994.x

131. Schilthuizen M, Chai H-N, Kimsin TE, Vermeulen JJ (2003) Abundance and diversity of land-snails (Mollusca: Gastropoda) on limestone hills in Borneo. *Raffles Bulletin of Zoology* 51:35–42
132. Simon-Nutbrown C, Hollingsworth PM, Fernandes TF, et al (2020) Species Distribution Modeling Predicts Significant Declines in Coralline Algae Populations Under Projected Climate Change With Implications for Conservation Policy. *Front Mar Sci* 7:. <https://doi.org/10.3389/fmars.2020.575825>
133. Solem A (1975). Notes on Salmon River Valley oreohelcid land snails, with description of *Oreohelix waltoni*. *The Veliger* 18.1:16-30.
134. Sonter LJ, Ali SH, Watson JEM (2018) Mining and biodiversity: key issues and research needs in conservation science. *Proceedings of the Royal Society B: Biological Sciences* 285:20181926. doi: 10.1098/rspb.2018.1926
135. Stamatakis A (2006) RAxML-VI-HPC: maximum likelihood-based phylogenetic analyses with thousands of taxa and mixed models. *Bioinformatics* 22:2688–2690. doi: 10.1093/bioinformatics/btl446
136. Stankowski S (2013) Ecological speciation in an island snail: evidence for the parallel evolution of a novel ecotype and maintenance by ecologically dependent postzygotic isolation. *Molecular Ecology* 22:2726–2741. <https://doi.org/10.1111/mec.12287>
137. Sterck F, Markesteijn L, Schieving F, Poorter L (2011) Functional traits determine trade-offs and niches in a tropical forest community. *Proceedings of the National Academy of Sciences* 108:20627–20632. <https://doi.org/10.1073/pnas.1106950108>
138. Storch D, Evans KL, Gaston KJ (2005) The species-area-energy relationship. *Ecology Letters* 8:487–492. doi: 10.1111/j.1461-0248.2005.00740.x
139. Swofford DL, Sullivan J (2003) Phylogeny inference based on parsimony and other methods using PAUP. *The Phylogenetic Handbook* 267–312. doi: 10.1017/cbo9780511819049.010
140. Talavera G, Dincă V, Vila R. (2013). Factors affecting species delimitations with the GMYC model: Insights from a butterfly survey. *Methods in Ecology and Evolution*, 4(12), 1101-1110. doi:10.1111/2041-210x.12107

141. Terhaar J, Kwiatkowski L, Bopp L (2020) Emergent constraint on Arctic Ocean acidification in the twenty-first century. *Nature* 582:379–383.
<https://doi.org/10.1038/s41586-020-2360-3>
142. Teshima H, Davison A, Kuwahara Y, Yokoyama J, Chiba S, Fukuda T, Ogimura H, Kawata M. (2003) The evolution of extreme shell shape variation in the land snail *Ainohelix editha*: a phylogeny and hybrid zone analysis. *Molecular Ecology* 12:1869–1878. doi: 10.1046/j.1365-294x.2003.01862.x
143. Tropek R, Kadlec T, Karesova P, Spitzer L, Kocarek P, Malenovsky I, Banar P, Tuf IH, Hejda M, Konvicka M (2010) Spontaneous succession in limestone quarries as an effective restoration tool for endangered arthropods and plants. *Journal of Applied Ecology* 47:139–147. doi: 10.1111/j.1365-2664.2009.01746.x
144. Van Riel P, Jordaens K, Van Houtte N, Martins AM, Verhagen R, Backeljau T. (2005) Molecular systematics of the endemic Leptaxini (Gastropoda: Pulmonata) on the Azores islands. *Molecular Phylogenetics and Evolution*. Oct 1;37(1):132-43
145. Vermeij GJ (1995) *A Natural History of Shells*. Princeton University Press
146. Vermeij GJ (2015) Gastropod skeletal defences: land, freshwater, and sea compared. *Vita Malacologica* 13:1–25
147. Vermeij GJ, Covich AP (1978) Coevolution of Freshwater Gastropods and Their Predators. *The American Naturalist* 112:833–843
148. Wägele H, Klussmann-Kolb A (2005) Opisthobranchia (Mollusca, Gastropoda) – more than just slimy slugs. Shell reduction and its implications on defence and foraging. *Frontiers in Zoology* 2:3. <https://doi.org/10.1186/1742-9994-2-3>
149. Waldbusser G, Bergschneider H, Green M (2010) Size-dependent pH effect on calcification in post-larval hard clam *Mercenaria* spp. *Mar Ecol Prog Ser* 417:171–182. <https://doi.org/10.3354/meps08809>
150. Wang C-Y, Bochkovskiy A, Liao H-YM (2021) Scaled-YOLOv4: Scaling Cross Stage Partial Network. arXiv:201108036 [cs]
151. Wang J, Ai B, Kong H, Kang M (2017) Speciation history of a species complex of *Primulina eburnea* (Gesneriaceae) from limestone karsts of southern China, a biodiversity hot spot. *Evolutionary Applications* 10:919–934. doi: 10.1111/eva.12495

152. Watson S-A, Peck LS, Tyler PA, et al (2012) Marine invertebrate skeleton size varies with latitude, temperature and carbonate saturation: implications for global change and ocean acidification. *Global Change Biology* 18:3026–3038.
<https://doi.org/10.1111/j.1365-2486.2012.02755.x>
153. Weaver KF (2006) Biogeography, systematics, and conservation genetics in the mountain snail group *Oreohelix* (Oreohelicidae). PhD Thesis, University of Colorado, CO, USA.
154. Weaver KF, Perez-Losada M, Guralnick RP, Nelson A, Blatt S, Crandall KA (2008) Assessing the conservation status of the land snail *Oreohelix peripherica wasatchensis* (Family Oreohelicidae). *Conservation Genetics* 9:907–916. doi: 10.1007/s10592-007-9415-y
155. Weaver KF, Weaver PF, Guralnick R (2010). Origin, diversification and conservation status of talus snails in the Pinaleno Mountains: A conservation biogeographic study. *Animal Conservation*, 13(3), 306-314. doi:10.1111/j.1469-1795.2009.00341.x
156. Welter-Schultes FW (1998) Albinaria in central and eastern Crete: distribution map of the species (Pulmonata: Clausiliidae). *Journal of Molluscan Studies* 64:275–279
157. Welter-Schultes FW (2010) Revision of the genus *Albinaria* in Crete (Greece): presence of geographically variable monotypic and polytypic species (Gastropoda: Clausiliidae). *Archiv für Molluskenkunde International Journal of Malacology* 143–245
158. Whipkey CE, Capo RC, Hsieh JCC, Chadwick OA (2002) Development of Magnesian Carbonates in Quaternary Soils on the Island of Hawaii. *Journal of Sedimentary Research* 72:158–165. <https://doi.org/10.1306/050801720158>
159. Woodruff DS, Gould SJ (1987) Fifty Years of Interspecific Hybridization: Genetics and Morphometrics of a Controlled Experiment on the Land Snail *Cerion* in the Florida Keys. *Evolution* 41:1022–1045. <https://doi.org/10.1111/j.1558-5646.1987.tb05874.x>
160. Xia X (2018) DAMBE7: New and Improved Tools for Data Analysis in Molecular Biology and Evolution. *Molecular Biology and Evolution* 35:1550–1552. doi: 10.1093/molbev/msy073

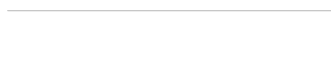
161. Xia X, Xie Z, Salemi M, Chen L, Wang Y (2003) An index of substitution saturation and its application. *Molecular Phylogenetics and Evolution* 26:1–7. doi: 10.1016/s1055-7903(02)00326-3
162. Yanes Y, Delgado A, Castillo C, et al (2008) Stable isotope ($\delta^{18}\text{O}$, $\delta^{13}\text{C}$, and δD) signatures of recent terrestrial communities from a low-latitude, oceanic setting: endemic land snails, plants, rain, and carbonate sediments from the eastern Canary Islands. *Chemical Geology* 249:377–392
163. Zakharova L, Meyer KM, Seifan M (2019) Trait-based modelling in ecology: A review of two decades of research. *Ecological Modelling* 407:108703
164. Zheng Z, Wang P, Liu W, et al (2020) Distance-IoU Loss: Faster and Better Learning for Bounding Box Regression. *AAAI* 34:12993–13000. <https://doi.org/10.1609/aaai.v34i07.6999>
165. Zizka A, Silvestro D, Andermann T, et al (2019) CoordinateCleaner: Standardized cleaning of occurrence records from biological collection databases. *Methods in Ecology and Evolution* 10:744–751. <https://doi.org/10.1111/2041-210X.13152>

Appendix A: Copyright from Conservation Genetics for Chapter 1

SPRINGER NATURE LICENSE

TERMS AND CONDITIONS

Jul 16, 2021



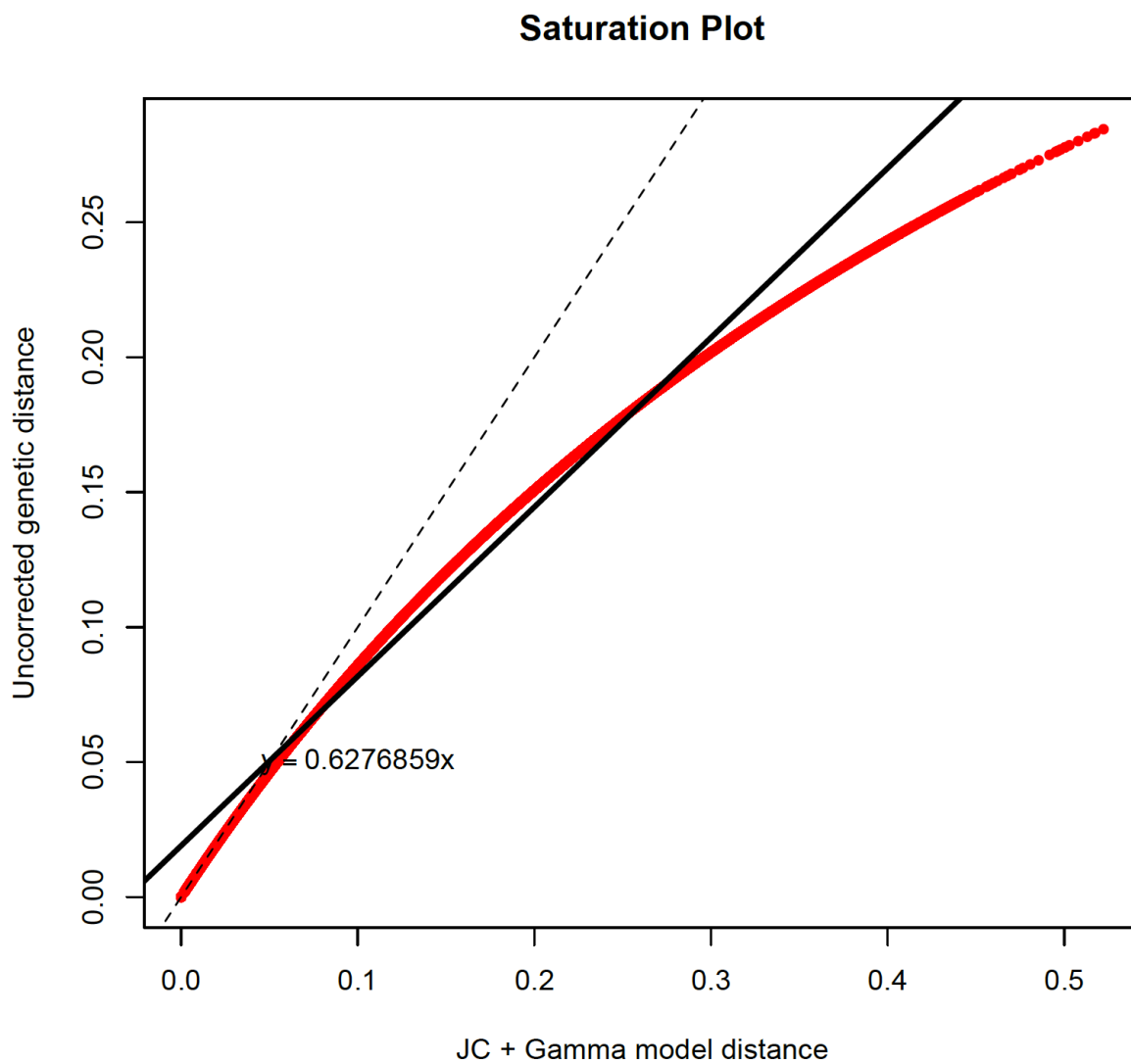
This Agreement between Thomas Linscott ("You") and Springer Nature ("Springer Nature") consists of your license details and the terms and conditions provided by Springer Nature and Copyright Clearance Center.

License Number	5107250219881
License date	Jul 13, 2021
Licensed Content Publisher	Springer Nature
Licensed Content Publication	Conservation Genetics
Licensed Content Title	Assessing species number and genetic diversity of the Mountainsnails (Oreohelicidae)
Licensed Content Author	T. Mason Linscott et al
Licensed Content Date	Aug 25, 2020
Type of Use	Thesis/Dissertation
Requestor type	academic/university or research institute
Format	print and electronic
Portion	full article/chapter
Will you be translating?	no
Circulation/distribution	1 - 29
Author of this Springer Nature content	yes

Title	Resource Constrained Adaptive Evolution of Mollusc Shell Form
Institution name	University of Idaho
Expected presentation date	Aug 2021
	Thomas Linscott 6822 N Old Fort Dr
Requestor Location	SPOKANE, WA 99208 United States Attn: University of Idaho
Total	0.00 USD

Appendix B: Supplementary tables and figures for Chapter 1

Chapter 1 Supplementary Figure 1:



Chapter 1 Supplementary Figure 1: Saturation plot of Oreohelix COI genes.

Chapter 1 Supplementary Table 1:

Model:	Number of Delimited Species:
Birth-Death	284
Birth-Death without singletons:	231
Birth-Death without singletons:and strigosa clade:	81
Coalescent:	394
Coalescent without singletons:	343
Coalescent without singletons and strigosa clade:	67

Chapter 1 Supplementary Table 1: GMYC delimitations using different dataset compositions and model parameters.

Chapter 1 Supplementary Table 2:

Delimited Species	Private Allele Position	Nucleotide
O. strigosa complex	None	N/A
O. grahamensis 1	None	N/A
O. grahamensis 2	None	N/A
O. grahamensis 3	None	N/A
O. subrudis	None	N/A
O. haydeni/yavapai complex	None	N/A
O. yavapai complex	None	N/A
O. jugalis complex	None	N/A
O. sp. 'kiabab'		264 G
O. concentrata		210 G
O. metcalfei complex	138, 174	T, C
O. barbata 1	247, 382, 468	T, T, T
O. barbata 2	382, 384, 424	C, T, A
O. amariradix	204, 435	G, G
R. avalonensis	352, 439, 571	C, A, A
R. chiricahuana	261, 303, 322	G, C, C
R. clappi	282, 312, 335, 366, 498, 549	C, G, C, C, C, G

Chapter 1 Supplementary Table 2: Private alleles and nucleotide information for all delimited species in the study.

Appendix C: Supplementary tables and figures for Chapter 2

Chapter 2 Supplementary Material Note 1

Predictor Dataset Creation

The predictors used in this study came from a variety of sources (Supplementary Table 1). In this section, we will detail how they were made to allow facilitate replication of our results. All predictors were reprojected in ArcGIS pro v.2.6.0 to WGS1984 and clipped to the same raster resolution. Predictor names used in R code are shown in parentheses. See Supplemental Table 1 for references.

Elevation (elevation): This layer was sourced from the publicly available ASTER Global Digital Elevation data reprojected to 90m resolution using the Project tool and clipped to the desired extent using the Clip Raster tool.

Slope (slope): This layer was created using the Slope tool in ArcGis on the 90m elevation data using a z-factor of 0.00001171 appropriate for 40 degrees latitude (<https://pro.arcgis.com/en/pro-app/latest/tool-reference/3d-analyst/applying-a-z-factor.htm>) which is close to the mean latitude of our study area.

Compound topographic index (CTI): This layer was created using the GradientMetrics ArcGIS toolbox (<https://github.com/jeffrejevans/GradientMetrics>) compound topographic index tool on the 90m resolution elevation data.

Heat load index (HLI): This layer was created using the GradientMetrics ArcGIS toolbox (<https://github.com/jeffrejevans/GradientMetrics>) heat load index tool on the 90m resolution elevation data.

Height distance above nearest drainage (HAND): This layer was created by first creating a stream layer using the Con tool in ArcGIS pro on the perennial and intermittent streams present in the USGS National Hydrography Dataset (<https://www.usgs.gov/core-science-systems/ngp/national-hydrography>). Then, we used the Flow Distance tool using the stream

layer and 90m elevation data as inputs and set the function to measure only vertical flow distance.

Horizontal distance to nearest drainage e(DTND): This layer was created by first creating a stream layer from the perennial and intermittent streams present in the National Hydrography Dataset (<https://www.usgs.gov/core-science-systems/ngp/national-hydrography>) using the Con tool in ArcGIS pro. Then, we used the Flow Distance tool with the stream layer and 90m elevation data as inputs and set the function to measure only horizontal flow distance.

Global horizontal irradiance (GHI): This layer was sourced from the Global Solar Atlas (Solar Atlas 2020). No modifications were made other than reprojecting and clipping were necessary.

Soil ph (soilph): We downloaded tiled POLARIS probabilistic mean soil ph data from across the western USA from

http://hydrology.cee.duke.edu/POLARIS/PROPERTIES/v1.0/ph/mean/0_5/.

Tiled data were combined using the Mosaic to New Raster tool in ArcGIS pro. Missing data were filled in based on a sliding window average of 20 x 20 pixels using the Cell Statistics tool and the Mosaic to New Raster tool.

Soil clay content (soilclay): We downloaded tiled POLARIS probabilistic mean soil clay content data across the western USA from

http://hydrology.cee.duke.edu/POLARIS/PROPERTIES/v1.0/clay/mean/0_5/.

Tiled data were combined using the Mosaic to New Raster tool in ArcGIS pro. Missing data were filled in based on a sliding window average of 20 x 20 pixels using the Cell Statistics tool and the Mosaic to New Raster tool.

Normalized Difference Vegetation Index (NDVI): We used modified SEBALIGEE Google Earth Engine code (Mhawej and Faour 2020; original code used in Mhawej and Faour here: <https://code.earthengine.google.com/48200ed2b76ff4acc530c618bb047635>; code used in this paper is provided on Dryad) to take the mean NDVI across the month of July for the entirety

of LANDSAT8's available data (2013 – 2020). We chose the month of July to gather NDVI data as cloud cover artifacts are usually less prevalent in summer months and that this time of the year represents some of the greatest extremes in temperature/desiccation land snails will experience. Regional segments were combined using the Mosaic to New Raster tool in ArcGIS pro.

LANDSAT8 Surface Temperature (LST): We used modified SEBALIGEE Google Earth Engine code (Mhawej and Faour 2020; original code used in Mhawej and Faour here: <https://code.earthengine.google.com/48200ed2b76ff4acc530c618bb047635>; code used in this paper is provided on Dryad) to download regional mean NDVI across the month of July for the entirety of LANDSAT8's available data (2013 – 2020). We chose the month of July to gather NDVI data as cloud cover artifacts are usually less prevalent in summer months and that this time of the year represents some of the greatest extremes in temperature/desiccation land snails will experience. Regional segments were combined using the Mosaic to New Raster tool in ArcGIS pro.

Distance to nearest developed area (developed): We used the Con tool in ArcGIS pro on the National Land Cover Database (<https://pubs.er.usgs.gov/publication/fs20123020>; Homer et al. 2012) pasture, crops, moderately developed, and highly developed areas to create a layer of developed areas. We then input the developed area as the feature of interest in the Path Distance tool and the cost raster of equal values (in this case, 1) for the entire Western USA. This value was then multiplied by the distance of the original projection (90m) to generate real distance away from developed areas.

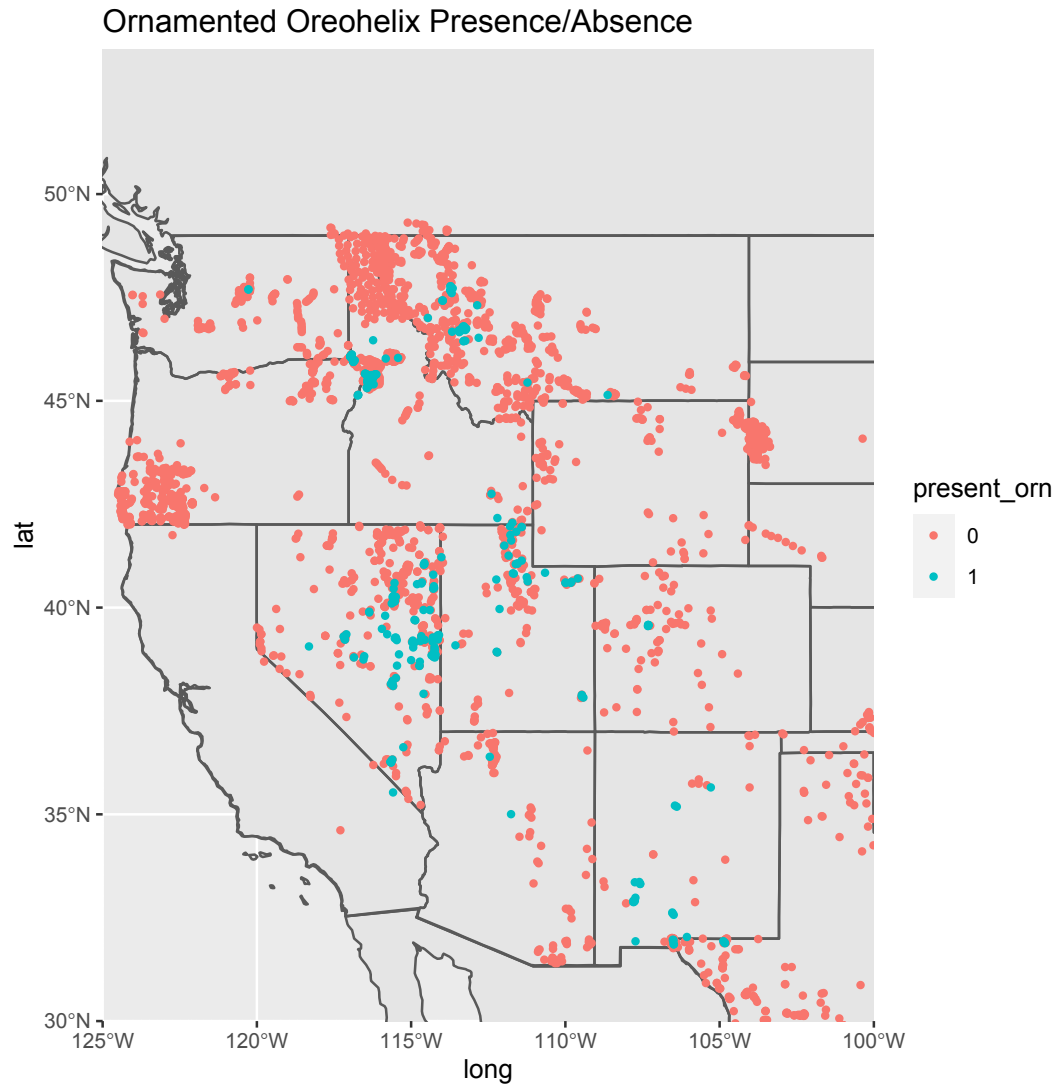
Distance to CaCO₃ rock (LS): We used the Con tool in ArcGIS pro on the National Karst Map's (<https://pubs.usgs.gov/of/2014/1156/>; Weary and Doctor 2014) near surface carbonate layers from wet and dry environments to create our initial CaCO₃ rock layer. This layer was then improved locally in the Salmon and Snake river area (Idaho, USA) with carbonate layers from Kauffman et al. (2014) as this information was already available from a preliminary study. The two CaCO₃ rock layers were combined using the Mosaic to New Raster tool to create the final CaCO₃ rock layer. We then input the CaCO₃ rock areas as the

feature of interest in the Path Distance tool and the cost raster of equal values (in this case, 1) for the entire Western USA. This value was then multiplied by the distance of the original projection (90m) to generate distance away from CaCO₃ rock.

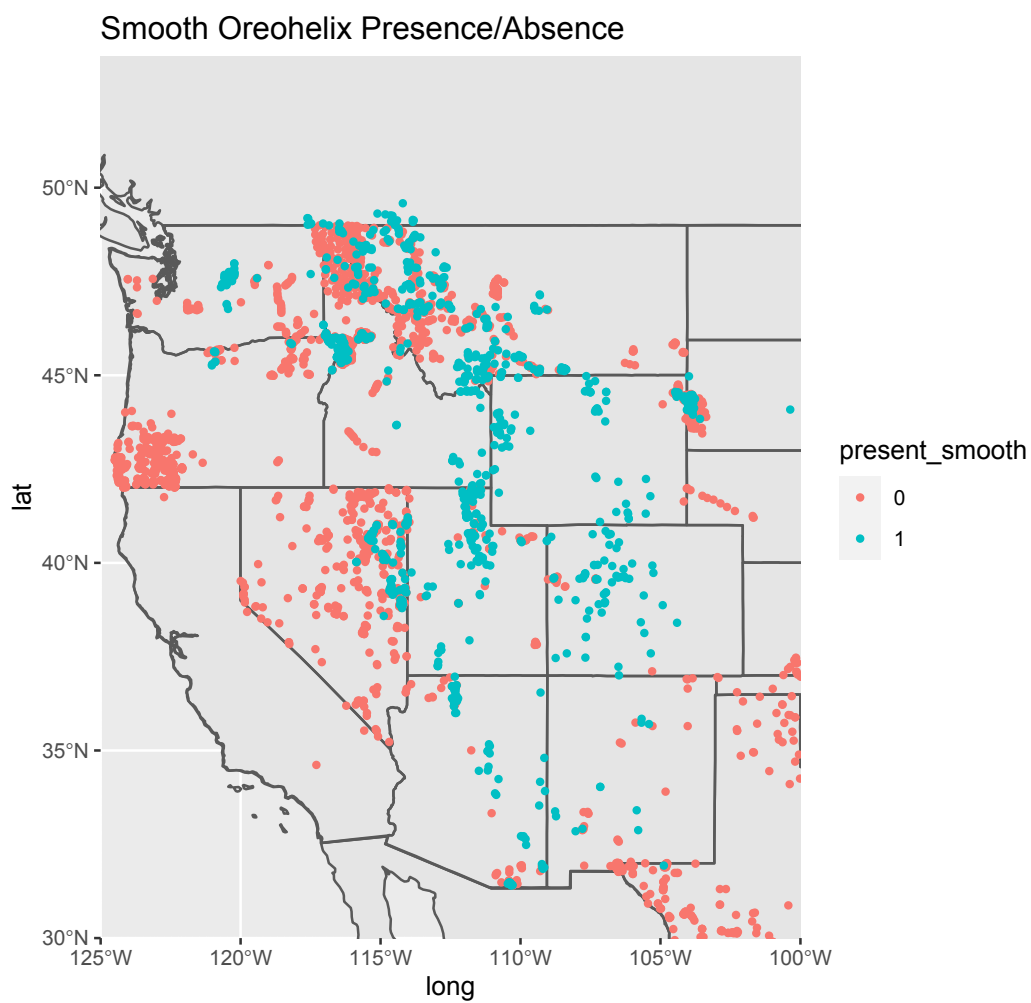
Dataset Composition:

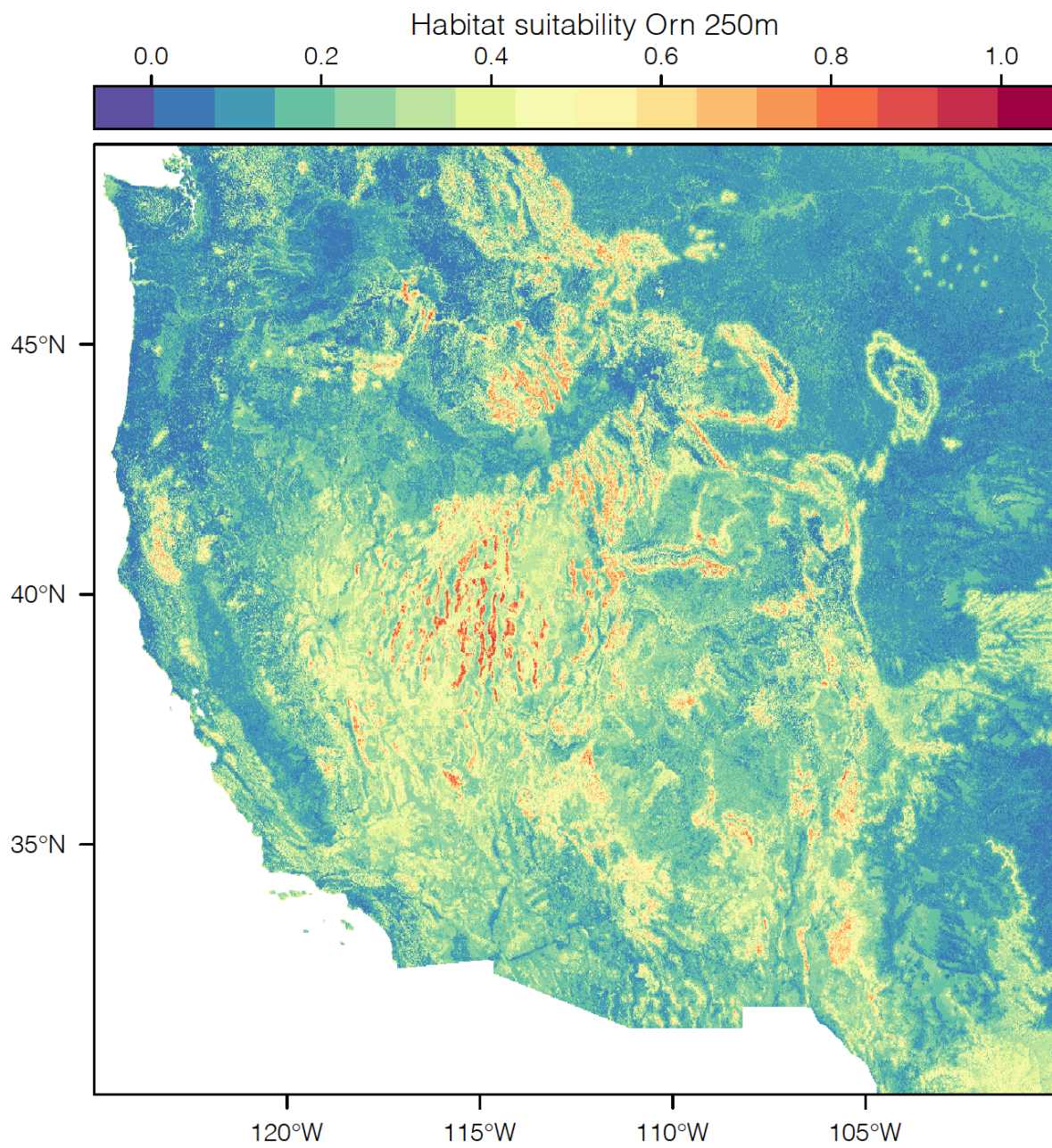
Number of records for classification and regression models were taken from a combination of government and private surveys. All records are less than 500m spatial uncertainty. All records on Dryad are obfuscated to greater than 1km in accordance with state and federal government data use agreements.

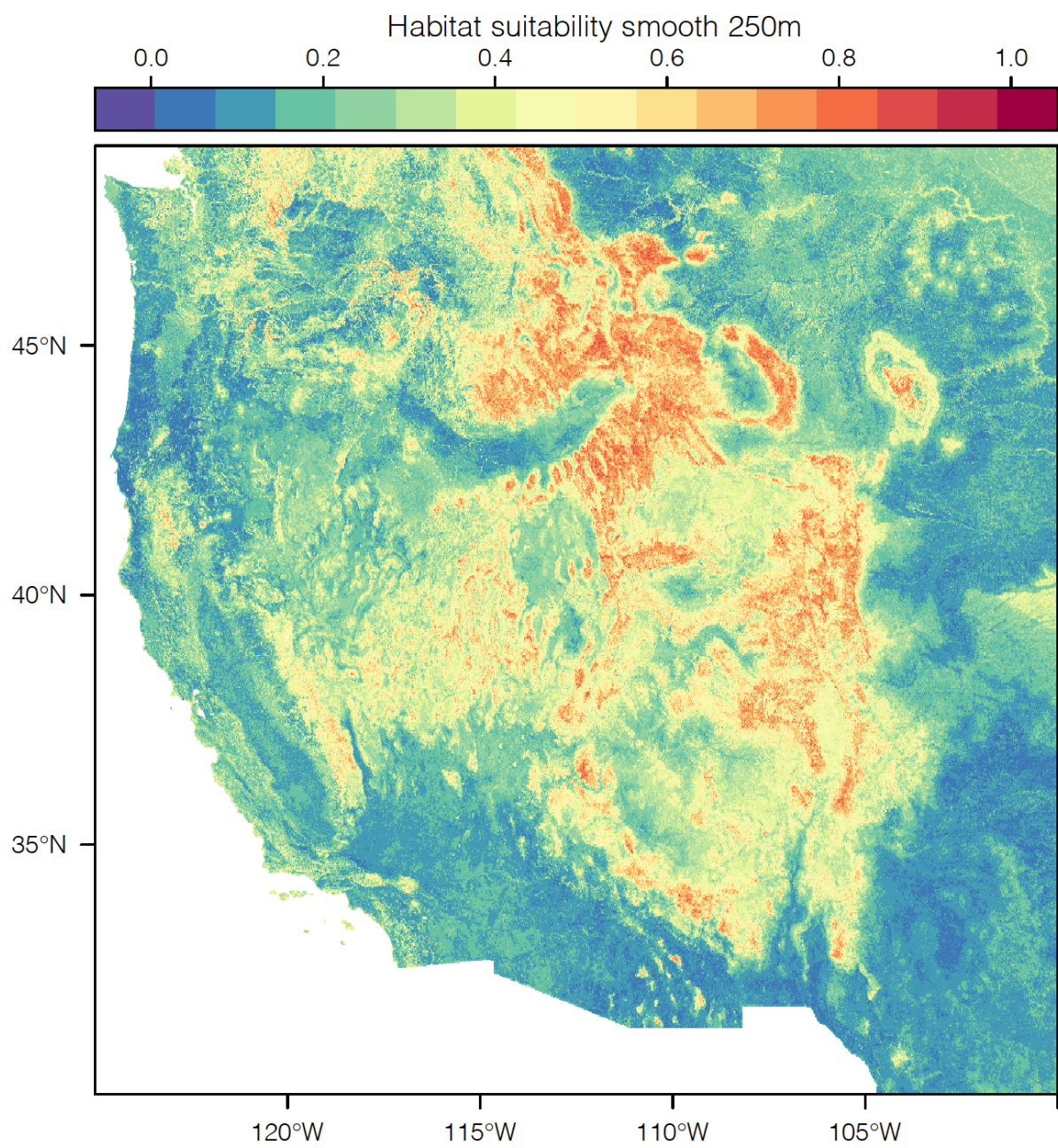
Chapter 2 Supplementary Figure 1:

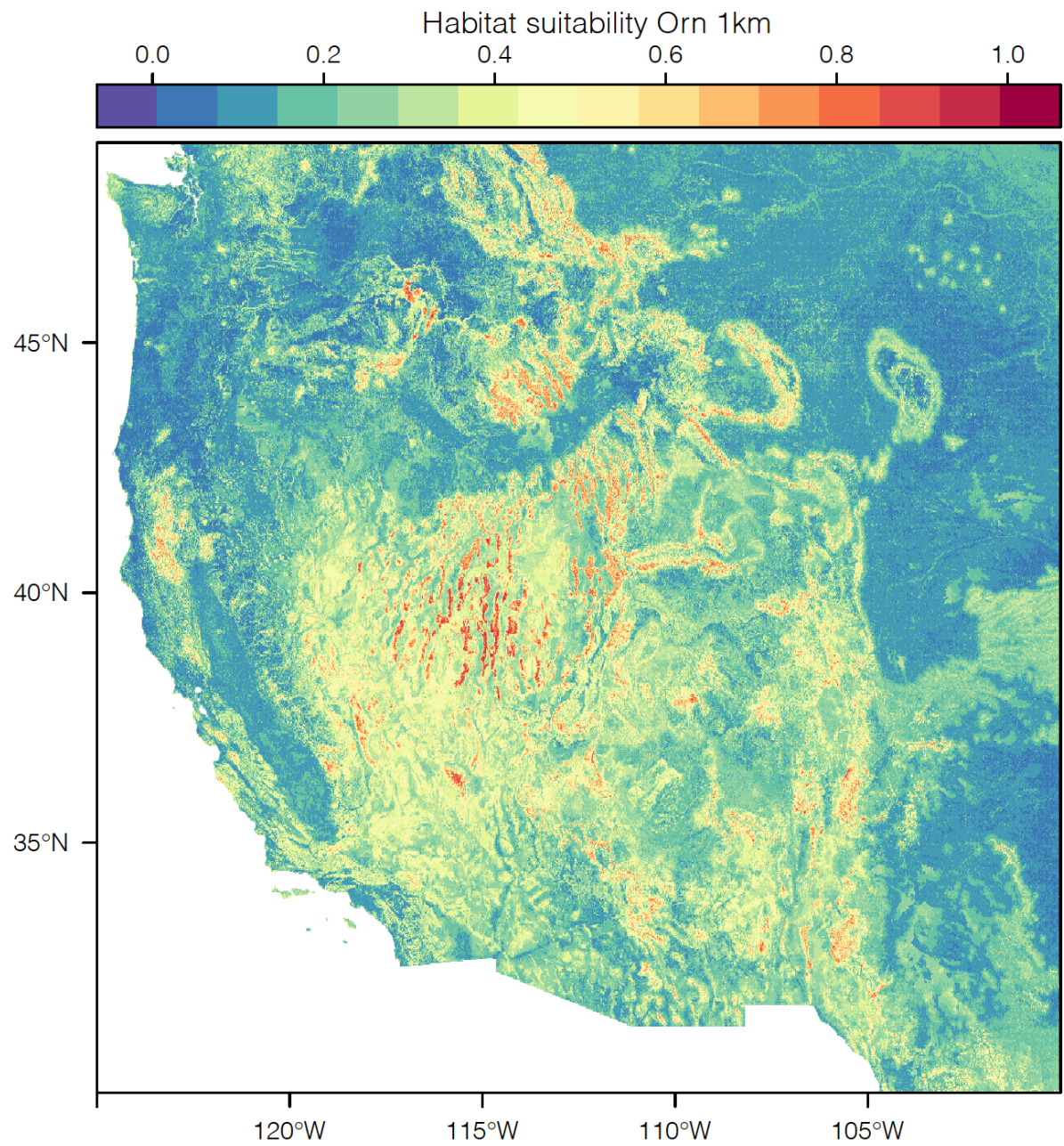
Chapter 2 Supplementary Figure 1: Ornamented *Oreohelix* presence and absence map.

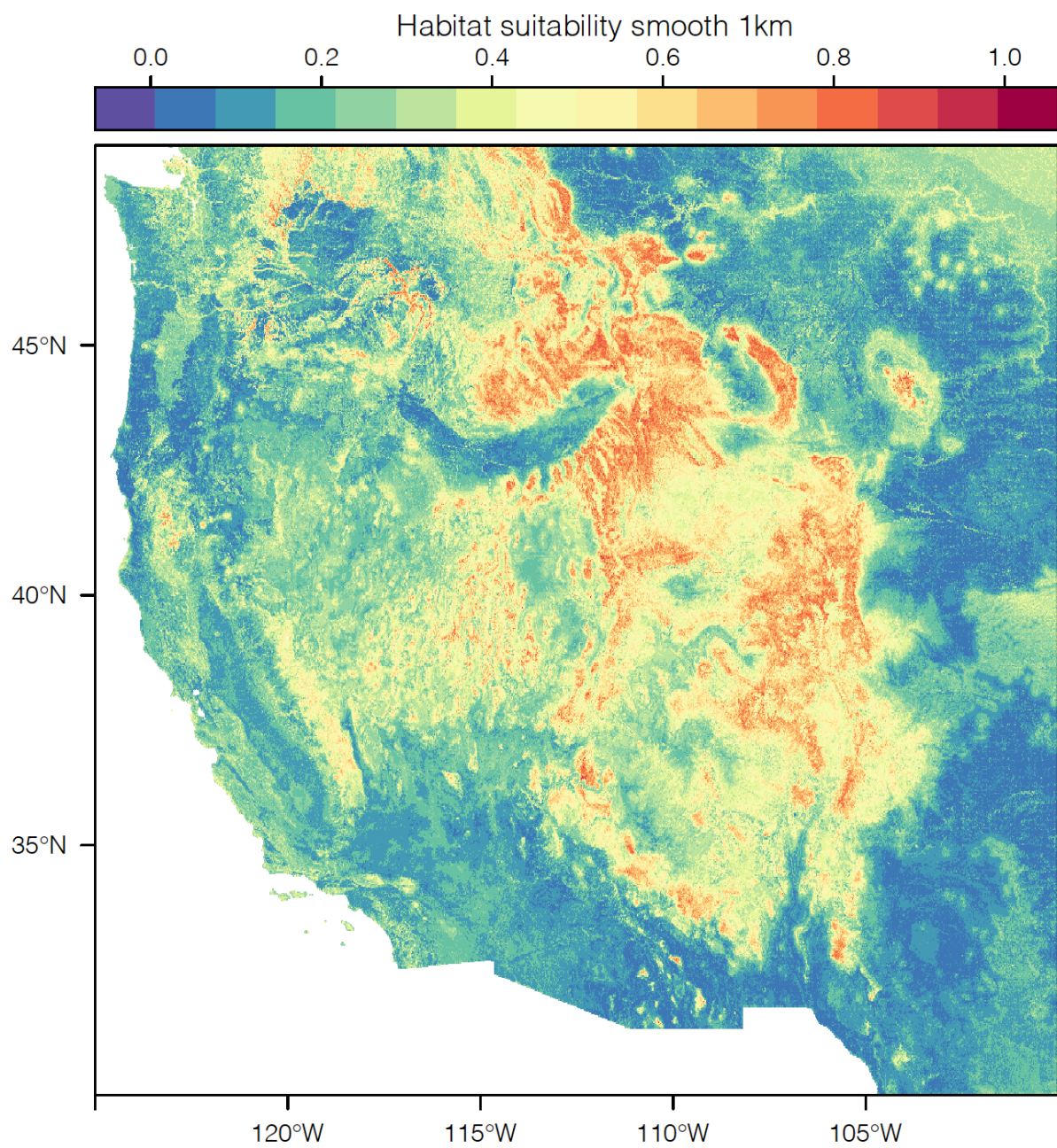
Chapter 2 Supplementary Figure 2:

Chapter 2 Supplementary Figure 2: Smooth *Oreohelix* presence and absence map.

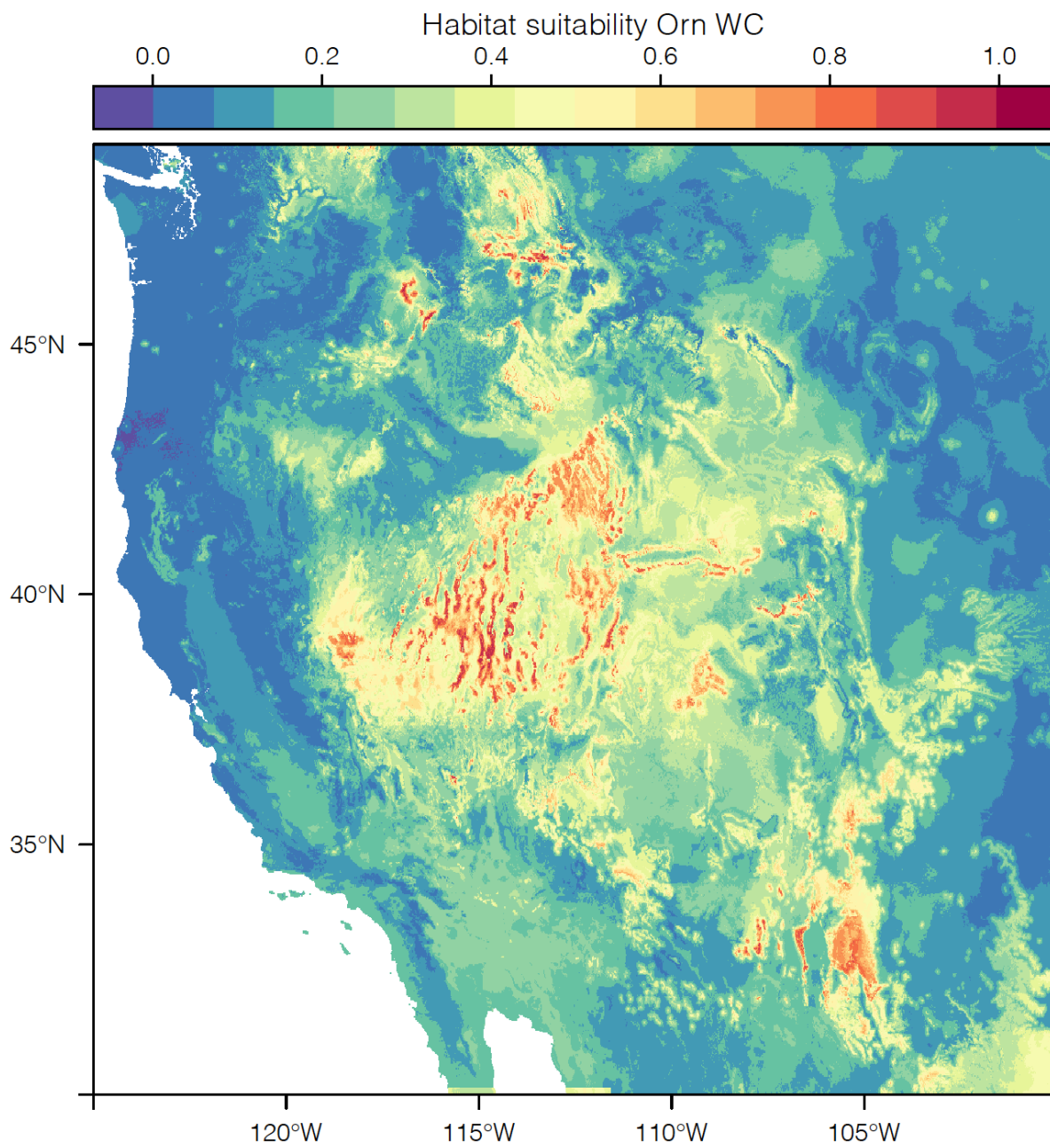
Chapter 2 Supplementary Figure 3:**Chapter 2 Supplementary Figure 3:** Ornamentated 250m² distribution map.

Chapter 2 Supplementary Figure 4:**Chapter 2 Supplementary Figure 4:** Smooth 250m² distribution map.

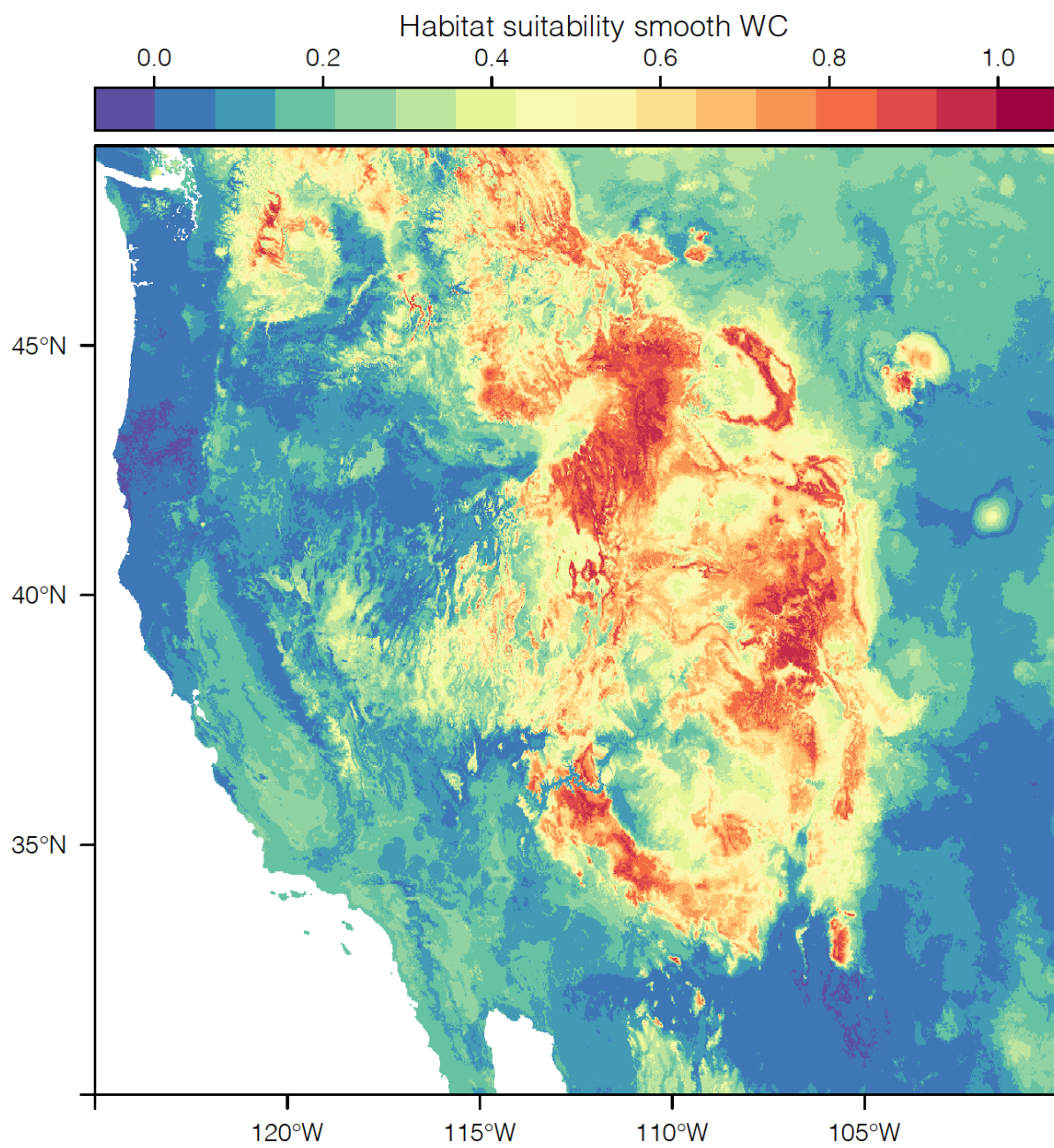
Chapter 2 Supplementary Figure 5:**Chapter 2 Supplementary Figure 5:** Ornamented 1km² distribution map.

Chapter 2 Supplementary Figure 6:**Chapter 2 Supplementary Figure 6:** Smooth 1km² distribution map.

Chapter 2 Supplementary Figure 7:



Chapter 2 Supplementary Figure 7: Ornamented WorldClim distribution map.

Chapter 2 Supplementary Figure 8:**Chapter 2 Supplementary Figure 8:** Smooth WorldClim distribution map.

Chapter 2 Supplemental Table 1:

Predictor	30m2	90m2	250m2	1km2	1km2 WorldClim	Native Resolution	Biological Study	Source
Compound topographic index (CTI)	1	1	1	1	-	30m2	West et al. 2019	Tachikawa et al. 2011; Evans et al. 2014
Heat Load Index (HLI)	1	1	1	1	-	30m1	Rykken et al. 2007	Tachikawa et al. 2011; McKay et al. 2011
Height above nearest drainage (HAND)	1	1	1	1	-	30m2	Ström et al. 2009; Hettenbergerová et al. 2013	Tachikawa et al. 2011; McKay et al. 2012
Horizontal distance to nearest drainage (DTND)	1	1	1	1	-	30m2	Ström et al. 2009; Hettenbergerová et al. 2013	Tachikawa et al. 2011; McKay et al. 2012
Slope	1	1	1	1	-	30m2	West et al. 2019	Tachikawa et al. 2010
Elevation	1	1	1	1	-	30m2	Klorvuttimontara et al. 2017	Tachikawa et al. 2011
Global Horizontal Irradiance (GHI)	1	1	1	1	-	250m2	Schweizer et al. 2019	Holden et al. 2018; Solargis 2019
Soil clay content (soilclay)	1	1	1	1	-	30m2	Gomot et al. 1989; Charrier et al. 2013	Chaney et al. 2019
Soil ph (soilph)	1	1	1	1	-	30m2	Gomot et al. 1989; Charrier et al. 2013	Chaney et al. 2019
Normalized Difference Vegetation Index (NDVI)	1	1	1	1	-	30m2	Pratumchart et al. 2019	Mhawej and Faor 2020
Mean July LANDSAT8 Surface Temperature	1	1	1	1	-	30m2	Baur and Baur 1993	Mhawej and Faor 2020
Distance to developed area (developed)	1	1	1	1	-	30m2	Frest and Johannes 1997; Rosin et al. 2017	Yang et al. 2018
Distance to calcareous rock (LS)	1	1	1	1	1	30m2	Kalisz and Powell 2003; Juříčková et al. 2008;	Weary and Doctor 2014

WorldClim Annual Mean Temperature	-	-	-	-	1	1km2	Hof 2011; Lei et al. 2017	Fick and Hijmans 2017
WorldClim Mean Diurnal Range	-	-	-	-	1	1km2	Hof 2011; Lei et al. 2017	Fick and Hijmans 2017
WorldClim Isothermality	-	-	-	-	1	1km2	Hof 2011; Lei et al. 2017	Fick and Hijmans 2017
WorldClim Annual Precipitation	-	-	-	-	1	1km3	Hof 2011; Lei et al. 2018	Fick and Hijmans 2018
WorldClim Temperature Annual Range	-	-	-	-	1	1km2	Hof 2011; Lei et al. 2017	Fick and Hijmans 2017
WorldClim Mean Temperature of Wettest Quarter	-	-	-	-	1	1km2	Hof 2011; Lei et al. 2017	Fick and Hijmans 2017
WorldClim Mean Temperature of Driest Quarter	-	-	-	-	1	1km2	Hof 2011; Lei et al. 2017	Fick and Hijmans 2017
WorldClim Precipitation Seasonality	-	-	-	-	1	1km2	Hof 2011; Lei et al. 2017	Fick and Hijmans 2017
WorldClim Precipitation of Driest Quarter	-	-	-	-	1	1km2	Hof 2011; Lei et al. 2017	Fick and Hijmans 2017
WorldClim Precipitation of Warmest Quarter	-	-	-	-	1	1km2	Hof 2011; Lei et al. 2017	Fick and Hijmans 2017

Chapter 2 Supplementary Table 1: Predictor dataset composition, data source, original resolution, and usage in previous land snail distribution studies.

Chapter 2 Supplementary Table 2:

Training				
Resolution	Ornament Presence	Ornament Absence	Smooth Presence	Smooth Absence
Class 90m2:	237	0	857	0
Class 250m2:	237	0	857	0
Class 1km2:	237	0	857	0
Class WC:	237	0	857	0
Distribution 90m2: Distribution	234	2456	848	1837
250m2:	234	2456	848	1837
Distribution 1km2:	234	2456	848	1837
Distribution WC:	234	2456	848	1837
Validation				
Resolution	Ornament Presence	Ornament Absence	Smooth Presence	Smooth Absence
Class 90m2:	62	0	209	0
Class 250m2:	62	0	209	0
Class 1km2:	62	0	209	0
Class WC:	62	0	209	0
Distribution 90m2: Distribution	65	605	220	455
250m2:	65	605	220	455
Distribution 1km2:	65	605	220	455
Distribution WC:	65	605	220	455

Chapter 2 Supplementary Table 2: Presence and absence locality numbers for different Random-forest classification and distributional models.

Chapter 2 Supplemental Table 3:

Predictor	90m ²	250m ²	1km ²	1km ² WC
Soil pH	18.78 / 25.30	22.54 / 20.43	19.60 / 15.33	-
Soil clay content	11.86 / 18.02	11.93 / 35.71	11.18 / 31.53	-
Horizontal distance to nearest drainage	13.89 / 18.25	10.78 / 16.14	8.49 / 8.55	-
Height above nearest drainage	14.47 / 14.89	12.51 / 12.15	16.17 / 10.86	-
Compound topographic index	3.76 / 11.37	4.27 / 7.04	3.56 / 2.97	-
Global Horizontal Irradiance (W·H/m ²)	26.86 / 66.06	20.36 / 58.57	12.38 / 51.85	-
Heat load index	0.39 / 9.31	3.57 / 8.38	2.08 / 1.18	-
Slope	19.16 / 8.87	14.62 / 9.46	25.58 / 14.52	-
Elevation	27.61 / 73.78	25.76 / 70.48	11.66 / 68.79	-
Normalized Difference Vegetation Index	27.81 / 30.94	22.06 / 23.26	17.05 / 25.42	-
July Mean Land Surface Temperature	25.54 / 19.22	24.13 / 16.54	13.90 / 13.94	-
Distance to developed area	9.06 / 25.83	8.76 / 21.61	1.16 / 21.70	-
Distance to calcareous rock	78.00 / 61.35	74.97 / 58.59	64.16 / 50.75	70.71 / 59.48
WorldClim Annual Mean Temperature	-	-	-	19.98 / 38.47
WorldClim Isothermality	-	-	-	25.19 / 28.96
WorldClim Temperature Annual Range	-	-	-	33.31 / 42.90
WorldClim Mean Annual Precipitation	-	-	-	18.61 / 24.09
WorldClim Mean Temperature of Wettest Quarter	-	-	-	30.71 / 47.62
WorldClim Mean Temperature of Driest Quarter	-	-	-	23.59 / 57.18
WorldClim Precipitation Seasonality	-	-	-	14.26 / 45.07
WorldClim Precipitation of Driest Quarter	-	-	-	22.31 / 29.81
WorldClim Precipitation of Warmest Quarter	-	-	-	17.36 / 38.16

Chapter 2 Supplementary Table 3: Predictor variable importance for Random-forest distribution models. Bolded values indicate it is the most important variable for the classification model. The first values in each column denote the variable importance values for ornamented distribution models and the second value for smooth forms.

Chapter 2 Supplemental Table 4:

Scientific Name	Ornamentation Classification	Global Status	State Status
<i>Oreohelix alpina</i>	0	G2	S1
<i>Oreohelix amariradix</i>	0	G1G2	S1S2
<i>Oreohelix anchana</i>	0	GH	SNR
<i>Oreohelix barbata</i>	0	G1	S1,S1
<i>Oreohelix californica</i>	1	G1	SNR
<i>Oreohelix carinifera</i>	1	G1	S1
<i>Oreohelix concentrata</i>	P	G2	SNR; SNR
<i>Oreohelix confragosa</i>	0	G1	S1
<i>Oreohelix cooperi</i>	0	G1Q	S2, S1
<i>Oreohelix elrodi</i>	1	G2G3Q	S1
<i>Oreohelix eurekaensis</i>	1	G2	S1
<i>Oreohelix eurekaensis uinta</i>	1	G1	SNR
<i>Oreohelix grahamensis</i>	1	G2	S2
<i>Oreohelix hammeri</i>	1	GX	S1
<i>Oreohelix handi</i>	1	G1	SNR, S1
<i>Oreohelix haydeni alta</i>	1	G1	SNR
<i>Oreohelix haydeni betheli</i>	1	-	SNR
<i>Oreohelix haydeni bruneri</i>	1	-	SNR
<i>Oreohelix haydeni corrugata</i>	1	G2	S1
<i>Oreohelix haydeni haydeni</i>	1	-	S2
<i>Oreohelix haydeni hesperia</i>	1	G2T1	S1
<i>Oreohelix haydeni hybrida</i>	1	-	SNR
<i>Oreohelix haydeni mixta</i>	P	-	SNR
<i>Oreohelix haydeni oquirrhensis</i>	1	-	SNR
<i>Oreohelix haydeni perplexa</i>	1	G2T1T3	SNR
<i>Oreohelix hemphilli</i>	1	G2T1T3	S2
<i>Oreohelix hendersoni</i>	0	G1G3	SNR
<i>Oreohelix houghi</i>	0	G1	SNR
<i>Oreohelix howardi</i>	0	G1	SNR
<i>Oreohelix idahoensis idahoensis</i>	1	G1	S1
<i>Oreohelix idahoensis baileyi</i>	1	G1	S1
<i>Oreohelix intersum</i>	1	G1T1	S1
<i>Oreohelix jaegeri</i>	1	G1	S1
<i>Oreohelix jugalis</i>	0	G1	S1
<i>Oreohelix junii</i>	0	G1G2	S2S3
<i>Oreohelix litoralis</i>	0	G2	S1
<i>Oreohelix loisae</i>	0	G1	S2
<i>Oreohelix magdalenae</i>	0	G1G3	S1
<i>Oreohelix metcalfei acutidiscus</i>	1	G2	SNR

<i>Oreohelix metcalfei concentrica</i>	1	G2T1	SNR
<i>Oreohelix metcalfei cuchillensis</i>	0	G2T1	S1
<i>Oreohelix metcalfei hermosensis</i>	0	G2T1	SNR
<i>Oreohelix metcalfei metcalfei</i>	1	G2T1T2	SNR
<i>Oreohelix metcalfei radiata</i>	1	G2T1	SNR
<i>Oreohelix neomexicana</i>	P	G2T2	S3, SNR
<i>Oreohelix nevadensis</i>	0	G3	S1
<i>Oreohelix parawanensis</i>	0	G1	S1
<i>Oreohelix peripherica newcombi</i>	P	G1	SNR
<i>Oreohelix peripherica peripherica</i>	P	G2	SNR
<i>Oreohelix peripherica wasatchensis</i>	1	G2T1T2	S1
<i>Oreohelix peripherica weberiana</i>	P	-	SNR
<i>Oreohelix pilsbryi</i>	1	G2T1	S1
<i>Oreohelix pygmaea</i>	0	G1	S1, S1
<i>Oreohelix pygmaea maculata</i>	0	-	SNR
<i>Oreohelix strigosa berryi</i>	0	G5T2	S1S2, SH
<i>Oreohelix strigosa buttoni</i>	0	-	SNR
<i>Oreohelix strigosa capax</i>	0	G5T2Q	SNR
<i>Oreohelix strigosa delicata</i>	0	G5T1	S1, S1
<i>Oreohelix strigosa depressa</i>	0	G5T5	SNR, S2S3, S2?, SNR
<i>Oreohelix strigosa fragilis</i>	0	-	SNR
<i>Oreohelix strigosa goniogyra</i>	1/P	G5T1	S1
<i>Oreohelix strigosa nogalensis</i>	0	G5T2	S1
<i>Oreohelix strigosa strigosa</i>	0	-	S5
<i>Oreohelix subrudis</i>	0	G5	SNR, S3, SNR; SNR, SNR, S5, S3, S3, SNR, SNR
<i>Oreohelix swopei</i>	0	G1	S1
<i>Oreohelix tenuistriata</i>	0	GH	SH, SNR
<i>Oreohelix variabilis</i>	0	G2Q	S2
<i>Oreohelix vortex</i>	0	G2?	S1
<i>Oreohelix waltoni</i>	1	G1	S1
<i>Oreohelix yavapai clutei</i>	0	-	SNR
<i>Oreohelix yavapai cummingsi</i>	1	G5T3Q	S1
<i>Oreohelix yavapai extremitatis</i>	1	G5TNR	SNR, SNR, SNR
<i>Oreohelix yavapai fortis</i>	0	-	SNR
<i>Oreohelix yavapai magnicornu</i>	1	-	SNR
<i>Oreohelix yavapai mariae</i>	1	G5T1	S1
<i>Oreohelix yavapai profundorum</i>	0	-	SNR
<i>Oreohelix yavapai yavapai</i>	1	G5	S1
<i>Oreohelix sp.</i>	Classified based on image	-	-

Chapter 2 Supplemental Table 4: *Oreohelix* ornamentation type and NatureServe conservation rank.

Oramentation classification values of 1 mean the species is ornamented, 0 mean the species is smooth, and P indicate the species is polymorphic for ornamentation. NatureServe ranks correspond to global (G) or state (S) on a scale of 1-5 with 5 being the least threatened. NR, U, Q, T correspond to not ranked, unrankable due to possible lack of information, questionable taxonomic status, and intraspecific status, respectively.

Chapter 2 Supplemental Table 5:

term	.y.	group1	group2	df	statistic	p	p.adj	p.adj.signif
w_shell*h_shell*ornamentation	mass	horiz_rib	keeled	1.25E+02	2.83E+00	5.37E-03	0.054	ns
w_shell*h_shell*ornamentation	mass	horiz_rib	smooth	1.25E+02	5.13E+00	1.05E-06	1E-05	****
w_shell*h_shell*ornamentation	mass	horiz_rib	smooth limestone	1.25E+02	1.86E+00	6.51E-02	0.651	ns
w_shell*h_shell*ornamentation	mass	horiz_rib	vert rib	1.25E+02	-2.06E+00	4.11E-02	0.411	ns
w_shell*h_shell*ornamentation	mass	keeled	smooth	1.25E+02	1.74E+00	8.37E-02	0.837	ns
w_shell*h_shell*ornamentation	mass	keeled	smooth limestone	125	-0.651	5.16E-01	1	ns
w_shell*h_shell*ornamentation	mass	keeled	vert rib	125	-3.97	1.21E-04	0.001	**
w_shell*h_shell*ornamentation	mass	smooth	smooth limestone	125	-2.82	5.63E-03	0.056	ns
w_shell*h_shell*ornamentation	mass	smooth	vert rib	125	-7.01	1.31E-10	1E-09	****
w_shell*h_shell*ornamentation	mass	smooth limestone	vert rib	125	-4.07	8.42E-05	8E-04	***

Chapter 2 Supplemental Table 5: Pairwise comparison of estimated marginal means of shell mass after controlling for shell height and width. Significant differences are considered below a 0.05 adjusted p-value.

Chapter 2 Supplemental Table 6:

term	.y.	group1	group2	df	statistic	p	p.adj	p.adj.signif
mass*ornamentation	cf	horiz_rib	keeled	1.26E+02	-0.915	3.62E-01	1.00E+00	ns
mass*ornamentation	cf	horiz_rib	smooth	1.26E+02	10.1	6.30E-18	6.30E-17	****
mass*ornamentation	cf	horiz_rib	smooth_limestone	1.26E+02	5.23	6.99E-07	6.99E-06	****
mass*ornamentation	cf	horiz_rib	vert_rib	1.26E+02	4.15	6.13E-05	6.13E-04	***
mass*ornamentation	cf	keeled	smooth	1.26E+02	8.73	1.27E-14	1.27E-13	****
mass*ornamentation	cf	keeled	smooth_limestone	1.26E+02	5.28	5.58E-07	5.58E-06	****
mass*ornamentation	cf	keeled	vert_rib	1.26E+02	4.37	2.56E-05	2.56E-04	***
mass*ornamentation	cf	smooth	smooth_limestone	1.26E+02	-2.38	1.87E-02	1.87E-01	ns
mass*ornamentation	cf	smooth	vert_rib	1.26E+02	-3.83	2.03E-04	2.03E-03	**
mass*ornamentation	cf	smooth_limestone	vert_rib	126	-1.08	2.83E-01	1.00E+00	ns

Chapter 2 Supplemental Table 6: Pairwise comparison of estimated marginal means of shell strength after controlling for shell mass. Significant differences are considered below a 0.05 adjusted p-value.

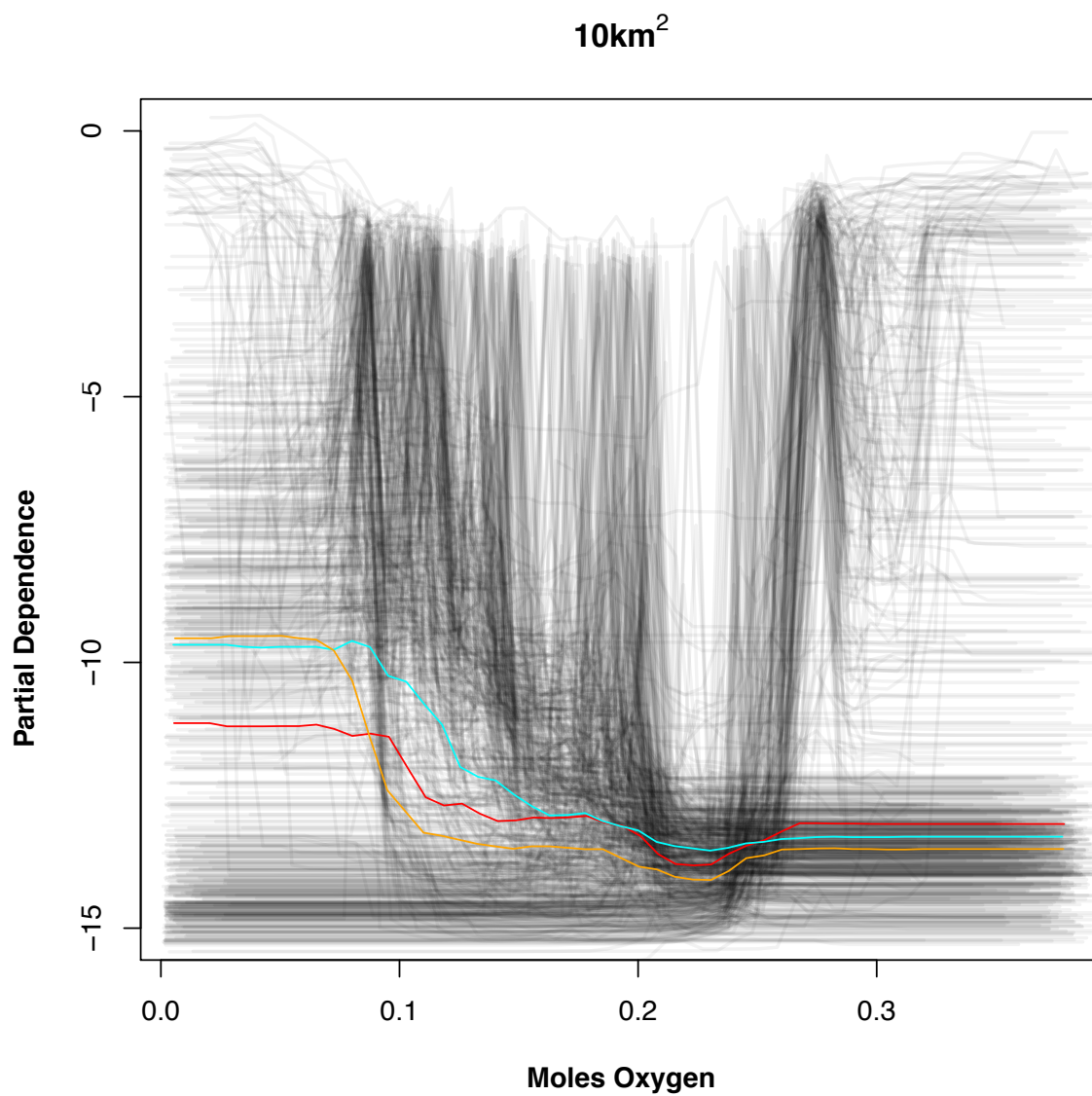
Chapter 2 Supplemental Table 7:

Ornamented 90m	CTI90	slope90	LST90	NDVI90	DTND90	elevation90	GHI90
Min	-4.4629	0	257.7	0.02804	0	256	3.181
Median:	-0.02607	17.61	296	0.41346	217.3	1667	4.404
Mean:	0.35805	19.03	295.2	0.44356	6606.6	1610.7	4.377
Max:	11.46183	45.79	309.7	0.85868	177490	3237	5.941
	HAND90	HLI90	LS90	developed90	soilclay90	soilph90	
Min	0	0.5823	0	0	2.123	5.091	
Median:	36	0.8046	0	4935	14.851	6.76	
Mean:	158.9	0.7994	2313	6244	14.809	6.846	
Max:	1270	0.9901	113192	35885	26.447	8.334	
Smooth 90m	CTI90	slope90	LST90	NDVI90	DTND90	elevation90	GHI90
Min	-4.4387	0.000	270.4	-0.4193	0.0	50	3.016
Median:	0.2457	13.150	292.8	0.5820	127.3	1755	4.156
Mean:	0.9258	14.823	293.0	0.5542	1679.2	1620	4.215
Max:	13.7685	55.268	309.2	0.8888	106260.1	3391	5.782
	HAND90	HLI90	LS90	developed90	soilclay90	soilph90	
Min	0.00	0.5695	0.0	0	0.9053	4.174	
Median:	11.00	0.7995	696.8	4304	15.0582	6.454	
Mean:	80.03	0.7976	11078.5	6200	14.8177	6.502	
Max:	1387.00	0.9793	220756.1	35885	55.1244	9.084	

Chapter 2 Supplemental Table 7: Summary statistics for ornamented and smooth predictor variables. See Supplemental Table 1 for predictor abbreviations.

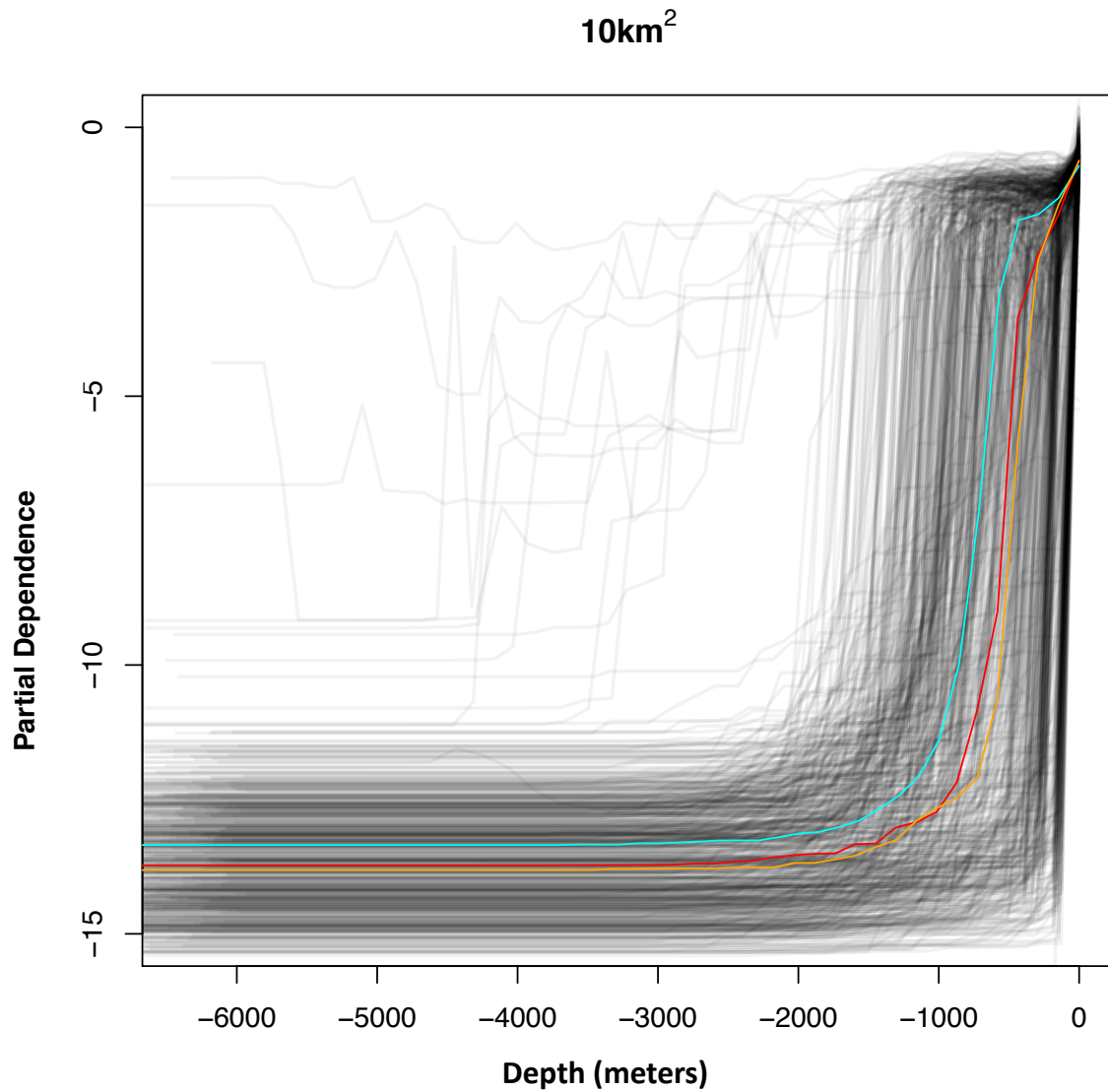
Appendix D: Supplementary tables and figures for Chapter 3

Chapter 3 Supplemental Figure 1:



Chapter 3 Supplemental Figure 1: Partial dependence plot of moles oxygen and gastropod morphotype presence. Higher partial dependence values indicate higher likelihood for class presence. Colored lines depict median partial dependence lines for morphotype groups and black lines denote species. Cyan: ornamented; Red: smooth; Orange: sea slug.

Chapter 3 Supplemental Figure 2:



Chapter 3 Supplemental Figure 2: Partial dependence plot of depth and gastropod morphotype presence. Higher partial dependence values indicate higher likelihood for class presence. Colored lines depict median partial dependence lines for morphotype groups and black lines denote species. Cyan: ornamented; Red: smooth; Orange: sea slug.